WIND-TUNNEL MODELLING OF HILL AND VEGETATION INFLUENCE ON WIND POWER AVAILABILITY

TASK 1: LITERATURE REVIEW

Prepared by

Robert N. Meroney, Ph.D., P.E.*

for

Meteorological Services

U.S. WINDPOWER, INC.

6592 Preston Avenue

Livermore, California 94550

* Professor, Civil Engineering

Director, Fluid Dynamics and Diffusion Laboratory

FLUID MECHANICS AND WIND ENGINEERING PROGRAM

Colorado State University

CSU Contract No. 29-8610

CER92-93-RNM-1

October 1992, revised February 1993

WIND-TUNNEL MODELLING OF HILL AND VEGETATION INFLUENCE ON WIND POWER AVAILABILITY

TASK 1: LITERATURE REVIEW

Prepared by

Robert N. Meroney, Ph.D., P.E.*

for

Meteorological Services
U.S. WINDPOWER, INC.
6592 Preston Avenue
Livermore, California 94550

* Professor, Civil Engineering
Director, Fluid Dynamics and Diffusion Laboratory

FLUID MECHANICS AND WIND ENGINEERING PROGRAM

Colorado State University

CSU Contract No. 29-8610

CER92-93-RNM-1

October 1992, revised February 1993

EXECUTIVE SUMMARY

A literature review was performed of agricultural meteorology and wind engineering literature to identify the parametric effects of hill shape, vegetation density, and clearing size on hill-top wind speed. Forest meteorology research was examined which considered forest canopy density, tree height, understory structure and tree species effects on wind speed parameters such as displacement height, d; surface roughness, z_o ; and surface drag, u_* / u_{ref}. Field and laboratory measurement programs were surveyed which studied the variation of winds downwind of tree stands and the effect of clearings on clearing winds. Numerical and mathematical models were evaluated to determine the state-of-the-art of predictions of combined effects of hill terrain height and vegetation cover on wind fields.

The survey identified several tables and algorithms which may be used to estimate forest canopy displacement height and roughness length. Surface drag data seems to be much less systematic; hence, large variations in magnitude are recorded, and no one algorithm is reliable.

Field and laboratory measurement programs find that the presence or absence of vegetation can produce significant changes in wind speed. Vegetation may also enhance or inhibit the presence of flow separation over hill crests. Limited data taken near wind turbines erected near tree stands confirms that lower turbine productivity occurs at significant distances downwind of vegetation.

Analytic models based on linear-perturbation theories were identified which can predict the combined effects of hill height, hill slope, hill shape and surface roughness variation on hill top wind speeds. These perturbation models have been validated against field and laboratory measurements, and they are found to predict trends correctly, but in some cases may overpredict hill crest wind speeds. Numerical models (FLOWSTAR, MS3DJH/3) based on linear-perturbation methods and Fourier decomposition of complex terrain are available which can predict the joint effects of terrain elevation, thermal stratification, and non-homogeneous surface roughness. These models are constructed to work on small workstations or PC computers. These models are currently limited to stationary situations, "mild" terrain and roughness variations, and mild stratification such that flow separation and blocking do not occur.

Spreadsheet results are provided which estimate the added value of different size clearcut areas over various two-dimensional ridges. Predicted information includes depth of the inner layer of the flow at crest height, wind speeds in the outer and inner region, and fractional speed-up factors. Data is provided for roughness change speed-up, hill induced speed-up, and combined effect of hill slope and roughness variations.

Alternative diagnostic models based on the concept of mass consistency are also available which have been used to examine hill crest flows in the presence of vegetation (NOABL, UICWINDS, NUWINDS, ASL, etc.) Some of these models use ad hoc type modifications to allow for stratification and vegetation effects. These models are also limited to flows which have no separation or blocked regions.

Some authors have also proposed modifications to finite difference or finite element equation sets to account for vegetation drag on wind fields (HOTMAC, CSURAMS). The principle adjustment used is the addition over the vegetation filled portion of the grid of a drag term related to vegetation density. These models have been used to predict winds over meso-scale size regions, are often computer memory and time intensive, and require a fast workstation with considerable memory.

Robert N. Meroney, Professor
Fluid Mechanics and Wind Engineering
Civil Engineering, Colorado State University

ACKNOWLEDGEMENTS

The author wishes to acknowledge the assistance and discussions provided by Dr. Scott Veenhuizen, formerly of United Industries, Inc., Kent, WA; Dr. Michael Sestak, Bureau of Land Management, Fort Collins, CO; Ms. Bernadette Connell, Dr. Evgeny Donev, Dr. William Massman and Dr. Karl Zeller of the Rocky Mountain Forest and Range Experiment Station, Fort Collins, CO; Dr. Tetsuji Yamada, Yamada Science and Art, Inc., Los Alamos, NM; and Dr. Peter Taylor, York University, Canada. The effective and friendly assistance of Mr. Lindsey Weiss of the Colorado State University library staff is also appreciated.

TABLE OF CONTENTS

EXECUTIVE SUMMARY i

ACKNOWLEDGEMENTS iii

LIST OF TABLES vi

LIST OF FIGURES vii

LIST OF SYMBOLS xi

I. **INTRODUCTION** 1

II. **WIND FLOW OVER HILLS/COMPLEX TERRAIN** 2
- 2.1 General Wind Speed and Turbulence Characteristics 2
- 2.2 Field and Laboratory Measurements 9
- 2.3 Summary 10

III. **WIND FLOW OVER VEGETATIVE CANOPIES** 17
- 3.1 Flow Within and Downwind of an Individual Tree 19
- 3.2 Under-canopy Forest Flow Field 26
- 3.3 Above-canopy Forest Flow Field 30
  - 3.3.1 *Logarithmic velocity profile models* 30
  - 3.3.2 *Power-law velocity profile models* 35
- 3.4 Wind Flow Near Clearings, Clearcuts, and Forest Edges 38
- 3.5 Change of Surface Roughness 52
  - 3.5.1 *Change of Roughness Models* 52
  - 3.5.2 *Multiple changes of roughness* 55
- 3.6 Summary 55

IV. **VEGETATIVE/SURFACE ROUGHNESS EFFECTS ON FLOW OVER HILLS /MOUNTAINS** 57
- 4.1 Homogeneous Surface Roughness Over Hills/Mountains 57
  - 4.1.1 *Field and Laboratory Data* 57
  - 4.1.2 *Inviscid -Rotational Numerical Model Results* 60
  - 4.1.3 *Turbulence Model Insights* 60
  - 4.1.4 *Linear-perturbation Model Insights* 60
- 4.2 Change in Roughness Effects on Flow Over Hills/Mountains 64
  - 4.2.1 *Linear-perturbation Model Insights* 64
  - 4.2.2 *Field and Fluid Model Data* 65
- 4.3 Laboratory Measurements of Vegetation Covered Terrain 65
- 4.4 Summary 71

V. **ANALYTIC AND NUMERICAL MODELS** 72
5.1 Mass-consistent or Objective Analysis Models Applied to Vegetation Covered Terrain 72
5.1.1 *NOABL Predictions for Clearcut Effects Over Cape Blanco, Oregon* 73
5.1.2 *Atmospheric Science Laboratory (ASL) Model Predictions* 77
5.1.3 *NUATMOS Predictions of Complex Terrain Flows* 77
5.2 Linear-perturbation Models Applied to Vegetation Covered Terrain 81
5.2.1 *FLOWSTAR Model Predictions* 81
5.2.2 *MS3DJH and MS-MICRO Model Predictions* 81
5.2.3 *Mass-consistent and Linear-perturbation Model Comparisons* 87
5.3 Primitive Equation Models Applied to Vegetation Covered Terrain 87
5.3.1 *HOTMAC Predictions of Forest and Vegetation Effects* 87
5.3.2 *FITNAH Vegetation Modifications to Predict Deforestation Effects on Drainage Flows and Local Climate* 89
5.4 Spread-sheet Predictions of Wind Effects of Clearcutting 91
5.4.1 *Linear-perturbation Expressions for Combined Changes in Roughness and Elevation* 91
5.4.2 *Results of Spreadsheet Calculations* 91
5.5 Summary 102

VI. **CONCLUSIONS** 103

APPENDIX: REVIEW AND CLASSIFICATION OF COMPLEX TERRAIN MODELS 105

REFERENCES 125

LIST OF TABLES

Table 2.2.1 Laboratory Simulations of Flow Over Complex Terrain 12
Table 2.2.1 (Continued) 13
Table 2.2.1 (Continued) 14
Table 2.2.1 (Continued) 15
Table 2.2.1 (Concluded) 16
Table 3.3.1 Table of roughness length data 32
Table 3.4.1 Wake behavior of buildings, trees and shelterbelts (Meroney, 1977) 45
Table 4.1.4 Maximum increase of velocity in potential flow over various two-dimensional hills with low slopes. 61
Table 5.2.1 MS3DJH/3R and finite-difference model predictions for flow over Gaussian hills with roughness modulation. (Walmsley *et al.*, 1986) 84

LIST OF FIGURES

Figure 2.1.1 Characteristic wind speed and power availability over the crest of a two-dimensional ridge. 3
Figure 2.1.2 Velocity, turbulence, and static pressure profiles over a 1:6 slope triangular hill. (Meroney, et al., 1976) 4
Figure 2.1.3 Velocity, turbulence and static pressure profiles over a 1:4 slope triangular hill. (Meroney, et al. 1976) 5
Figure 2.1.4 Velocity, turbulence, and static pressure profiles over a 1:2 slope triangular hill. (Meroney,et al. 1976) 6
Figure 2.1.5 Velocity speedup between approach flow and crest over different hill shapes. (Meroney et. al. 1978) 7
Figure 2.2.1 Vertical profiles of speedup at the hilltop for two wind directions in wind-tunnel (AES, OXR, NZR) and full-scale (FS) flows (Teunissen *et al.*, 1987) 11
Figure 3.0.1 Drag coefficients of live and model trees: Dashed line (after Hsi and Nath, 1968); solid circles (after Rayner, 1962) (Meroney, 1968) 18
Figure 3.1.1 Geometry of idealized trees for numerical calculations. (Gross, 1987) . . . 20
Figure 3.1.2 Vertical profiles of u at different point along the symmetry axis. The dotted line shows the undisturbed profile of the inflow boundary. (Gross, 1987) 21
Figure 3.1.3 Vertical profiles of shear stress, σ, at different points along the symmetry axis. The dotted line shows the reference (inflow) value. (Gross, 1987) 22
Figure 3.1.4 Streamlines of the horizontal airflow for 1 m above the ground. The contour of the tree is dotted, the dashed line indicates cases where $u < 0$. (Gross, 1987) 23
Figure 3.1.5 Vertical profiles of u at different points along the symmetry axis (———— ball-tree, - - - cone-tree) (Gross, 1987) 24
Figure 3.1.6 Wind deformation and the wind velocity that may produce that deformation. (Hewson *et al.*, 1979) 25
Figure 3.2.1 Meteorological wind tunnel at Colorado State University and artificial tree canopy. (Meroney, 1968) 27
Figure 3.2.2a Velocity profiles in and above model forest canopy (Meroney, 1968) 28
Figure 3.2.2b Longitudinal turbulent intensity for model forest canopy. (Meroney, 1968) 28
Figure 3.2.3 Under-forest canopy mean velocity profiles for expressions developed by Cowan, 1968; Inoue, 1953, and Cionco, 1965; and Massman, 1987. 29
Figure 3.2.4 Optimal fits of observed wind profile for a Ponderosa pine canopy. Observations are denoted by circles from Raupach and Thom (1981).(Massman, 1987) 29
Figure 3.3.1 Above canopy wind profiles for various average forest canopy heights when $d = 0.63$ h, $z_o = 0.125$ h, and $u_* = 0.316$ u(h). 34

Figure 3.3.2 Effective roughness for sinusoidal orography. Measurements, finite difference models, and Equation 3.3.4. (Grant and Mason, 1990) 36
Figure 3.3.3 Variation of the power-law index with increasing roughness and corresponding roughness classes for Equations 3.3.8 and 3.3.9. (Baron, 1981) 37
Figure 3.3.4 Variation of the power-law index with increasing height of roughness elements. (Baron, 1981) 39
Figure 3.3.5 Variation of the power-law index with increasing roughness length. (Baron, 1981) 40
Figure 3.4.1 Windflow and vertical profiles of meteorological variables within and above a forest. (Cionco, 1982) 41
Figure 3.4.2 Figure 3.4.1 with smoke plumes deployed. (Cionco, 1982) 41
Figure 3.4.3 Mean velocity profiles within and above the roughness. (Kawatani, 1971) 42
Figure 3.4.4 Shear plate drag for model forest canopy (Meroney, 1968) 43
Figure 3.4.5 Study areas in the High Ridge Evaluation Area, Umatilla National Forest, Oregon. (Fowler, *et al.*, 1987) 47
Figure 3.4.6 Wind passage at 6 and 20m in watersheds 4 and 1 during two 11 month periods--one before and one after treatment. (Fowler *et al.*, 1987) 48
Figure 3.4.7 Goodnoe Hills, WA. Radials show directions to towers. Percent reduction in wind speed and increase in turbulence [$\Delta U\%/\Delta u'\%$] (Elliott and Barnard, 1990) 49
Figure 3.4.8 Wind speed ratios (to tower 9) versus tower 9 wind direction. Directions of major groves and wind turbines are indicated (Elliott and Barnard, 1990) 50
Figure 3.4.9 Turbulence intensity ratios (to tower 9) versus tower 9 wind direction. (Elliott and Barnard, 1990) 51
Figure 3.5.1 Wind profile transition height resulting from a change in surface roughness (Park Schwind, 1977, in Meroney, 1977) 53
Figure 3.5.2 Wind profile shapes and wind power profile shapes for various types of flat terrain. (Park and Schwind, 1977) 54
Figure 3.5.3 Internal boundary layer thickness versus normalized distance referenced to larger z_o. Line is best fit to points. (Hunt and Simpson, 1982) 56
Figure 4.1.1 Effect of surface roughness on wind flow over a sharp-crested ridge. (Wegley, Orgill and Drake, 1978) 58
Figure 4.1.2 Fractional speedup ratio profiles at crest of triangular hills. Field data,Bradley (1978); Laboratory data, Bouwmeester *et al.* (1978) 59
Figure 4.1.3 Approach flow velocity profiles for numerical inviscid flow calculations. (Bouwmeester *et al.*, 1978) 62
Figure 4.1.4 Fractional speedup ratios predicted from numerical inviscid flow calculations (Bouwmeester *et al.*, 1978) 62
Figure 4.1.5 Flow over elliptical obstacles. Heights are scaled by object height. Velocities are scaled by upstream velocity at z/h = 3. (Jensen and Petersen, 1978) 63

Figure 4.2.1 Measured fractional speed-up at top of the smooth and rough hills. (Britter *et al.*, 1981) 66
Figure 4.2.2 Horizontal isotachs over Rakaia Gorge, N.Z. z_p = 10 m. (Meroney *et al.*, 1978) 67
Figure 4.2.3 Horizontal isotachs over Rakaia Gorge, N.Z., z_p = 50 m. (Meroney *et al.*, 1978) 68
Figure 4.2.4 Vertical section G-G isotachs at Rakaia Gorge, N.Z. (Meroney *et al.*, 1978) 69
Figure 4.2.5 Vertical section F-F isotachs at Rakaia Gorge, N.Z. (Meroney *et al.*, 1978) 70
Figure 5.1.1 Smoothing scheme for aerodynamic roughness length (Lin *et al.*, 1985) . . 74
Figure 5.1.2 Vertical wind profiles over a surface of smoothed surface roughness (Lin *et al.*, 1985) 75
Figure 5.1.3 Initialization of vertical wind profiles for 3-D wind flow computations. (Lin *et al.*, 1985) 76
Figure 5.1.4 Typical complex terrain scenario with grass and forest ($\wedge$)vegetation and villages (□). (Cionco, 1982) 78
Figure 5.1.5 Surface layer windfield solution for Figure 5.1.4. (Cionco, 1982) 78
Figure 5.1.6 Schematic of 3-dimensional coupled wind model (Cionco, 1982) 79
Figure 5.1.7 Cross-section analysis of adjacent grid point wind profiles. (Cionco, 1982) 80
Figure 5.2.2 Crest velocities for sinusoidal hill and ln[z_o], ———MS3DJH/3R; Finite diff. m_r= 4. (Walmsley *et al.*, 1986) 83
Figure 5.2.1 Sinusoidal hill & ln{z_o].——— MS3DJH/3R, finite diff. model, m_r = 4; + , m_r = 100. (Walmsley *et al.* 1987) 83
Figure 5.2.4 Crest velocities over rough-crested 2-D Gaussian hill (See Figure 5.2.3 for notation) (Walmsley *et al.*, 1986) 85
Figure 5.2.3 Rough-crested 2-D Gaussian hill,(2β=1000m, h=100m, m_r=10)———u,---roughness only fd model;○, + roughness only MS3DJH/3R model, ... 85
Figure 5.2.7 Cresttop velocities for the Coastal Hill and Island experiments. (Walmsley *et al.*, 1986) 86
Figure 5.2.6 Wind speed at z = 2m for Coastal and Island experiments. Dashed curves are roughness change alone. (Walmsley *et al.*, 1986) 86
Figure 5.2.8 Mean wind speeds for each of 12 directions computed by WAsP, NOABL*, and MS-MICRO and measured values at Vounaros. (Lalas *et al.*, 1988) 88
Figure 5.3.1 Distribution of tree canopies. Units are in decimal, *i.e.*, 3 indicates 0.3, 2 for 0.2, and 0 for no trees. (Yamada and Bunker, 1989) 90
Figure 5.3.2 HOTMAC modeling of horizontal wind vectors at z = 24 m at 0200 LST. (Yamada and Bunker, 1989) 90
Figure 5.3.3 Computed wind vectors at 2 m above Finkenbach valley terrain: (a) with canopy, (b) after deforestation. (Gross, 1987) 92

Figure 5.4.1 Linear-perturbation. Inverse-polynomial hill. $h_{hill} = 100$ m, $L = 1000$ m, $z_{o1} = 3.71$ m, $z_{o2} = 0.1$ m. $U_{10m} = 10$ m/s. 94
Figure 5.4.2 Effects of clearcutting upwind to the hill half-height, $h_{hill}/L = L$ for various hill slopes. $z_{o1} = 3.71$ m. 95
Figure 5.4.3 Influence on windspeed of clearcutting different distances upwind for a hill slope $h_{hill}/L = 0.10$. $z_{o1} = 3.71$ m. 96
Figure 5.4.4 Influence on wind speed of clearcutting different distances upwind for a hill slope $h_{hill}/L = 0.20$. $z_{o1} = 3.71$ m. 97
Figure 5.4.5 Influence on windspeed of clearcutting different distances upwind for a hill slope $h_{hill}/L = 0.40$. $z_{o1} = 3.71$ m. 98
Figure 5.4.6 Influence on windspeed of clearcutting various distances upwind for hill slope $h_{hill}/L = 0.10$, $z_{o1} = 1.85$ m. 99
Figure 5.4.7 Influence on windspeed of clearcutting different distances upwind for hill slope $h_{hill}/L = 0.20$, $z_{o1} = 1.85$ m. 100
Figure 5.4.8 Influence on windspeed of clearcutting different distances upwind for hill slope $h_{hill}/L = 0.40$, $z_{o1} = 1.85$ m. 101

LIST OF SYMBOLS

Symbol	Description	[Dimension]
A	Silhouette area	[L^2]
C_D	Drag coefficient	
C_f	Skin friction coefficient	
C_p	Surface pressure coefficient	
d	Displacement height	[L]
D	Crown diameter	[L]
h, h_{hill}, H	Hill, mountain, or escarpment height	[L]
h, H	Forest canopy height	[L]
K	Tree crown height	[L]
H	Peak to trough height sinusoidal terrain	[L]
l, l_z, δ_1	Inner layer depth	[L]
l_{zh}	Inner layer depth for hill effects	[L]
l_{zr}	Inner layer depth for roughness change	[L]
L	Distance from crest to hill half-height	[L]
L	Hill characteristic width	[L]
L_{mo}	Monin-Obukhov stratification scale	[L]
ΔP	Fractional power change	
Ri	Richardson number	
S	Horizontal area occupied by roughness element	[L^2]
ΔS	Fractional speedup factor	

SYMBOLS (Contd.)

Symbol	Description	[Dimension]
ΔT	Fractional turbulent intensity change	
u, U, V	Wind speed	$[LS^{-1}]$
u_h	Wind speed at top of vegetative canopy	$[LS^{-1}]$
u_o	Upwind wind speed	$[LS^{-1}]$
u_{ref}	Reference wind speed	$[LS^{-1}]$
u_*	Surface friction velocity	$[LS^{-1}]$
u_{*1}	" " " due to upwind roughness	$[LS^{-1}]$
u_{*2}	" " " due to downwind roughness	$[LS^{-1}]$
Δu	Perturbation wind speed increment	$[LS^{-1}]$
Δu_{hill}	" " " " from hill	$[LS^{-1}]$
Δu_{rough}	" " " " from roughness	$[LS^{-1}]$
x, y, z	Coordinate distances	[L]
z, Δz	Vertical distance above ground	[L]
z_o	Surface roughness	[L]
z_{o1}	" " upwind	[L]
z_{o2}	" " downwind	[L]
z_o^{eff}	Effective surface roughness from both hills and local roughness	[L]
z_m	Matching height	[L]
α	Power-law velocity exponent	
β	Deacon's parameter	
κ	von Karman's coefficient	
λ	Wavelength, sinusoidal hills	[L]
δ	Boundary layer thickness	[L]

I. INTRODUCTION

Wind turbine aerodynamics is concerned with the interaction between atmospheric flows and the turbine's rotor. The wind-turbine rotor operates in the atmospheric surface layer, where wind shear, gustiness, and the local micro-meteorology of terrain shape and vegetation change the operating environment. Since wind turbine performance is critically linked to the availability of wind energy at turbine hub height, preferred sites are those with moderate and persistent winds (20-40 mph).

Hills or ridges are known to cause wind "speed-up" associated with streamline convergence. Convergence will occur in neutrally stratified flows at hill crest; whereas maximum streamline convergence will often occur on the lee of a hill or ridge when the wind flows between the surface and an elevated inversion. Tall vegetation such as woods, windbreaks, or forests may degrade the wind environment over a hill. Eddies created by a tree canopy can enhance surface mixing reducing near-surface wind speeds, and the eddies themselves may cause gustiness which increases turbine blade loading and fatigue.

Given the simple-minded assumption that wind power is proportional to wind-speed cubed, even a 10% decrease in hub-height winds speed may reduce available wind power by 25%. Thus, knowledge of how vegetation cleared regions over hills may enhance or diminish hill crest velocities would be valuable planning information. Often the key question is how much clear cutting on the site of a proposed wind energy farm is required along the ridge tops and hilltops to maximize wind resources while minimizing environmental impact.

Wind energy specialists have focused frequently on the potential for wind speed amplification found in hilly terrain. Their concerns have led to additional field and laboratory data on the behavior of neutral and stratified flows over both two-dimensional ridges as well as three-dimensional isolated hills, valleys and gorges. Agricultural and forest meteorologists are concerned with "blow-down" in vegetative canopies during wind storms and the air transport of insects, pheremones, insecticides, herbicides, moisture, CO_2 , soil, burning debris and smoke. Analytic and numeric models have been created to estimate wind flows above and within such canopies in complex terrain situations.

This review will focus primarily on information related to the operation of wind turbines on hill crests partially or totally covered with forests. Chapter 2 provides a short background about flow amplification over terrain covered with minimal vegetation (*ie.* no flow displacement and small local roughness; $d = 0.0$, $z_o = 0\text{-}0.10$ m). Chapter 3 summarizes what is understood about wind flow over vegetative canopies over essentially horizontal ground surfaces. Chapter 4 considers the joint effects of vegetation and roughness effects over hills/complex terrain. Analytic, physical and numerical models used to characterize such flows are noted in Chapter 5. Conclusions relevant to the problem of wind turbine installation in vegetated hilly terrain are provided in Chapter 6.

II. WIND FLOW OVER HILLS/COMPLEX TERRAIN

The earth's surface is covered with almost imperceptible bulges and depressions on the global scale. The highest mountain barriers only extend above the earth's radius by about one-tenth of one percent from it's sea level value. Nevertheless, the presence of hills, mountains and valleys determines a great portion of the weather we live within. Mountains and hills and valleys induce variations in wind speed and turbulence from the mean sufficient to justify location of wind energy devices in complex terrain. Unfortunately, for most of man's weather experience most measurements have been made over flat homogeneous sites. Thus, the understanding of wind flows over complex terrain has become a special area of meteorological consideration. Interest in weather modification, air pollution, and wind energy over the last twenty years has led to extensive additional information about mountain climatology. Today, there are numerous books and monographs specifically focusing on the climate and specifically the winds developed over complex terrain (Blumen, 1990; Frost and Shieh, 1981;Hiester and Pennell, 1981; Hunt and Simpson, 1982; Wegley et al., 1978).

2.1 General Wind Speed and Turbulence Characteristics

Single hills and isolated ridges are known to produce higher wind speeds at a given height over the crest than far upwind during high speed neutrally stratified air flow. The approximate improvement in wind speed should be of the order of h/L, where h is hill height above the surrounding terrain and L is some characteristic horizontal hill width (say the distance from the crest to half-hill height). Thus, a smooth surfaced hill with average approach slopes ($h_{hill}/(2L)$) of 0.10, 0.2, 0.3, 0.4, or 0.5 should produce fractional speedup [$\Delta S = (u(z) - u_o(z))/u_o(z)$] increases at crest of the order 20%, 40%, 60%, 80% and 100%, respectively, or corresponding order increases in wind power up to 73%, 174%, 309%, 483%, and 700%, respectively **(See Figure 2.1.1)**. Speedup does not seem to be as sensitive to hill shape for the same average slope as long as flow separation does not occur **(See Figure 2.1.2)** . These values may be reduced by the presence of forests, local undulations, and regions of flow separation. In particular, when hill slopes exceed 0.3 it is likely that flow separation may occur at hill crest decreasing wind speeds and inducing large gustiness. **Figures 2.1.3 through 2.1.4** display wind and turbulence profiles measured over different slope triangular hills in a boundary-layer wind tunnel (Bouwmeester et al., 1978). Fractional speed up is defined as $\Delta S = (u(z) - u_o(z))/u_o(z)$, where $u_o(z)$ is the upstream profile and z is the height above local grade. Typically wind decreases at the foot of the hill then accelerates to hill crest. Over steep hills separation may occur at the hill crest **(Figure 2.1.4)**, which decreases crest wind speeds and produces gustiness and excess turbulence downstream.

Figure 2.1.5 displays the effect of 2-dimensional hill shape on fractional wind speedup. Note that hill slope is more significant than hill shape on defining wind profiles as long as the elevation is not so abrupt as to generate separation regions downwind. Three dimensional hills are found to produce lower wind speed increases than similar cross-section ridges.

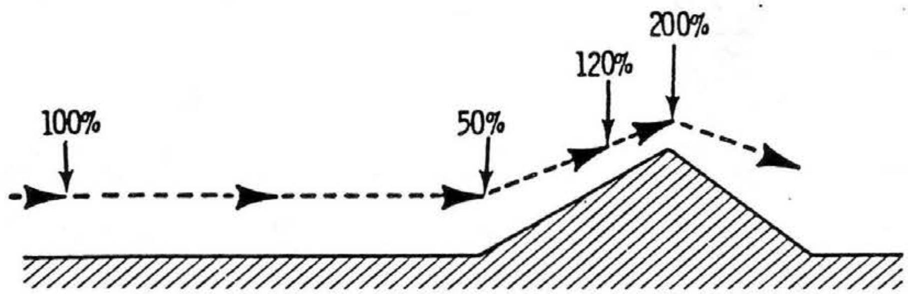

Figure 2.1.1 Characteristic wind speed and power availability over the crest of a two-dimensional ridge.

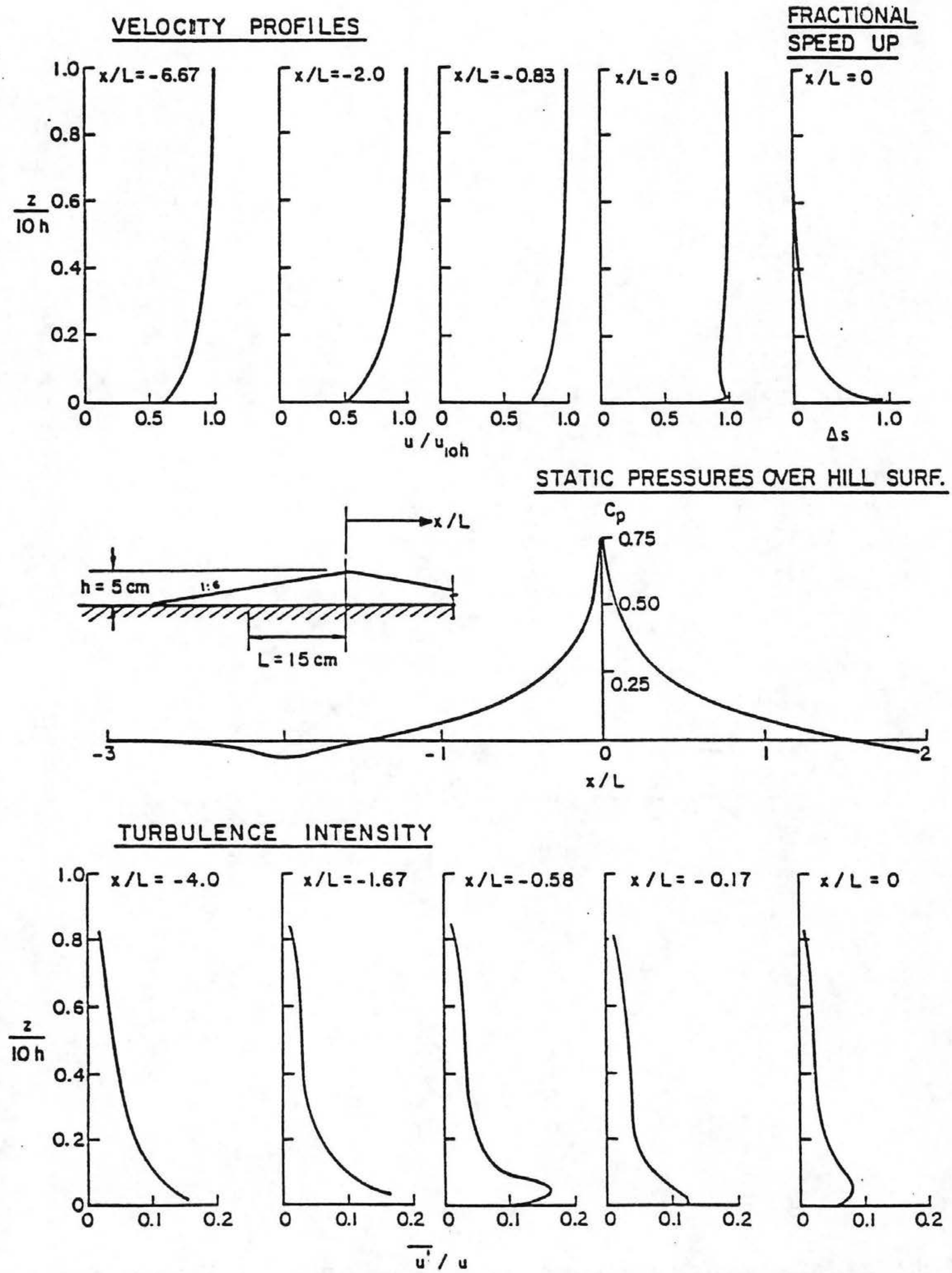

Figure 2.1.2 Velocity, turbulence, and static pressure profiles over a 1:6 slope triangular hill. (Meroney, et al., 1976)

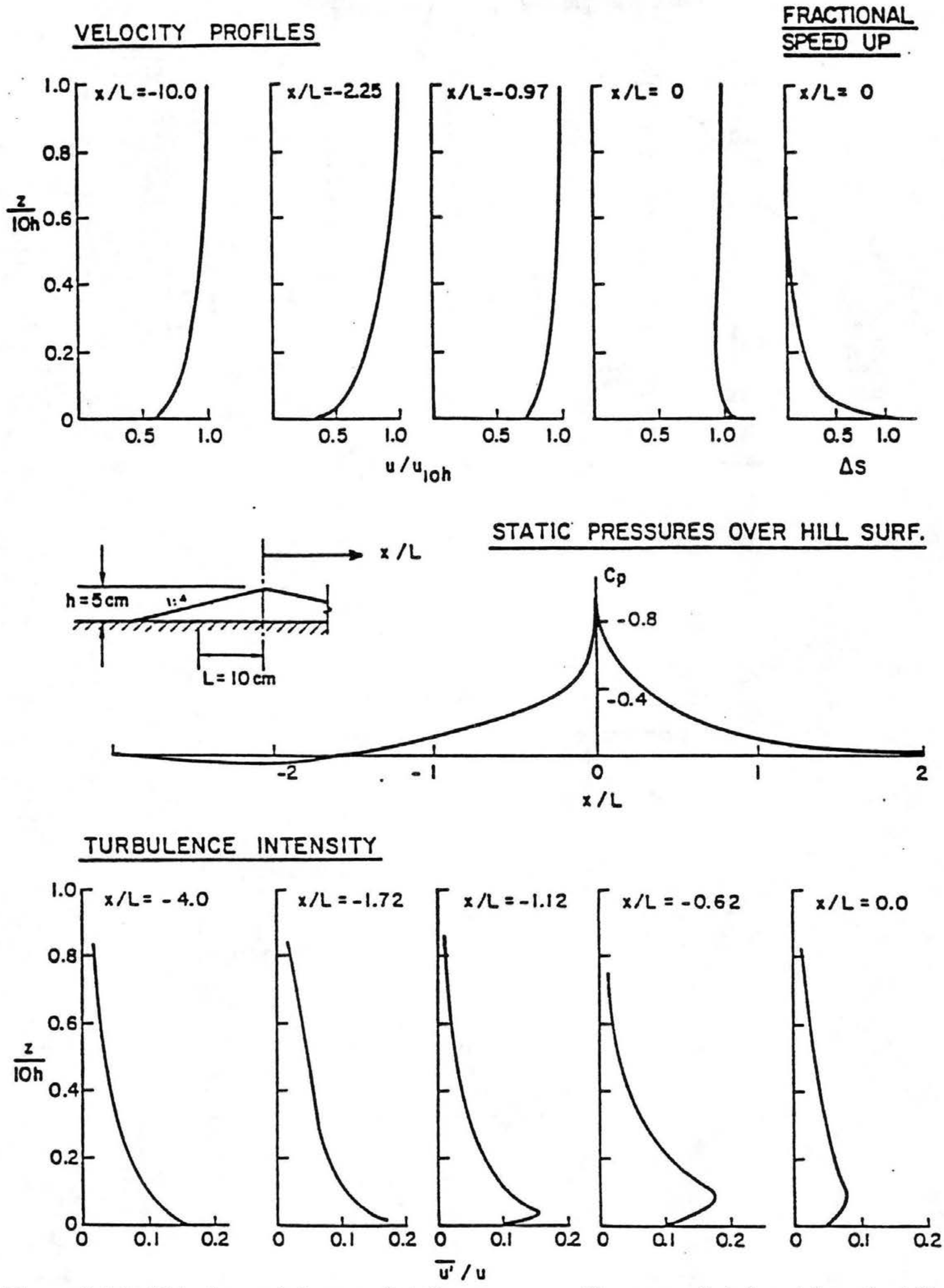

Figure 2.1.3 Velocity, turbulence and static pressure profiles over a 1:4 slope triangular hill. (Meroney, et al. 1976)

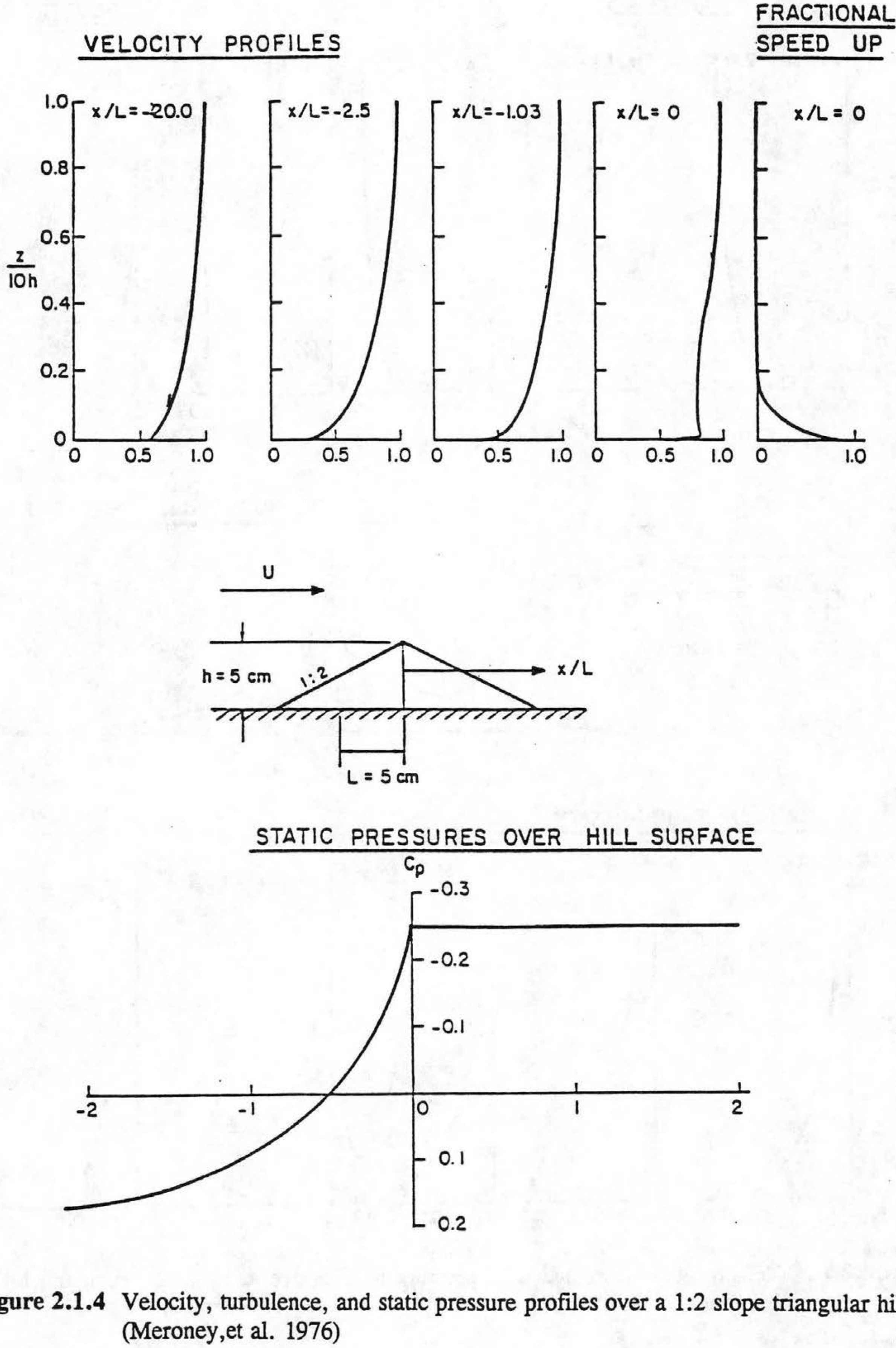

Figure 2.1.4 Velocity, turbulence, and static pressure profiles over a 1:2 slope triangular hill. (Meroney,et al. 1976)

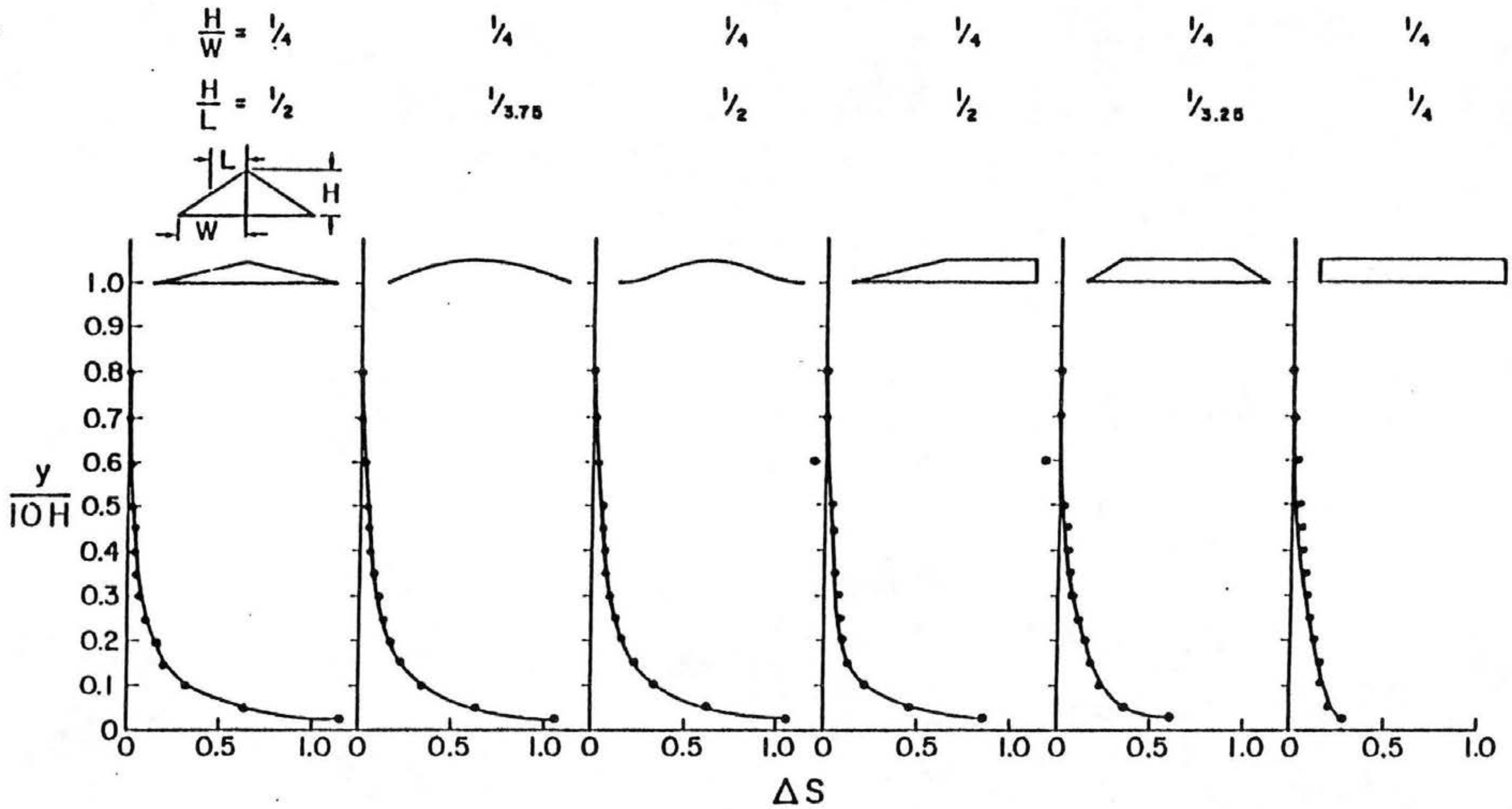

Figure 2.1.5 Velocity speedup between approach flow and crest over different hill shapes. (Meroney et. al. 1978)

It is more difficult to predict quantitatively the exact wind patterns in complex terrain where multiple hills, mountains and valleys occur over an extensive area. Flow interactions, blocking, and channeling may either enhance or decrease wind speeds. Indeed, at the present state of the meteorological art the serious wind-turbine meteorologist may be limited to field measurements, large meso-scale numerical models, or physical models in such cases.

Thermal stratification will also change the air flow over single hills and mountains substantially. Stable stratification may cause low level winds to move laterally around a hill barrier decreasing crest top winds but enhancing hill side winds, or alternatively an elevated inversion just above hill crest may induce very strong winds on the downslope side of a hill or ridge. Indeed some of the most persistent and attractive wind-energy locations appear to be associated with such downslope conditions. Blumen (1990) has edited a series of articles about such flows in hills, mountains and valleys into a monograph on atmospheric processes over complex terrain. In particular chapter 4 on mountain waves and downslope winds by D.R. Duran, chapter 5 on perturbation solutions to flow over hills by D.J. Carruthers and J.C.R. Hunt, and chapter 7 on physical modeling of flow over hills and mountains by R.N. Meroney are relevant reading for the wind-energy climatologist interested in wind power meteorology in hills and mountains.

Turbulence behavior over hills depends upon upwind fetch, strength of stream line convergence over the crest, and regions of increased shear. For small hills such that surface flows have limited time to come into local equilibrium with the new hill flow conditions the upwind turbulence is primarily advected along streamlines with minor changes; hence changes in wind shear play a small role. On the other hand convergence and divergence of streamtubes may lead to "rapid-distortion" or stretching, twisting, or shortening of turbulent vortex elements. Stretching distortions can lead to enhanced local vorticity and increased turbulence. When the local turbulent velocity is scaled by local mean speed at the hill crest the net effect may be a decrease in turbulent intensity although in absolute terms the turbulent fluctuations are greater. Of course if separation over the crest occurs then elevated regions of increased turbulence downwind will occur.

Hills or mountains with small slope or long upwind fetch conditions permit the near ground flow to move toward local equilibrium with local shear. An inner boundary layer, l_z grows upward in which these effects are significant. To a first order the depth at crest should be related to $l_z \ln[l_z / z_o] = 2\kappa^2 L$, where z_o is surface roughness and L is characteristic hill width.[1] For most conditions $l_z = 0.05$ L when h/L is of order one. In such conditions over

---

[1] The characteristic hill width, L, may be defined in at least three different ways. It can be total base-width of hill from upstream base to downstream base; it can be the distance from up- or down-wind hill base to hill crest; or it can be the distance from hill crest to the location up- or down-wind where the hill is one-half the total hill height above the base. The half-height width is used for characteristic width throughout this report.

moderate slope hills analytic and numerical methods based on linear-perturbation concepts work quite well (See Section 5.0). To a first order the fractional wind speedup, ΔS, is still found to be proportional to h/L.

2.2 Field and Laboratory Measurements

As a result of environmental and energy concerns there now exists a large number of field data sets related to wind flow fields over hilly and mountainous terrains. Some were performed to answer questions about nuclear power safety, others were concerned with atmospheric transport of power plant plumes, and some were specifically posed to evaluate wind-energy potential over hill crests. Articles in Blumen (1990) refer to experiments of the Dept. of Energy ASCOT test series (Geysers, CA; Brush Creek, CO), the Environmental Protection Agencies CTMDP test series (Cinder Cone Butte,ID; Hog Back Ridge, NM; Tracy Power Plant, NV), and various international measurement efforts like the Askervein hill project (US, NZ, UK, CN). Meroney (1978, 1980) reviews pre-1980 field studies which had laboratory counterpart experiments (eg. Rakaia River Gorge, NZ; Gebbies Pass, NZ; Kahuku Point, Oahu, HA). During the 1980s a number of field studies over relatively smooth isolated hills and ridges were performed specifically to validate wind flow models proposed to predict wind-energy potential (Askervein Hill, Blashaval, Brent Knoll, Great Dun Fell, Nyland Hill, UK; Kettle Hill, CAN). Table 2.2.1 summarizes some details of 69 laboratory studies for 31 cases of which comparable field measurements are available.

Almost all of the isolated hill and ridge studies examined terrain with very small surface roughness (1-3 cm); hence, there are few published data (found during this review) for wind flow over simple terrain shapes incorporating forests, woods, shelterbelts, clearings or clearcut areas. (This is not to say individual meteorological measurements do not exist in clearings and clearcut areas in hills, but no extensive sets of measurements were made in such situations to document terrain wide flow.) One exception was the two-dimensional ridge study performed in Australia by Bradley (1978) (See discussion in Section 4.1).

The ASCOT Brush Creek study involved a 650 m deep valley in western Colorado where the southwest-facing walls were dry, and barren, while the northeast-facing walls were moist and brush covered. The vegetation was found to make a significant difference in diurnal absorption of thermal radiation, and the wind flows which developed in the valley. The ASCOT Geyser area study were performed over tree covered hills and meadow covered valleys. Again inclusion of the vegetation in analytic and numerical models was necessary to reproduce the wind flows observed. Unfortunately, no high wind conditions were observed in either ASCOT study, for the principal program goal was to evaluate the mechanisms of night time and daytime drainage flow in open-ended valleys.

An extensive set of physical model experiments were also performed during the 1980s. The Askervein Hill Project was a collaborative study of boundary-layer flow over low hills (Taylor and Teunissen, 1987). Two field experiments were conducted during fall 1982 and 1983 near and around Askervein, a 116 m high hill on the west coast of the island of South Uist in the Outer Hebrides of Scotland. Over 50 towers were deployed and instrumented for wind measurements. Most were cup anemometers mounted on simple 10 m posts, but two 50 m, one 30 m, one 16 m, and thirteen 10 m towers were instrumented for three-component turbulence measurements. Subsequently, wind tunnel simulations of the hill were carried out at three different length scales (1 to 800, 1 to 1200, and 1 to 2500) in two wind tunnel facilities (Teunissen et al. 1987) The wind-tunnel results compared well with each other and with full scale data **(Figure 2.2.1)** Changes in mean flow speedup over the physical models were reproduced very well, including those due to small local terrain features that may be physically small at model scale. Relaxation of the aerodynamic roughness criterion ($Re_* = u_* z_o/\nu > 2.5$) affected the flow only on the lee side of the model hills. Turbulence changes induced by the hill did not depend on the nature of the surface roughness (suggesting the inner boundary length was quite small). An excessively smooth surface reduced the degree and extent of separated flow and resulted in overestimation of hill crest wind speeds. Simulations in two facilities using three models at three different scales showed a gratifying degree of consistency. The only effect of model scale was a predictable increase in difficulty in making measurements very close to the surface as the size of the model decreased. The depth of the turbulent inner layer was similar to the value predicted by Jensen et al. (1984) discussed in Section 3.5.

2.3 Summary

The general behavior of wind flow over simple and complex terrain is qualitatively well understood. Measurements in field or laboratory situations have been made under an amazingly broad range of conditions. Nonetheless, the possible combinations of hill shape, slope, surface roughness, stratification conditions, upwind approach conditions, surrounding terrain undulations, and unsteadiness associated with the diurnal cycle and weather result in few quantitatively reliable estimators for hill crest wind speeds.

Actual measurements of wind flow over vegetation covered terrain which can be used to specify the effect of forrest edges, clearings or clearcuts on wind energy siting are minimal. The few studies identified will be discussed in Sections 3.5 and 4.2.

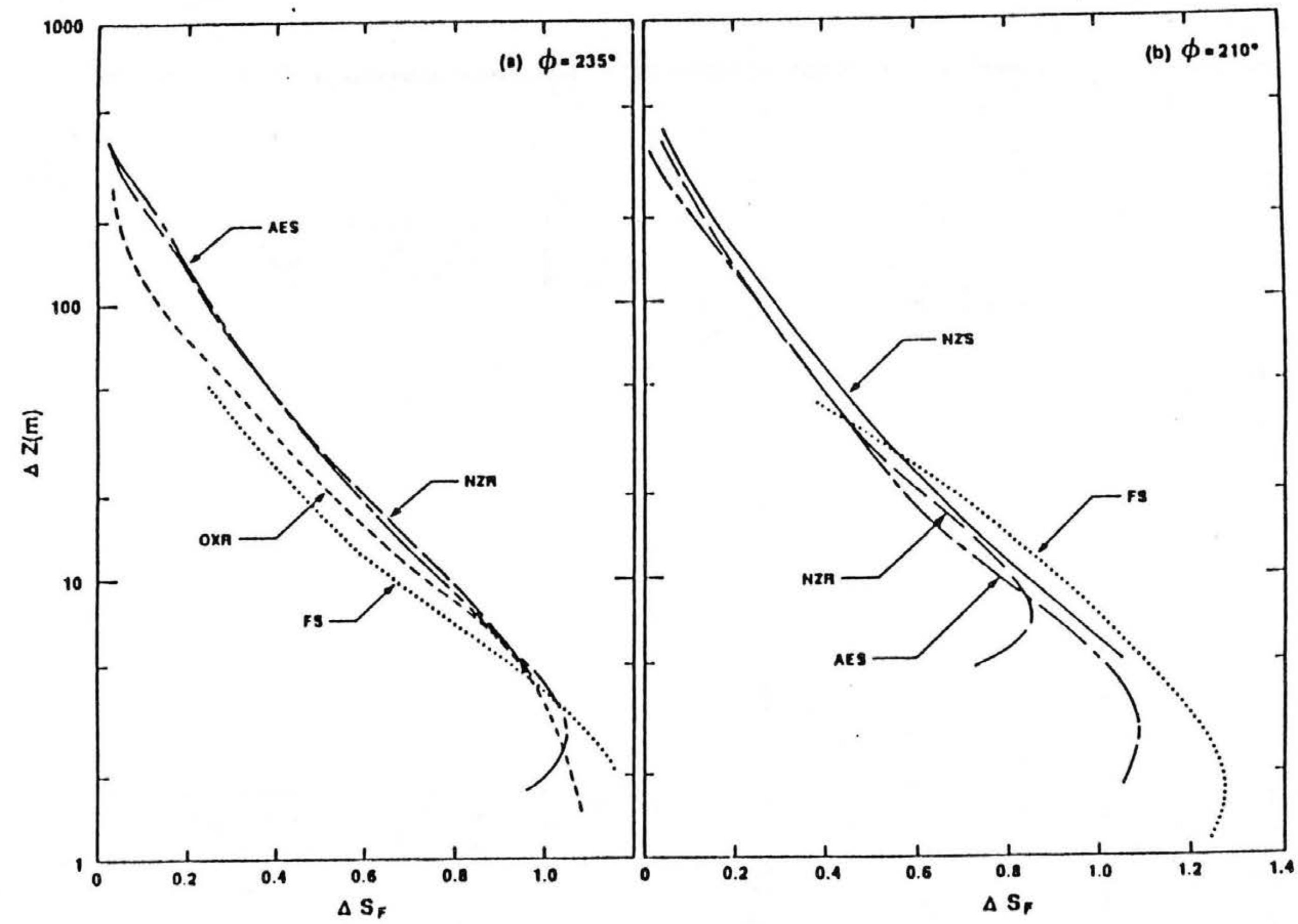

Figure 2.2.1 Vertical profiles of speedup at the hilltop for two wind directions in wind-tunnel (AES, OXR, NZR) and full-scale (FS) flows (Teunissen *et al.*, 1987)

Table 2.2.1 Laboratory Simulations of Flow Over Complex Terrain

	AUTHOR (DATE)	TOPOGRAPHIC SITE	PROBLEM STUDIED	TYPE OF AIRFLOW	MAXIMUM HEIGHT OF FEATURE (m)	LENGTH SCALE RATIO	Similitude Criteria						
							delta/H	alpha	$Z_o/H \times 10^4$	u'/U_*	u_*/U_∞	L_{ux}/H	Ri or PG Category
*1	Field and Warden (1929–1930)	Rock of Gibraltar	Topographical effects and turbulence	Neutral	520	5000	0.00	0.00					
*2	Abe (1941)	Mt. Fuji, Japan	Mountain clouds and topographic effects	Barostromatic (dry ice)	4000	50000							not accurate
*3	Putnam (1946)	Pond Glastenberg Mt. Washington	Topographic effects	Neutral	300 650 1154	5280 6280 5280		0.00 0.00 0.00					
4	Suzuki & Yabuki (1956)	Idealized hills	Mountain lee waves	Barostromatic (brine solution)			0.00	0.00					
5	Long (1953, 1954, 1955)	Idealized hills	Mountain lee waves	Barostromatic (brine solution)			0.00	0.00					13–94
*	Long (1959)	Sierra Nevada Mtns California	Mountain lee waves	Barostromatic (brine solution)	2750	75000	0.00	0.00					12–300
6	Nemoto (1961)	Enoshima & Akashi Channel, Japan	Turbulence & Velocity profiles	Neutral	60	600 3300/ 10000		1.00		0.20		1.33	
*7	Halitsky, Toleiss, Kaplin & Magony (1962–1963)	Bear Mountain New York	Turbulence & Wake patterns	Neutral	390	1920	1.25			0.16			
8	Briggs (1963)	Rock of Gibraltar	Turbulence Patterns	Neutral	520	5000	0.00	0.00					
9	Halitsky, Magony, & Halpern (1964–65)	Mountains near Manchester, Vermont	Topographic effects	Neutral									
10	Plate & Lin (1965) CSU	Idealized hill	Velocity & turbulence in wake	Neutral Unstable			3–9 3–5	0.15 0.19	1.50 1.50	0.14	0.03 0.03		 0.02
11	Chang (1966) CSU	Idealized hill	Velocity & turbulence in wake	Neutral			2.00	0.15	1.50				
*12	Cermak, Peterka & (Meroney) (1966) CSU	Pt. Arguello, CA	Topographic effects Diffusion	Barostromatic Neutral	500 500	12000 12000	9.00 9.00	0.25 0.25					0.31
*13	Meroney & Cermak (1967) CSU	San Nicolas Island, California	Topographic effects Diffusion	Neutral & Barostromatic	275 275	6200 6200	12.60 12.60	0.14 0.20	0.20		0.03		 0.30
14	Lin & Binder (1967) CSU	Idealized Mountain	Mountain lee waves	Barostromatic									4–25
15	Garrison & Cermak (1968) CSU	San Bruno Mountain, California	Topographic effects	Neutral Barostromatic (dry ice)	400 400 400	6000/4800 6000/4800 3000/2400	3.70 3.70 1.90	0.16 0.16	25.00 25.00		0.13		 0.32 0.32
*16	Hsi, Binder & Cermak (1968) CSU	Green River, Utah	Topographic effects	Neutral	65	800	6.00	0.14	2.00				

Table 2.2.1 (Continued)

AUTHOR (DATE)	TOPOGRAPHIC SITE	PROBLEM STUDIED	TYPE OF AIRFLOW	MAXIMUM HEIGHT OF FEATURE (m)	LENGTH SCALE RATIO	delta/H	alpha	Similitude Criteria $Z_o/H \times 10^4$	u'/U_*	u_*/U_*	L_w/H	Ri or PG Category
17 Sakagami and Kato (1968)	Seashore, Japan	Topographic effects Diffusion	Neutral	500	5000							
18 Zrajevsky, Doroshenko & Chepik (1968)	Idealized Hill	Topographic effects	Neutral									
*19 Lukey (1969)	Fort Martin West Virginia	Topographic effects Diffusion	Neutral		720							
*20 Kitabayashi, Orgill & Cermak (1971) CSU	Elk Mountain, WY	Topographic effects Diffusion	Neutral Barostromatic (Dry ice)	1200 1200	9600 9600	2.00 2.00	0.21 0.32	70.00		0.15		1.70
*21 Orgill, Cermak Grant (1971) a CSU	Eagle River Chalk Mountain area Colorado	Topographic effects Diffusion	Neutral Barostromatic (Dry ice)	1950 1950	9600 9600	4.00 2.00	0.25	3.00	0.28 0.50 0.05 0.60			6.00
*22 Orgill, Cermak Grant (1971) b CSU	San Juan Mountains Colorado	Topographic effects Diffusion	Neutral Barostromatic	2250 2250	hor 14,000 ver 9,600	2.00 2.00	0.35		0.15 0.20			
*23 Mori, Miyata & Mitsuta (1971)	Mt. Takakura Japan	Topographical effects	Neutral	300	5000							
24 Meroney, Chaudhry (1971–72) CSU	Rocky Flats Colorado	Topographic effects Diffusion	Neutral	140	1000	3.00	0.14	2.00	0.13			
25 de Bray (1973)	Idealized ramps and escarpments	Speedup	Neutral			3.00 3.00 0.05	0.14 0.11 0.00		0.12 0.15			
26 Sacre (1973)	Idealized ramps and hills	Speedup	Neutral			3.00	0.15					
27 Counihan (1973)	Idealized ramps and hills		Neutral			8, 12, 23			0.10			
28 Hewson, et.al. (1973–75)	Yaquina Head, Oregon	Speedup for WECS	Neutral	15	300	1.70						
29 Freeston (1974)	Idealized hill escarpments	Speedup	Neutral				0.14					
30 Meroney, Cermak (1974–1975) CSU	Mississippi River, Lansing, Iowa	Topographic effects Diffusion	Neutral Barostromatic	150 150	400 400	2.00 2.00	0.27 0.70	60.00 60.00				1.00
*31 Bowen & Lindley (1974)	River banks and Coastal Beach New Zealand	Speedup	Neutral	10,13	200–250	4.50	0.18	0.50	0.18	0.16		
*32 Lu & Lin (1976)	Idealized Saddle Mountain Garfield, utah	Topographic effects Diffusion	Barostromatic Barostromatic (brine solution)	1480	10000							0–58 9–36
33 Riley, Lu & Geller (1976)	Idealized hill 3–D	Topographic effects Diffusion	Barostromatic (brine solution)	1480	10000							5–288

Table 2.2.1 (Continued)

	AUTHOR (DATE)	TOPOGRAPHIC SITE	PROBLEM STUDIED	TYPE OF AIRFLOW	MAXIMUM HEIGHT OF FEATURE (m)	LENGTH SCALE RATIO	delta/H	alpha	Similitude Criteria $Z_0/H \times 10^4$	u'/U_*	u_*/U_∞	L_∞/H	Ri or PG Category
34	Meroney, et.al. (1976) CSU (1977) (1978)	Idealized hills Shapes: 2D 2D 3D	Topographic effects for WECS	Neutral Barostromatic Neutral			10.00 10.00 10.00	0.14 0.14	1.00 1.00 1.00	0.15 0.15	0.03 0.03		
*35	Kitabayashi (1977) CSU	Idealized hills	Stagnant Flows	Barostromatic			3.00						0.19–278
36	Petersen, Cermak & Ayad (1977–78) CSU	Geysers Area, California	Topographic effects Diffusion	Neutral	700	1920	2.50		7.00				
37	Cermak & Mutter (1977–78) CSU	Kahe, Oahu	Topographic effects Diffusion	Neutral	900	6500							
*38	Govind, et.al. (1977–78)	Kingston, TN	Topographic effects Diffusion	Neutral	150	800							
39	Ukeguchi, Okamato, Maeda & Ohba (1977)	Various terrain Japan	Nuclear power station Diffusion	Neutral		1000–2000							
*40	Meroney et.al. (1978) CSU, U. of Canterbury	Rakaia Gorge New Zealand	Topographic effects for WECS	Neutral	200	5000	2.50	0.15	1.00	0.13	0.03	0.75	
*41	Petersen and Cermak (1978) CSU	Geysers Area, California	Topographic effects Diffusion	Neutral	700	1920	2.15		0.15				0.06
*42	Graham, et al. (1978) CSU	Terrain near Kingston, Tenn	Topographic effects Diffusion	Neutral	100	960	6.34			0.2–0.3	0.1–0.2		
43	Hunt, Snyder & Long (1978)	Generic hill	Dividing streamline	Stable									6–25
44	Petersen and Cermak (1979) CSU	ASARCO Smelter Hayden, Arizona	Topographic effects Diffusion	Neutral	550	1920	2.09	0.07–0.60	0.06	0.2–0.3	0.03–0.21		
*45	Chien, Meroney, & Sandborn (1979) CSU	Kahuku Point Oahu, Hawaii	Topographic effects for WECS	Neutral	293	3840	4.78	0.13–0.15	3.75	0.17–0.18	0.02	0.57	
46	Petersen, Cermak & Hisato (1980) CSU	ASARCO Smelter Hayden, Arizona	Topographic effects Diffusion	Stable	550	3072	2.23	0.18–0.42	7–255		0.09		0.53
*47	Petersen and Cermak (1980) CSU	Alkali Creek Coal Creek Crested Butte, CO	Topographicl effects Diffusion	Stable/Neutral Stable/Neutral	1100 1000	1920 2560		0.07–0.23 0.18–0.30	0.002–14 6.90		0.03–0.06 0.05–0.08		3–14.2 0.07–22
*48	Briatore, Elisei & Longhetto (1980)	La Spezia coast Italy	Topographic effects Diffusion	Stable/Neutral	673	1800	5.20						
*49	Alessio, Briatore, Elisei & Longhetto (1981)	Grosseto, Italy	Dense plumes Valley flows	Stable	120	250, 3000, 4000							
50	Arya, et al. (1979–81)	Generic hills Two dimensional	Topographic effects Diffusion	Neutral									
51	Khurshudyan, Snyder & Nekrasov (1981)	Generic hills Two dimensional	Topographic effects Diffusion										

Table 2.2.1 (Continued)

AUTHOR (DATE)	TOPOGRAPHIC SITE	PROBLEM STUDIED	TYPE OF AIRFLOW	MAXIMUM HEIGHT OF FEATURE (m)	LENGTH SCALE RATIO	delta/H	alpha	Similitude Criteria $Z_o/H \times 10^4$	u'/U_*	u_*/U_*	L_m/H	RI or PG Category
52 Snyder, et al. (1980-85) •	Triangular ridges Sinusoidal ridges Fences Cinder Cone Butte Witch of Agnesi	Topographic effects Diffusion Dividing streamline	Stable/Neutral	 100	 690							
53 Lee, Barr, Snyder & Lawson (1981)	Generic long valley	Valley channeling	Neutral			10.00			-			
54 Pearse, Lindley & Stevenson (1981)	Generic hills Two dimensional	Topographic effects for WECS	Neutral									
54 Pearse (1982)	Generic conical hills	Topographic effects for WECS	Neutral	15	300	18.00	0.17		0.25		120.00	
*55 Neal (1983)	Gebbies Pass in Banks Penninsula, NZ	Topographic effects for WECS	Neutral	300	4000, 8000	2.13			0.10			
*56 Falvey (1983)	American river basin California	Topographic effects Diffusion	Stable	2600	250000 horiz. 125000 vertic.							
57 Ohba & Nakamura (1983)	Generic hills Two dimensional	Topographic effects Diffusion	Stable/Neutral									0.0, 0.7, 1.8
58 Castro, Snyder & Marsh (1983)	Generic hills Three dimensional	Topographic effects Diffusion	Stable									0.39-25
*59 Ohba & Nakamura (1983)	Coastline Japan	Topographic effects Diffusion	Stable/Neutral	175	2000	2.86						0.1, 0.8, 2.1, 2.9
*60 Teunissen, et al. (1982-88)	Askervein hill Outer Hebrides, Scotland	Topographic effects for WECS	Neutral	116	800 1200 2500	2.76 2.33 1.98	0.19 0.14 0.14	3.10 0.51 0.60	0.16 0.12 0.11	0.05 0.04 0.04		
61 Tampieri & Hunt (1985)	Generic valleys Two dimensional	Topographic effects Diffusion	Stable									0.31-16
62 Arya & Gadiyaram (1986)	Genric hills Three dimensional	Topographic effects Diffusion	Neutral			4.00	0.13	3.00	0.12			
63 Lohmeyer & Plate (1986)	Generic hills Three dimensional	Topographic effects Windblown dusts Diffusion	Neutral				0.12		0.15			
64 Neff & Meroney (1987) CSU	Savannah River Lab. South Carolina	Topographic effects Diffusion	Neutral Stable Neutral Unstable		400 1000 1000 1000		 0.23 0.00		0.24 0.07 0.24 0.23	 0.003 0.024 0.040		D B D F
*65 Salmon, Teunissen, Mickle & Taylor (1988)	Kettle Hill Alberta, Canada	Topographic effects	Neutral	100	1000							

Table 2.2.1 (Concluded)

AUTHOR (DATE)	TOPOGRAPHIC SITE	PROBLEM STUDIED	TYPE OF AIRFLOW	MAXIMUM HEIGHT OF FEATURE (m)	LENGTH SCALE RATIO	delta/H	alpha	Similitude Criteria $Z_o/H \times 10^4$	u'/U_∞	u_*/U_∞	L_{ux}/H	RI or PG Category
66 Briggs, Thompson & Snyder (1989)	Valley Two dimensional	Topographic effects Diffusion	Neutral but stable valley air									
67 Gong & Ibbetson (1989)	Generic hills Two dimensional Three dimensional	Topographic effects on WECS	Neutral									
68 Finnigan, Raupach, Bradley & Aldis (1990)	Rough generic hill Two dimensional	Topographic effects	Neutral									
*69 Meroney & Neff (1989-90) CSU	Jurupa Mountains California	Topographic effects Diffusion	Neutral Stable	420	1000 2500	4.50 5.40	0.17 0.28	7.62 7.62	0.25 0.03-0.05	 0.0021		D E-F

* Field observations available

III. WIND FLOW OVER VEGETATIVE CANOPIES

As early as 1893, a German scientist, Metzger, investigated the effects of wind action on trees. Subsequently, a variety of studies have been made of the behavior of winds well inside and directly above a forest canopy (Bayton, 1963; Cooper, 1965; Denmead, 1964; Dolman, 1986; Fons, 1940; Grant, 1984; Huston, 1964; Poppendiek, 1949; Sadeh et al., 1982; Sauer et al., 1951; Tiren, 1927; Tourin and Shen, 1966; etc.). Some measurements are available for the variation of the wind at the edge of a forest (Iizuka, 1952; Leahey and Hansen, 1987; Reifsnyder, 1955). Much of this data is accumulated in periodically issued reviews and books (Geiger, 1956; Monteith, 1976; Raupauch and Thom, 1981; Forests, Weather and Climate, 1989).

Laboratory simulation of canopy flow in the wind tunnel has been used by the forest meteorologist in his efforts to understand the complex nature of flow generated by the tree--a permeable, random shaped, elastic object. Tiren, 1927, attempted to estimate crown drag from conifer branch-drag measurements made in a wind tunnel as part of his study of stem forms. Wind-breaks have been studied by models to determine soil erosion and blow-down characteristics (Hirata, 1953; Iizuka, 1956; Malina, 1941; Woodruff and Zingg, 1952). Others performed studies to characterize the transport of scalar products into, within and above vegetation (Plate and Quarishi, 1965, Kawatani and Meroney, 1968; Meroney, Kesic and Yamada, 1968). These studies were conducted to deduce the qualitative behavior of tree barriers for specific problems. The investigators apparently made no attempt to scale dynamically the character of a live tree except to compensate intuitively for shape and porosity.

To model completely the complex geometry and structural characteristics of a live tree is obviously not practical; however, measurements made on coniferous and deciduous trees in the wind tunnel and the field suggest that equivalence of drag and wake characteristics between model and prototype trees should be sufficient to study the general flow phenomenon (Lai, 1955; Meroney, 1968; Rayner, 1962; Sauer et al., 1951; Walshe and Fraser, 1963). Subsequently, a number of studies have been completed with greater attention to the flow characteristics of individual canopy elements (Hsi and Nath, 1968; Finnigan and Mulhearn, 1978; Kawatani and Meroney, 1970; Meroney, 1968, 1969; Raupach et al., 1980; Kawatani, 1971).

These field and laboratory measurements have provided a rough picture of a highly complex and turbulent flow field within the forest canopy. Measurements made behind small to medium specimens of spruce, juniper and pine trees reveal that linear wake growth exists behind all trees, that the wake shadows of individual branches disappear within 1-2 tree crown diameters downstream and that the velocity defect becomes Gaussian within 3-4 crown diameters. Drag measurements made on live trees indicate the drag coefficient, $C_d = F_{drag}/(\frac{1}{2}\rho U^2_{ref}A)$, may vary with wind speed from 1.0 - 0.3 **(Figure 3.0.1)**. These measurements indicate that the flow is inertially dominated (i.e., Reynolds number independent), but that self-streamlining of the tree at high velocities can reduce the effective cross-sectional area for the more flexible species. Measurements made within and above real and model trees reveal quite different flow characteristics for the under-canopy and above-canopy forest regions.

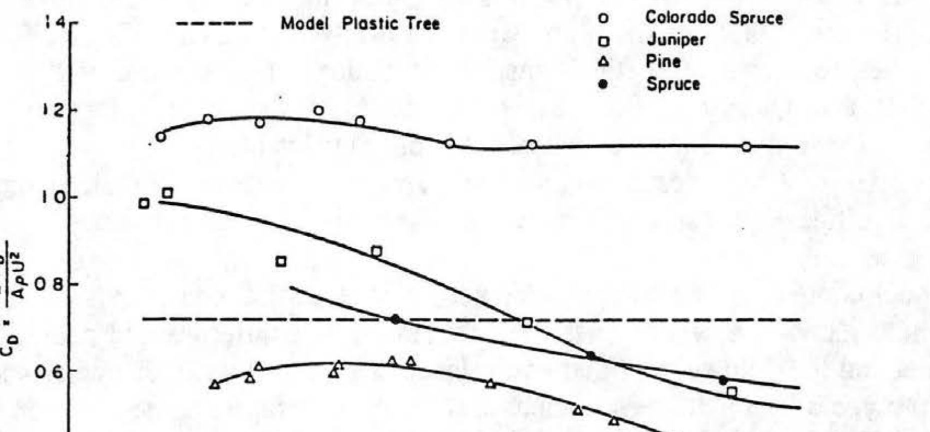

Figure 3.0.1 Drag coefficients of live and model trees: Dashed line (after Hsi and Nath, 1968); solid circles (after Rayner, 1962) (Meroney, 1968)

3.1 Flow Within and Downwind of an Individual Tree

Even a single tree can significantly reduce wind speeds and increase turbulence downwind of its stem and crown. Gross (1987) used a three-dimensional nonhydrostatic numerical model to investigate the air flow and turbulence around a single tree. For turbulence closure he used the Prandtl-Kolmogorov exchange coefficient and the Blackadar mixing length relation. The presence of the tree is simulated by an additional drag coefficient associated with tree foliage density or leaf area density. Time integrated solutions are obtained by the Adams-Bashforth scheme, centered differences are specified in space, and a fast Poisson solution solver is used to determine the pressure field.

Calculations were performed for both "cone" and "ball" shaped crown tree regions, with and without elevating trunks, and for neutral and stable air stratification. A tree porosity of 0.934 was assumed based on field measurements, calculations produced the anticipated wake deficits, turbulence excess, and a drag coefficient of 1.0 which are similar to individual tree values measured by Meroney (1968). All simulations show a reduction of wind speed inside the tree foliage, an accelerated flow over and around the tree and a wake region in the lee. The geometry of the crown seems to be the dominant factor. In a stable stratified atmosphere, the flow around the canopy is enhanced, while vertical motion is suppressed, and the strength and length of the reverse flow region behind the tree increases. These results agree well with available field and wind-tunnel experience.

Schematic tree shapes studied are shown in **Figure 3.1.1.** Crown heights considered were 16 m, crown diameters were 13 m, porosity was 0.93, trunk height varied from 0 to 6 m, and approach flow surface roughness was $z_o = 0.7$ cm. **Figure 3.1.2** displays centerline wake behavior behind a conifer shaped tree with no stem. **Figure 3.1.3** displays excess shear turbulence in the tree wake. **Figure 3.1.4** describes the streamlines of the horizontal airflow 1 m above the ground. The streamline pattern clearly shows the divergence around the tree and the recirculation region behind the tree. **Figure 3.1.5** compares mean velocities in the wake of ball and cone shaped trees elevated on 3 m trunk height.

Persistent strong winds can result in the deformation and growth distortion of individual trees. Hewson et al. (1979) describe methods which permit one to characterize persistent wind directions and speed. **Figure 3.1.6** provides sketches of tree deformation, the associated Griggs-Putnam index number, and the persistent wind velocity that is likely to produce such deformation.

The superposition of individual tree wakes result in the under-forest and above-forest velocity features found in extensive areas of forests or woods. The initial growth of wake deficits and the subsequent decay at greater downwind distances are characteristics of both individual tree and forest measurements.

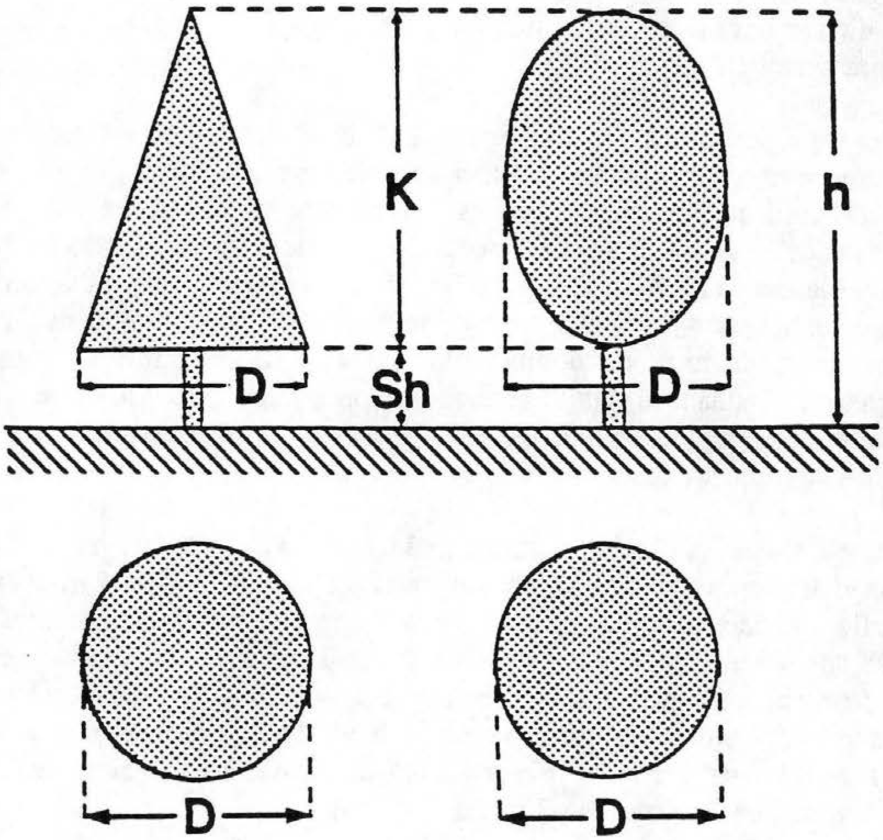

Figure 3.1.1 Geometry of idealized trees for numerical calculations. (Gross, 1987)

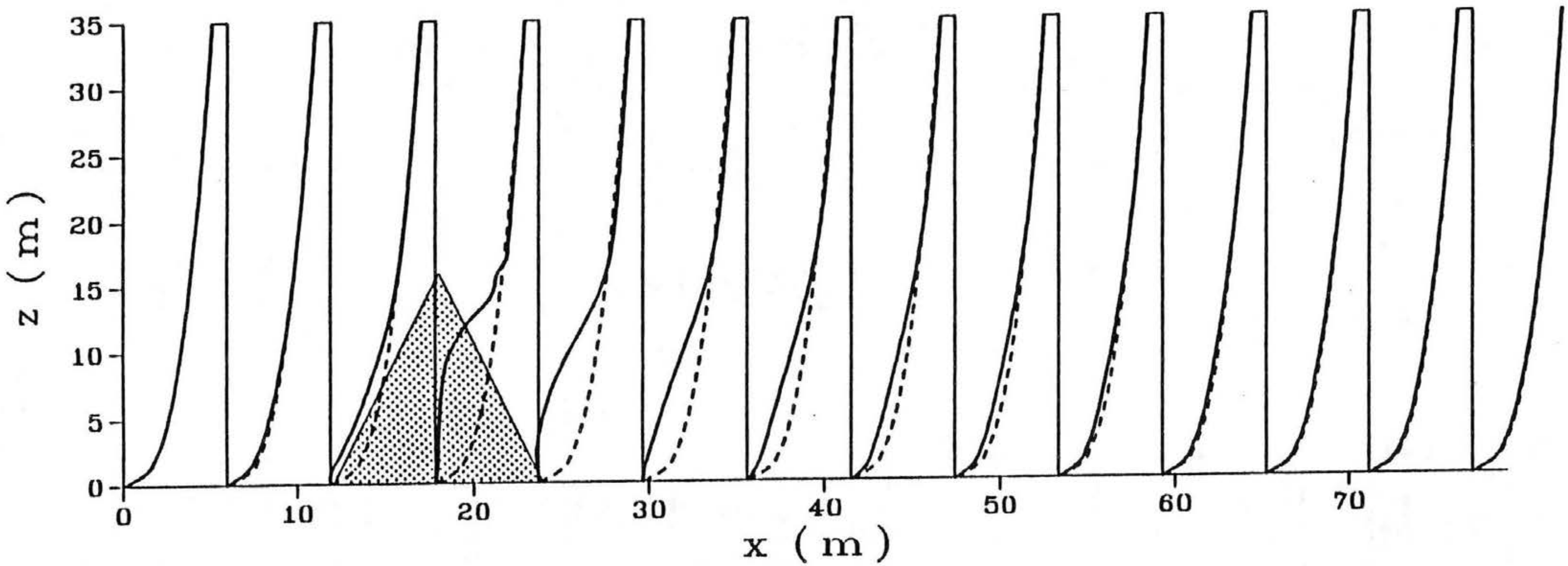

Figure 3.1.2 Vertical profiles of u at different point along the symmetry axis. The dotted line shows the undisturbed profile of the inflow boundary. (Gross, 1987)

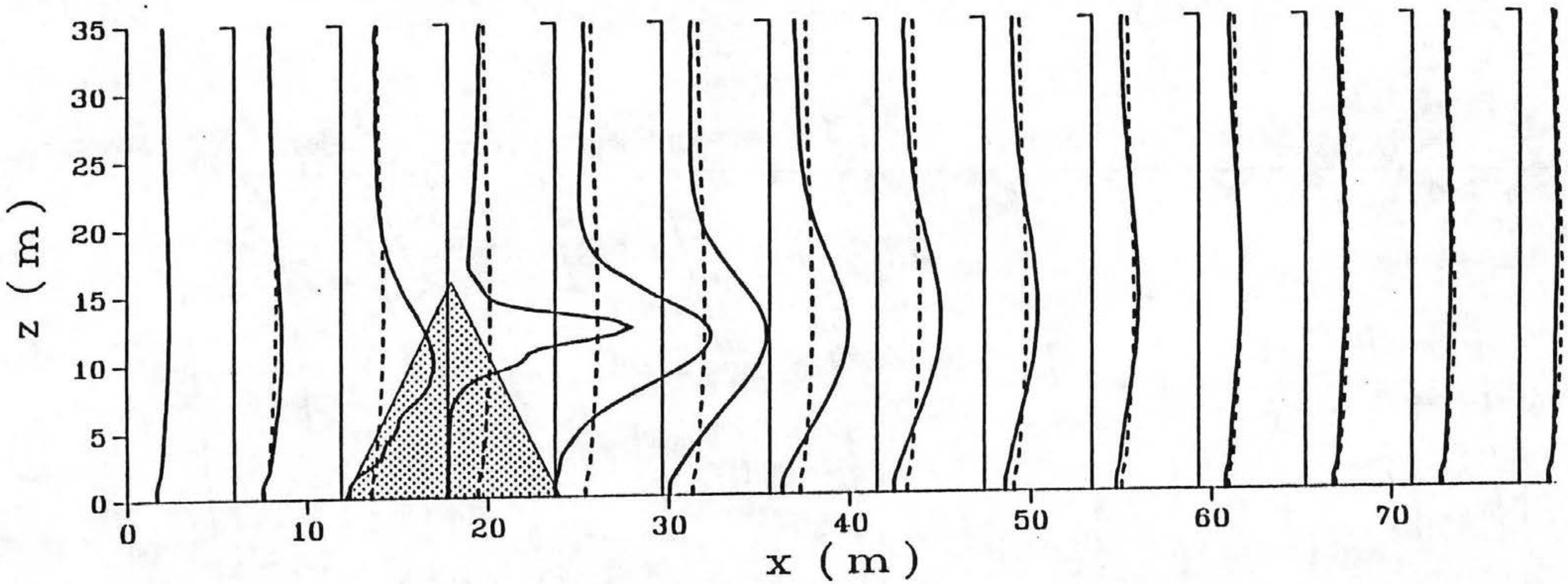

Figure 3.1.3 Vertical profiles of shear stress, σ, at different points along the symmetry axis. The dotted line shows the reference (inflow) value. (Gross, 1987)

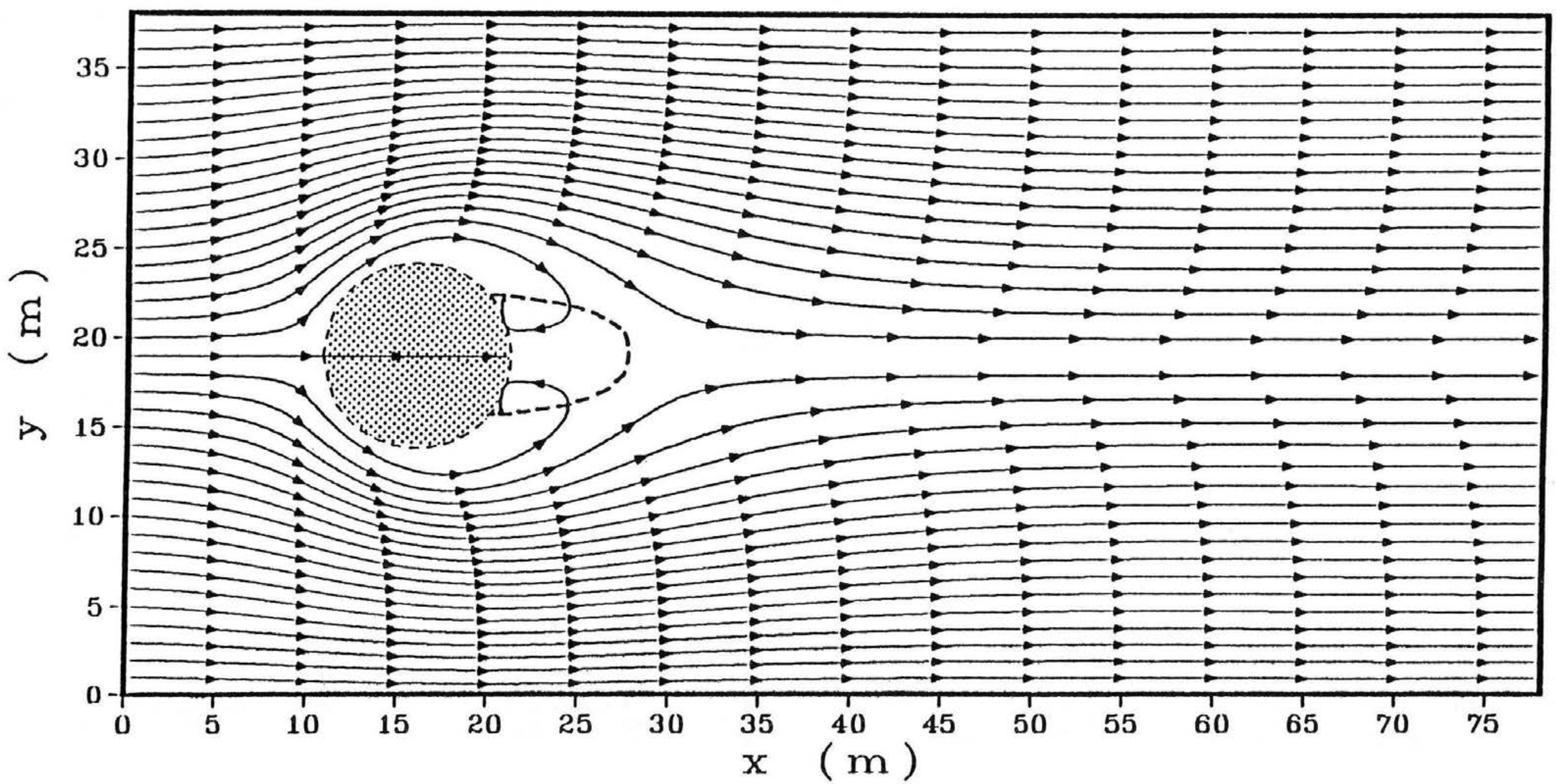

Figure 3.1.4 Streamlines of the horizontal airflow for 1 m above the ground. The contour of the tree is dotted, the dashed line indicates cases where $u < 0$. (Gross, 1987)

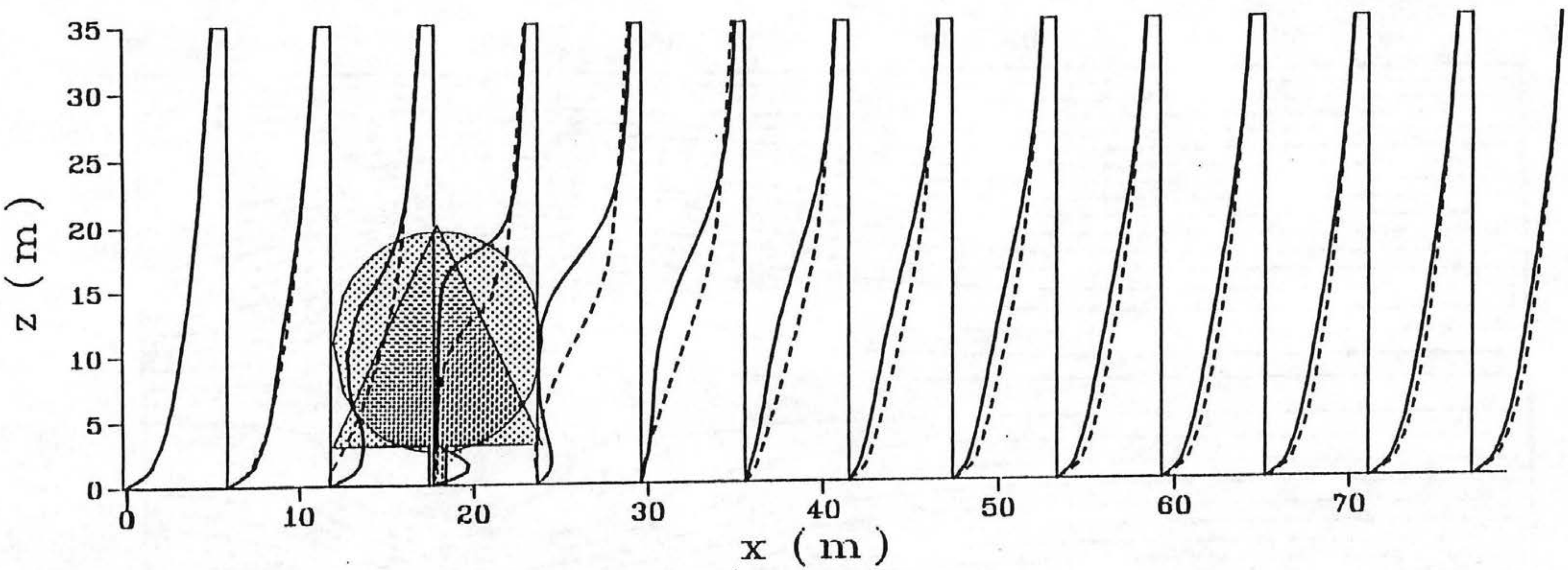

Figure 3.1.5 Vertical profiles of u at different points along the symmetry axis (———— ball-tree, - - - cone-tree) (Gross, 1987)

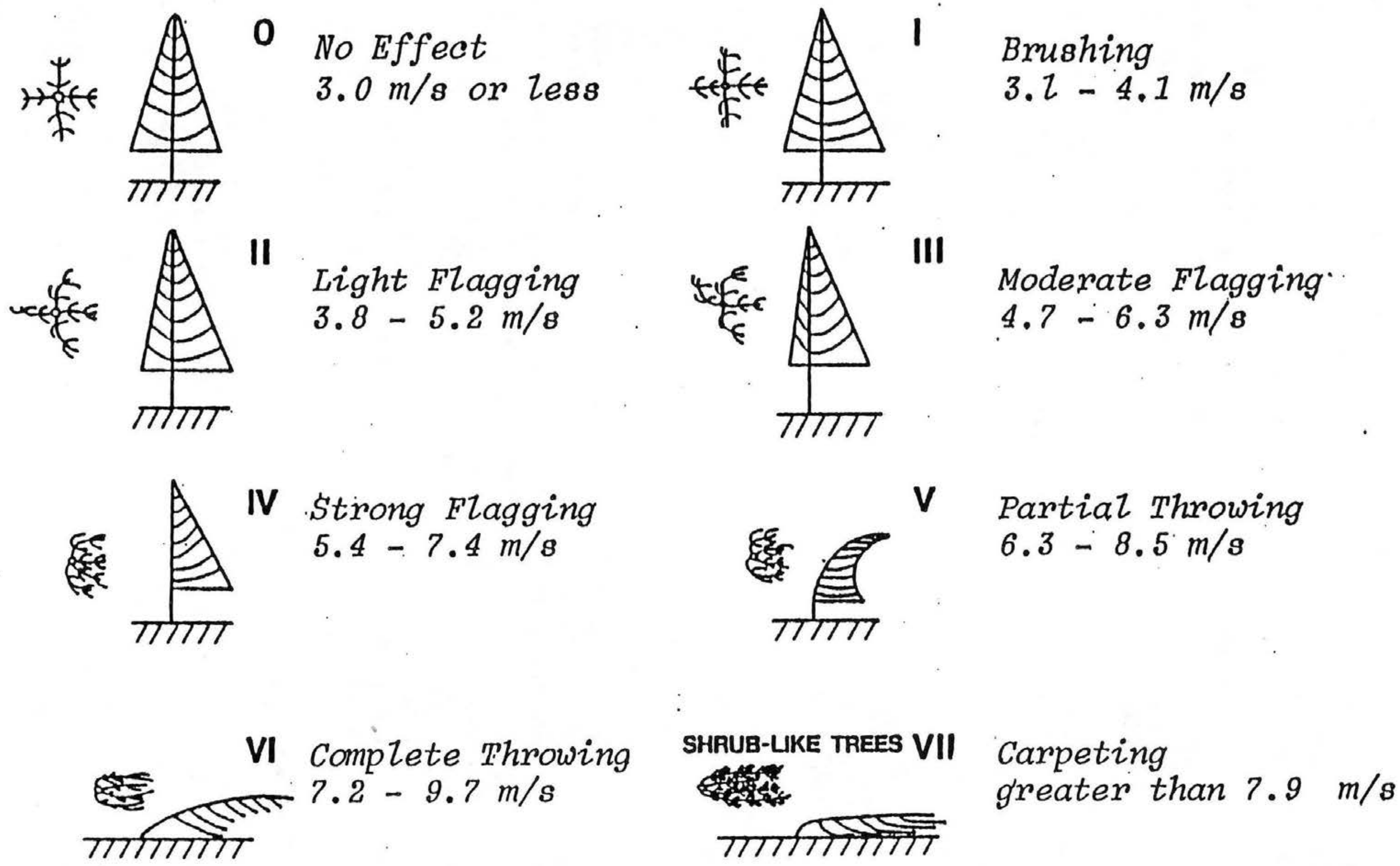

Figure 3.1.6 Wind deformation and the wind velocity that may produce that deformation. (Hewson *et al.*, 1979)

3.2 Under-canopy Forest Flow Field

The presence of tree trunks, branches, stems, and leaves (or needles) in a forest produces a barrier to air flow caused by form drag and skin friction which reduces the under-forest flow velocities substantially compared with wind speeds which occur above the canopy. Surface layer streamlines are displaced vertically, flow beneath the canopy is driven by shear from the flow above the canopy, and maximum winds occur at the top of the average height of the vegetation. Turbulence levels beneath the canopy may be similar to those found at ground level over small roughness surfaces (5-15%), but are significantly less than those which can occur in the strong shear which occurs above the canopy roof (20-40%). **Figures 3.2.1, 3.2.2a and 3.2.2b** display typical mean velocity and turbulence profiles found within and above forest canopies.

Different profiles have been proposed using first order closure models which specify a simple eddy diffusivity, K, and a drag coefficient, C_d, to describe that portion of the mean wind profile which exists beneath the forest ceiling for constant foliage distribution:

$$u/u_h = [(\sinh \beta\xi)/\sinh \beta]^{1/2} \qquad \text{(Cowan, 1968),} \quad [3.2.1]$$

$$u/u_h = \exp[-\beta(1 - \xi)/2] \qquad \text{(Inoue, 1963; Cionco, 1965), and} \quad [3.2.2]$$

$$u/u_h = [\cosh \beta\xi)/\cosh \beta]^{1/2} \qquad \text{(Massman, 1987),} \quad [3.2.3]$$

where $\xi = z/h$, u_h is the mean horizontal wind speed at the top of the canopy, h; and β is a maximum value of the foliage area density and the extinction coefficient given by:

$$\beta = [2C_d\, LAI/(\sigma\mu)]^{1/2}, \qquad [3.2.4]$$

which is a combination of the drag coefficient, C_d , the leaf-area-index, LAI, a measure of foliage distribution, σ, and a normalized eddy diffusivity, $\mu = K/hu = K_h/hu_h$. Only the expression proposed by Massman is consistent with the frequently observed zero wind gradient within the lower region of the canopy. Other authors have produced velocity profiles for non-constant foliage distributions and using higher order turbulence closure (Albini, 1981). **Figure 3.2.3** compares the three equations shown above for a $C_dLAI = 0.6$ and constant foliage distributions which result in β values of 4 and 6. For a constant foliage distribution the extinction coefficient β varies from 0 to 10.0 as the function C_dLAI varies from 0.0 to 1.0. Each of the under canopy velocity profiles may be associated with a companion shear stress distribution which looks similar to the velocity distribution. Typical under-canopy measurements made in a Ponderosa pine forest are shown in **Figure 3.2.4** .

Once a velocity distribution model is specified it is possible to solve by iteration for shear stand drag coefficient, $C_f = 2(u_*/u_h)^2$, displacement height, d, and surface roughness, z_o, parameters useful to characterize above canopy flow dynamics as functions of C_dLAI and foliage

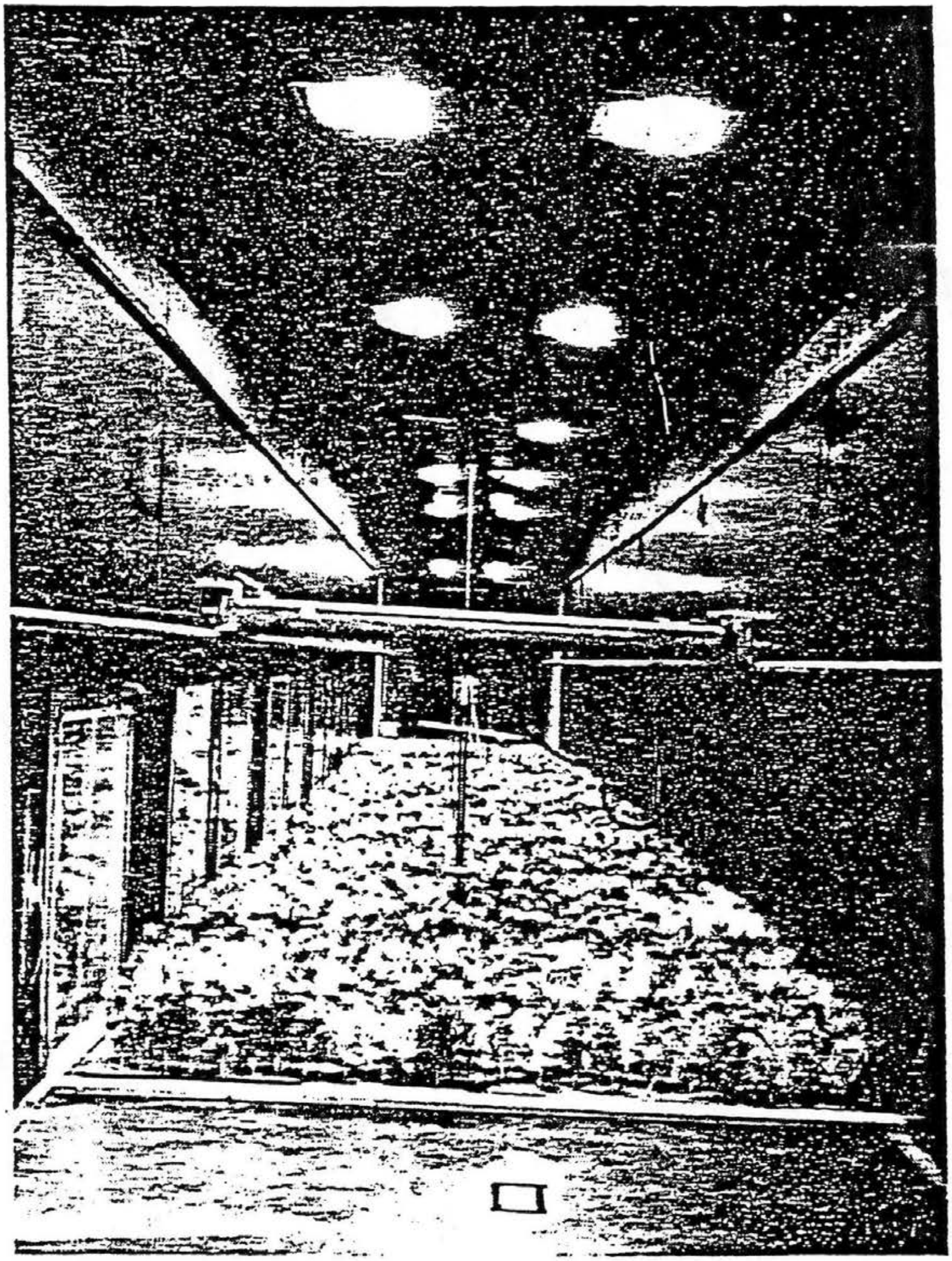

Figure 3.2.1 Meteorological wind tunnel at Colorado State University and artificial tree canopy. (Meroney, 1968)

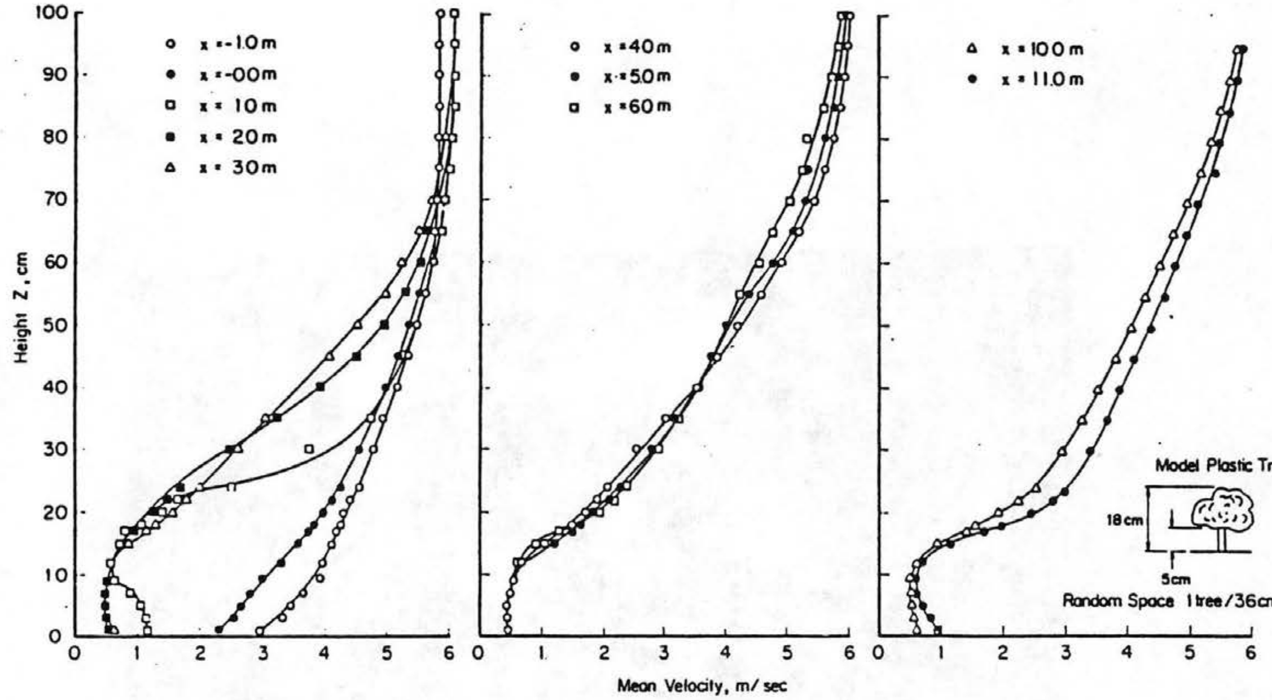

Figure 3.2.2 Velocity profiles in and above model forest canopy (Meroney, 1968)

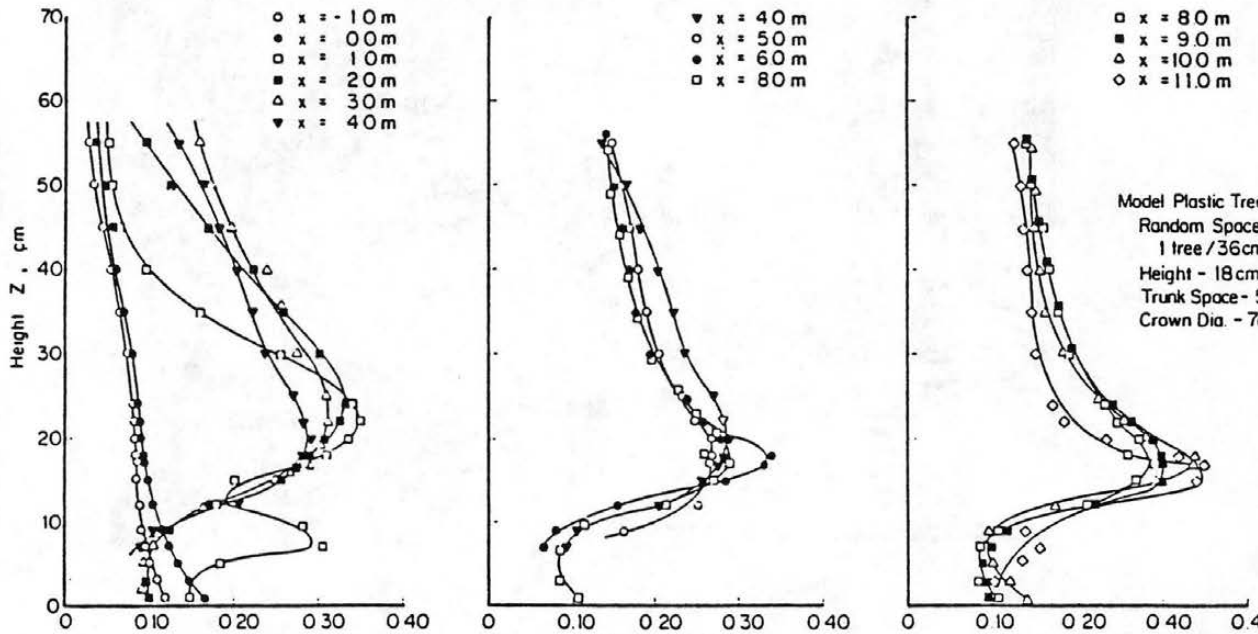

Figure 3.2.2 Longitudinal turbulent intensity for model forest canopy. (Meroney, 1968)

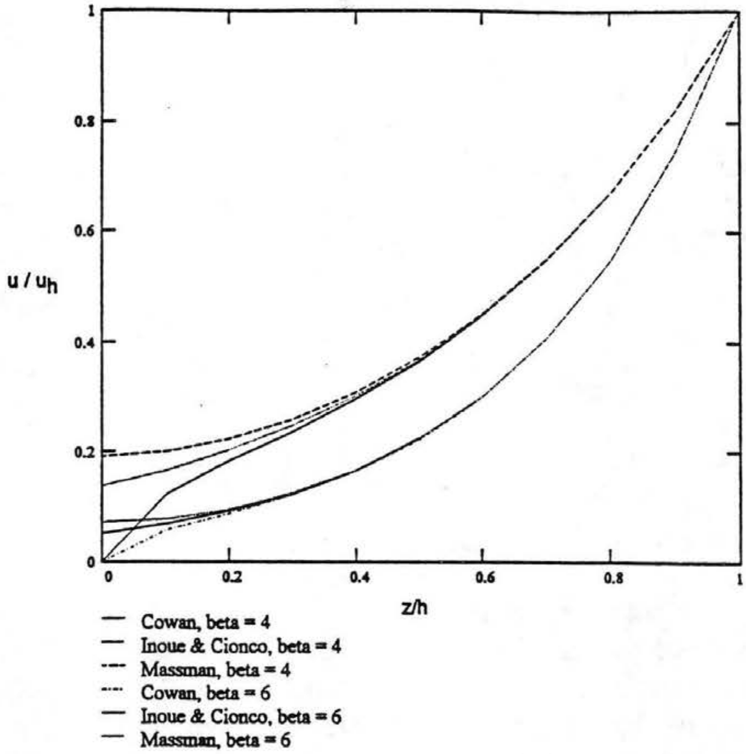

Figure 3.2.3 Under-forest canopy mean velocity profiles for expressions developed by Cowan, 1968; Inoue, 1953, and Cionco, 1965; and Massman, 1987.

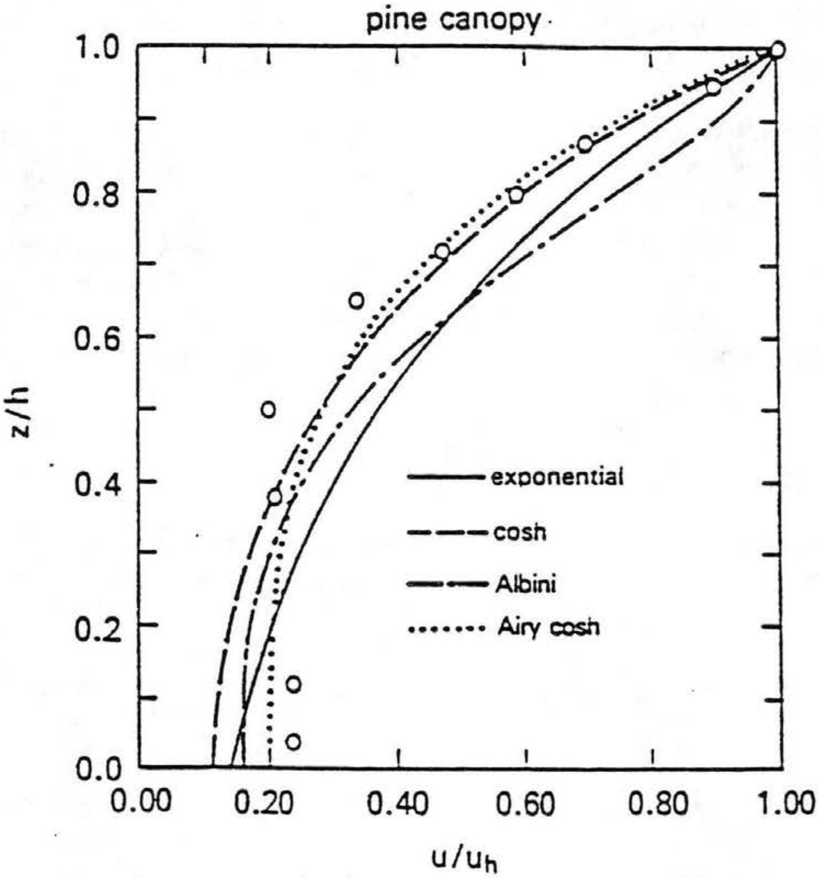

Figure 3.2.4 Optimal fits of observed wind profile for a Ponderosa pine canopy. Observations are denoted by circles from Raupach and Thom (1981).(Massman, 1987)

structure. Massman (1987) concludes that C_dLAI values from 0.25 to 0.50 characterize most full foliage canopies. Over this range almost any under-canopy model gives results very close to the following expressions:

$$0.10 < z_o/h < 0.13, \qquad [3.2.5a]$$

$$0.67 < d/h < 0.75, \text{ and} \qquad [3.2.5b]$$

$$0.17 < C_f < 0.20. \qquad [3.2.5c]$$

3.3 Above-canopy Forest Flow Field

The atmospheric boundary layer (ABL) is that portion of the atmosphere where surface drag due to the motion of the air relative to the ground modifies synoptic-scale motions caused by horizontal pressure gradients, Coriolis forces, and buoyancy. The depth of the ABL is highly variable (50 to 2000 m), but it generally increases with proximity to the equator, with wind speed, and as the earth surface roughens, but it decreases at night, and is strongly modified by thermal winds, inversions, and stratification. Counihan (1975) reviewed all adiabatic ABL data taken between 1880 to 1972. For high wind speeds (U_{10} > 5-7 ms^{-1}) Counihan recommended 600 m as a reasonable average boundary layer depth for both rural and urban cases independent of wind speed and roughness.

The lowest 10% of the atmospheric boundary layer is called the surface layer. It is characterized by the sharpest variations of wind speed, temperature, humidity, and turbulence characteristics with height. Counihan (1975) concluded the surface (or constant flux) layer would be about 100 m deep during adiabatic conditions. In diabetic (stratified) situations the surface layer depth is about equal to the absolute value of the Monin Obukhov length, $L_{mo} = -Tu_*^3/(\kappa g\, w't')$. For a summary of surface layer behavior for both neutral and stratified flows combined with both smooth and rough surfaces see Meroney (1986) or Panofsky and Dutton (1984).

3.3.1 *Logarithmic velocity profile models*

Within the surface layer the mean wind-speed profile is commonly described by logarithmic expressions. For situations when stratification has only a minor influence a modified logarithmic law has been proposed:

$$u(z) = (u_*/\kappa) \ln_e [(z - d + z_o)/z_o], \qquad [3.3.1]$$

where $u_* = (\tau/\rho)^{1/2}$ is the surface friction velocity, d is the zero-plane displacement, κ is Von Karman's shear layer constant, and z_o is the surface roughness. The displacement thickness, d, is important for tall roughness elements such as agricultural crops, forests, and cities. When the roughness elements are short, such that z_o < 0.2 m, one can set d = 0. The parameters can be determined from representative field measurements or models such as were discussed in Section 2.2. Fitting an expression which permits three free parameters to field measurements of wind speed in agricultural canopies is not trivial. It is not uncommon for some least-square fitting routines to produce negative displacement heights--which is, of course, inappropriate.

No exact definition of high roughness has been offered, but roughness of a height exceeding 10% of the surface layer is generally viewed as high roughness. (Alternatively, whenever the logarithmic expression with d set equal to zero fails to fit measured wind distributions, the full expression may be justified.) Generally, the von Karman universal constant κ is assumed equal to 0.4 based on extensive experimental study of fully developed turbulent flow through pipes and its relationship to the Kolmogorov dissipation constant. Some experimentalists treat the constant as another free parameter to improve curve fit to data; hence, values ranging from 0.15 to 0.5 have been recorded. Nonetheless, it is customary to accept the initial value of 0.4 unless there are very persuasive arguments to do otherwise.

Some derivations of the logarithmic expression depend upon the assumption that shear stress is nearly constant with height above the surface. Matching of inner and outer similarity solutions to a boundary layer demonstrates, however, that such an assumption is not really necessary to the existence of a region which depends logarithmically on displacement above a ground plane. Nonetheless, the shear stress may be expected to vary substantially above the canopy roof; hence, it would be best to associate the friction velocity with the average drag produced by the wind on the forest. In order to avoid negative displacement height values it is customary to assume the von Karman constant $\kappa = 0.4$, to prespecify displacement height as some fraction of the forest canopy depth (say $d = 0.67$ h) and to solve for friction velocity and surface roughness height by fitting the modified logarithmic expression to measured data.

The effective values of the parameters may vary locally when the surface roughness is non-homogeneous. A non-homogeneous surface occurs when the ground surface changes from water to land, urban to rural, or cleared to forested. Such changes may make it appear that effective surface roughness, surface friction, and displacement height vary with height within the velocity profile. This aspect of the flow field will be discussed further in another section.

Surface roughness estimates have been estimated by many scientists for flow data obtained over different agricultural crops and forests. There is a wide variance in results even for flow over the same surface. Frequently experimentalist fail to obtain data above the wake region of individual roughness elements ($z > 1.5h$); sometimes the data are taken during non-neutral conditions; and often upwind nonhomogenuities distort the measured profiles. Several sets of tabulated data are available prepared by Sutton (1949), Priestly (1959), Davenport, 1960, Counihan (1975), Simiu and Scanlan (1978) and Snyder (1981). See Table 3.3.1 for a summary of such estimates.

Jaeger (1965) recorded wind speed measurements over a ten year period over stands of Scotch pine located in southern Germany as they grew from 3 to 8 m height. He made estimates of the variation in u_*, z_o, d, β (Deacon parameter), and Richardson number, Ri, from wind and

Table 3.3.1 Table of roughness length data

Surface Type	Sutton (1949) (1953) Geiger (1950)	Priestly (1959)	Davenport (1965)	Counihan (1975)	Simiu & Scanlon (1978) & Snyder (1981)
Open sea	0.002-0.05		0.024-0.34	0.001-2	0.0003[a]-0.5[b]
Ice	0.001			0.001-2	
Smooth mud flat	0.001	0.001		0.001-2	
Sand	0.03-0.1	0.03			0.01-0.1
Snow on grass Snow on prairie	0.02 0.3	0.005 0.1		0.001-2	
Mown grass, 1 cm 3 cm 4.5 cm	0.1-0.2 0.7-2.0	0.2 0.7 1.7-2.4			0.1-1
Flat open country	2.0-3.0		1.75-6.5		
Low grass, steppe	1.0-4.0			0.1-20	1-4
Fallow field	5.0			0.1-20	2-3
High grass	3.0-9.0	3.7-9		0.1-20	4-10
Paletto	3.0-14.0				10-30
Pine forest (h = 15 m, d = 12 m)	20.0			100-150	90-100
Outskirts of towns, suburbs			20-90	100-150	20-40[c]
Centers of towns					35-45[c]
Centers of large cities			125-550		60-80[c]

[a] Wind speed at 10 m above sea surface equals 1.5 m/sec

[b] Wind speed at 10 m above sea surface is greater than 15 m/sec

[c] These values are exceptionally small

temperature data collected from meteorological towers placed within the forest stand. He found that the following correlations described the measurements:

$d = 0.63$ h, regression coefficient, $r = 0.73$-0.93; [3.3.2a]

$z_o = 0.174\ h + 0.227$, regression coefficient, $r = 0.44$; and [3.3.2b]

$u_* = (0.027\ h + 0.062)\ U_{9.6m} + b$, regression coefficient, $r = 0.84$. [3.3.2c]

The expressions for d and z_o are seen to be similar to those derived from examination of under-canopy flows. However, the correlation for z_o is rather poor, and in a personal communication Massman suggested universal expressions for friction velocity are not reliable.

Figure 3.3.1 display the variation of above-canopy wind speeds for typical forest values of displacement height and roughness where $d = 0.67$ h, $z_o = 0.125$ h, and $u_* = u(h) \int (C_f/2) = 0.316u(h)$. Given these dimensions one finds that the modified logarithmic law becomes:

$$u(z) = 0.316(u(h)/\kappa)\ln_e[8z/h - 4.34]. \qquad [3.3.3]$$

Of course, this expression is only approximate, since it assumes independence from drag coefficient, leaf area index, and foliage distribution variations. The expression should not be applied below $z = 1.5$ h.

Estimates of surface drag, roughness and displacement are also sought for use in meso-scale models where combinations of hilly terrain and vegetation can produce an "effective surface roughness" for flows above moderate heights. As noted by Taylor et al. (1989), "momentum transfer at the earth's surface can be considered as part 'skin friction' and part 'form drag.'" One can associate the surface shear stress as that portion of the drag associated with the roughness elements whose dimensions are of order size10 m or less. These include vegetation, buildings and small topographic features like ditches and embankments. The 'form drag' component of the momentum transfer is associated with terrain averaged over the minimum numerical grid used. In addition in stratified flow one may have 'wave drag' associated with waves propagating away from larger features (mountains, hills, and valleys). Taylor et al. used mixing length , turbulent kinetic energy closure, and Reynolds stress closure models to predict velocity profiles over sinusoidal roughness covered with different size surface roughness.. Logarithmic models were then fit to these profiles. A regression on the various calculations agrees with the following semi-empirical expression:

$$\ln[z_o^{eff}/z_o] = 3.5(ak)^2\ln[\lambda/z_o], \qquad [3.3.4]$$

where the surface terrain profile fits $z_s = a\cos(kx)$ and $k = 2\pi/\lambda$. This equation works well for $ak < 0.2$ and not bad at $ak = 0.3$ at which separation probably occurs over the hill crests. Thus, for cases with $\lambda = 500$ m and surface roughnesses, z_o , of 0.01, 0.1 and 1 m, the postulated maximum values of z_o^{eff} will be 2.37, 7.4, and 23.1 m, respectively.

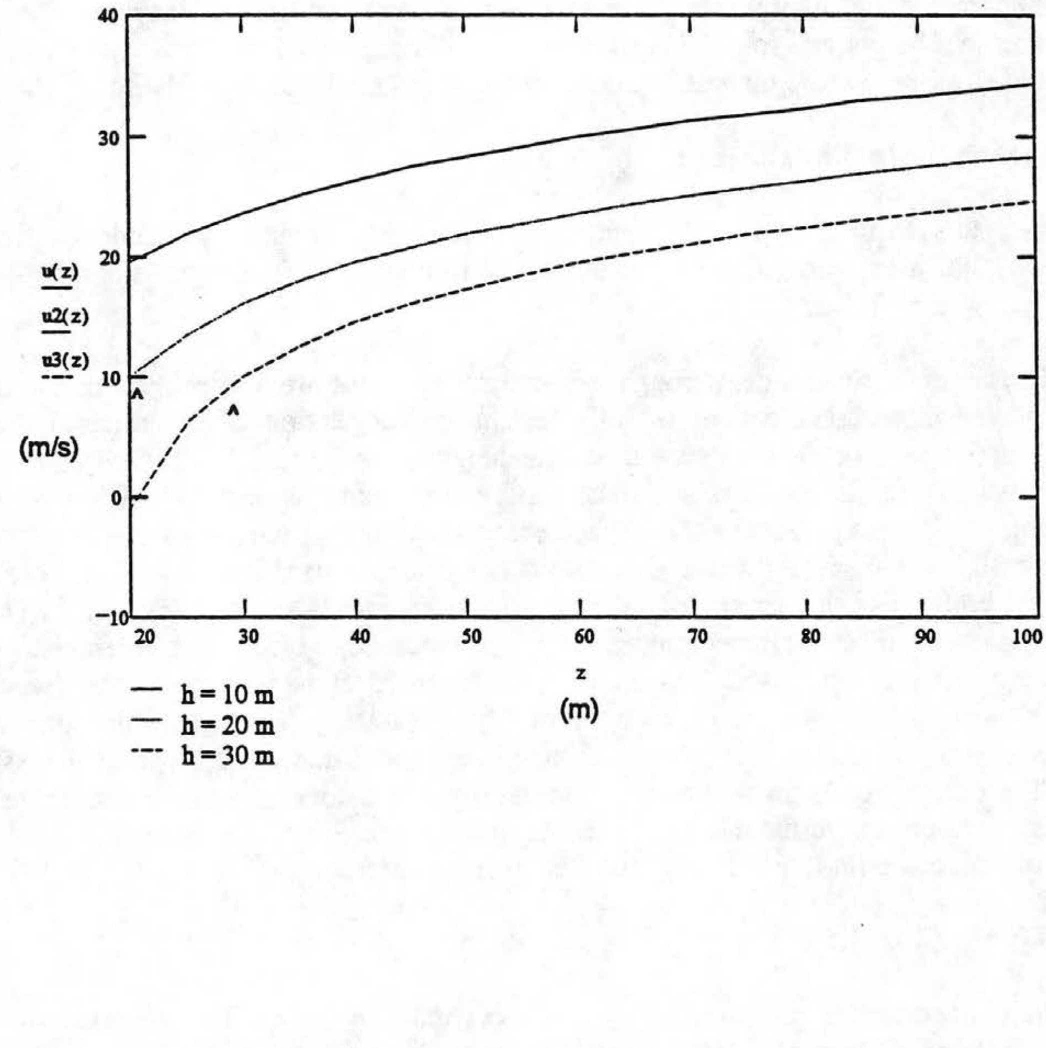

Figure 3.3.1 Above canopy wind profiles for various average forest canopy heights when d = 0.63 h, z_o = 0.125 h, and u_* = 0.316 u(h).

Grant and Mason (1990) reported the results of tether balloon measurements of flow over forest covered complex terrain in southern Wales, U.K. They wished to characterize the effective roughness over areas of the order of 100 km^2. Grant and Mason also generated wind data numerically with a two-dimensional, nonhydrostatic model using a second-order turbulence closure scheme over a hypothetical sinusoidal terrain with horizontal wave length of 2000 m and a peak-to-trough height of H = 300 m. The model was used to verify field measurements and expressions relating terrain undulation and local vegetative roughness.

Grant and Mason also propose that total drag is composed of two parts, a form drag term which represents the drag due to the main orographic elements and a shear stress term due to small scale features such as vegetation. They combined a shear stress estimate at the half-height of the terrain undulation, H/2, with the widely used formulae suggested by Lettau in 1969, $z_o/H = CA/S$, where A is the silhouette area of the roughness elements located in a horizontal area, S. The final expression is:

$$\ln^2 [H/(2z_o^{eff})] = \kappa^2 /\{0.5\ DA/S + \kappa^2/\ln^2[H/(2z_{o1})]\}, \qquad [3.3.5]$$

where D is a drag coefficient. For sinusoidal terrain, D = 0.3. The silhouette area should be averaged over about 12 km. As noted in **Figure 3.3.2** the effective roughness length, z_o^{eff}/H, is found to increase from 0.003 to 0.05 as A/S increases from 0 to 0.2.

3.3.2 *Power-law velocity profile models*

In an alternative empirical approach to describe the wind variation with height the velocity variation is described by a simple power law of elevation. It is widely used in describing the wind shear in the atmospheric surface and internal boundary layers in view of its simple format and engineering expediency. The general form of the expression used is:

$$u(z)/u_{ref} = (z/z_{ref})^{\alpha}, \qquad [3.3.6]$$

where u_{ref} is the reference wind at a reference height z_{ref}, and α is the power law index (exponent). The effect of turbulence induced by the surface roughness upon the wind shear is accounted for by the magnitude of the power law index, whose magnitude is normally smaller than unity but larger than zero. Often the power law index is determined empirically by fitting the expression above to measured data; however, it is also possible to match the magnitude of predicted velocity and shear at a specified height and relate the power law index, α, to logarithmic parameters (z_o, d, and L_{mo}). For neutral flow the expression is simply:

$$\alpha = z_m /[(z_m - d + z_o)(\ln_e [(z_m - d + z_o)/z_o)/z_o], \qquad [3.3.7]$$

where z_m is the matching or mid-height over which both profiles are presumed valid.

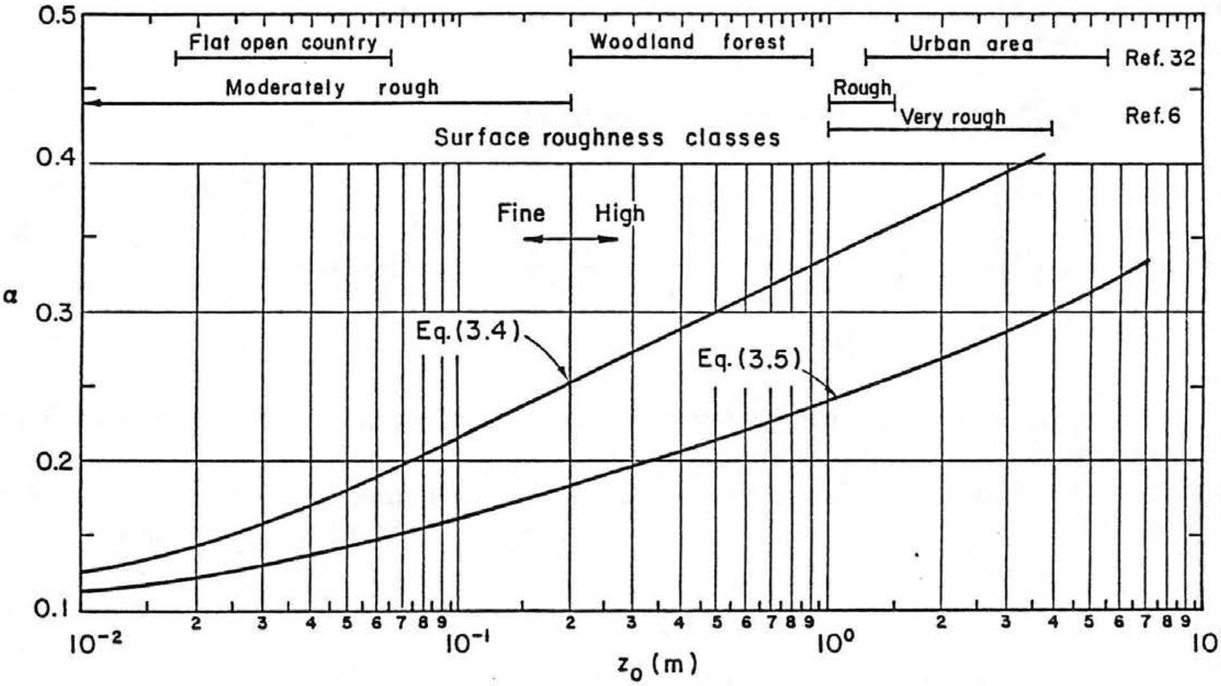

Figure 3.3.3 Variation of the power-law index with increasing roughness and corresponding roughness classes for Equations 3.3.8 and 3.3.9. (Baron, 1981)

Empirical expressions which relate power law index and surface roughness length have been proposed by Counihan (1975) and Baron (1982). Counihan's expression was developed by fitting logarithmic and modified logarithmic profiles to 70 different sites over data to a height of 100 m:

$$\alpha = 0.096 \log_{10} [z_o] + 0.016 (\log_{10} [z_o])^2 + 0.24, \qquad [3.3.8]$$

for $0.001 \leq z_o \leq 5$. Baron fit a similar relationship to the nomogram proposed by Davenport (1975) such that:

$$\alpha = 0.125 \log_{10} [z_o] + 0.0004/z_o + 0.336, \qquad [3.3.9]$$

for a roughness range $0.01 \leq z_o(m) \leq 5.5$. However, the two functions produce significantly different estimates. For example Baron's expression produces power index values 17 to 38% greater than Counihan's expression over the range from smooth to rough roughness **(See Figure 3.3.3)** . This variation may simply be the result of using different data sets, the influence of stratification, or it may be that displacement height was not considered in a similar manner for the two data sets.

Baron (1982) examined a wide cross-section of field and laboratory data and created **Figures 3.3.4 and 3.3.5** which predict power law index in terms of element, h, and roughness height, z_o , respectively. Given canopy heights, h, ranging from 10 to 30 m in depth, associated roughness length, z_o , varying from 1.25 to 3.75 m in size, one expects power law index, α, to vary from 0.45 to 0.52.

3.4 Wind Flow Near Clearings, Clearcuts, and Forest Edges

When airflow passes from a cleared area into a forest winds initially penetrate into the canopy space, but then the streamlines are lifted upward to the canopy roof **(See Figures 3.2.1 and 3.2.2)**. The penetration distance among the trunk space in the canopy understory may persist for 5 to 10 tree heights. Subsequently the wind rises above a recirculation region and re-enters the forest about 20h from the windward forest edge. Cionco (1982) sketched how such entrance flows might look from the perspective of smoke plumes on the battle field in **Figures 3.4.1 and 3.4.2.** But when the airflow passes from a forest canopy to a cleared area the under canopy flow begins to accelerate as much as 5 tree heights upwind as streamlines move toward the ground, but downwind of the forest edge low-level winds may require substantial distance to readjust to the new smaller surface roughness. **(See Figures 3.4.3a and 3.4.3b). Figure 3.4.4** from Meroney (1968) displays the effect of initial wind penetration at the windward forest edge, the low speed recirculating zone, and the flow acceleration before the downstream forest edge on canopy drag. Models which predict wind speed profile variations after changes in roughness are discussed in Section 3.5.

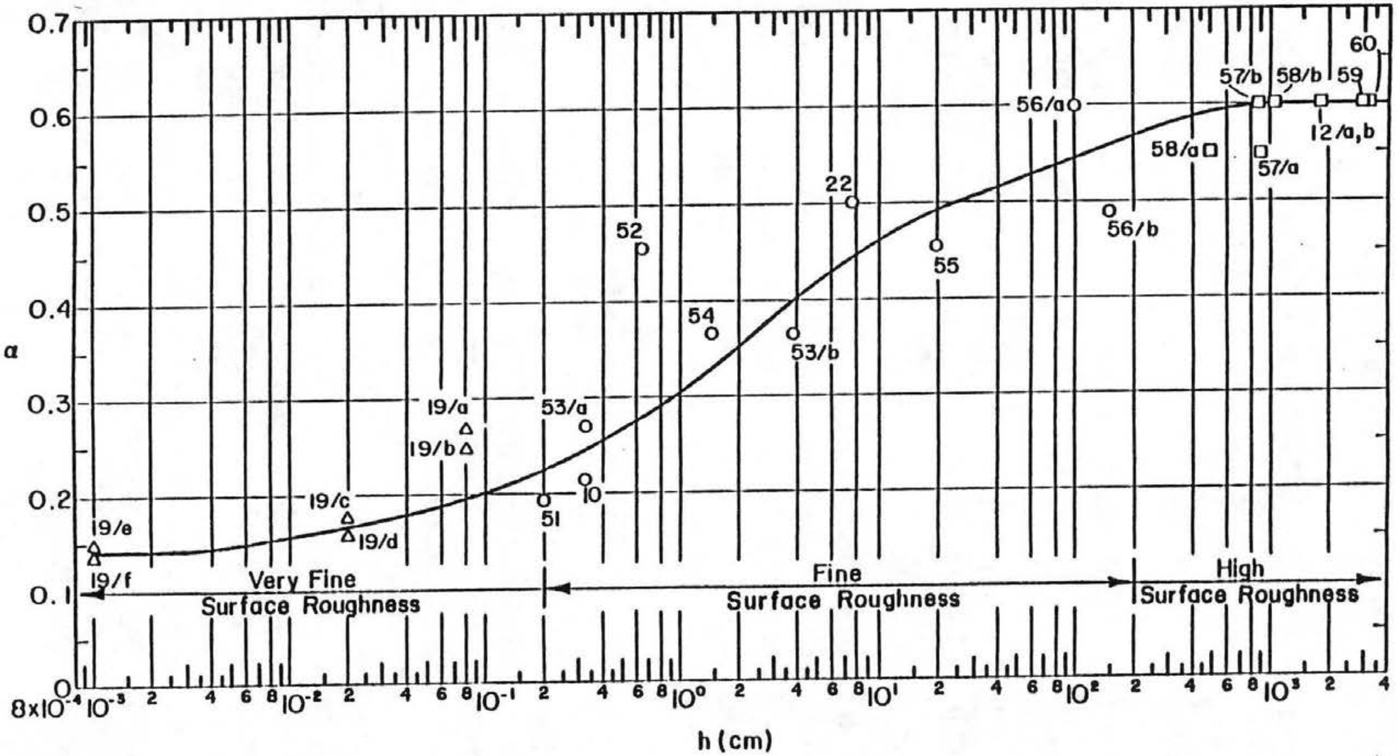

Figure 3.3.4 Variation of the power-law index with increasing height of roughness elements. (Baron, 1981)

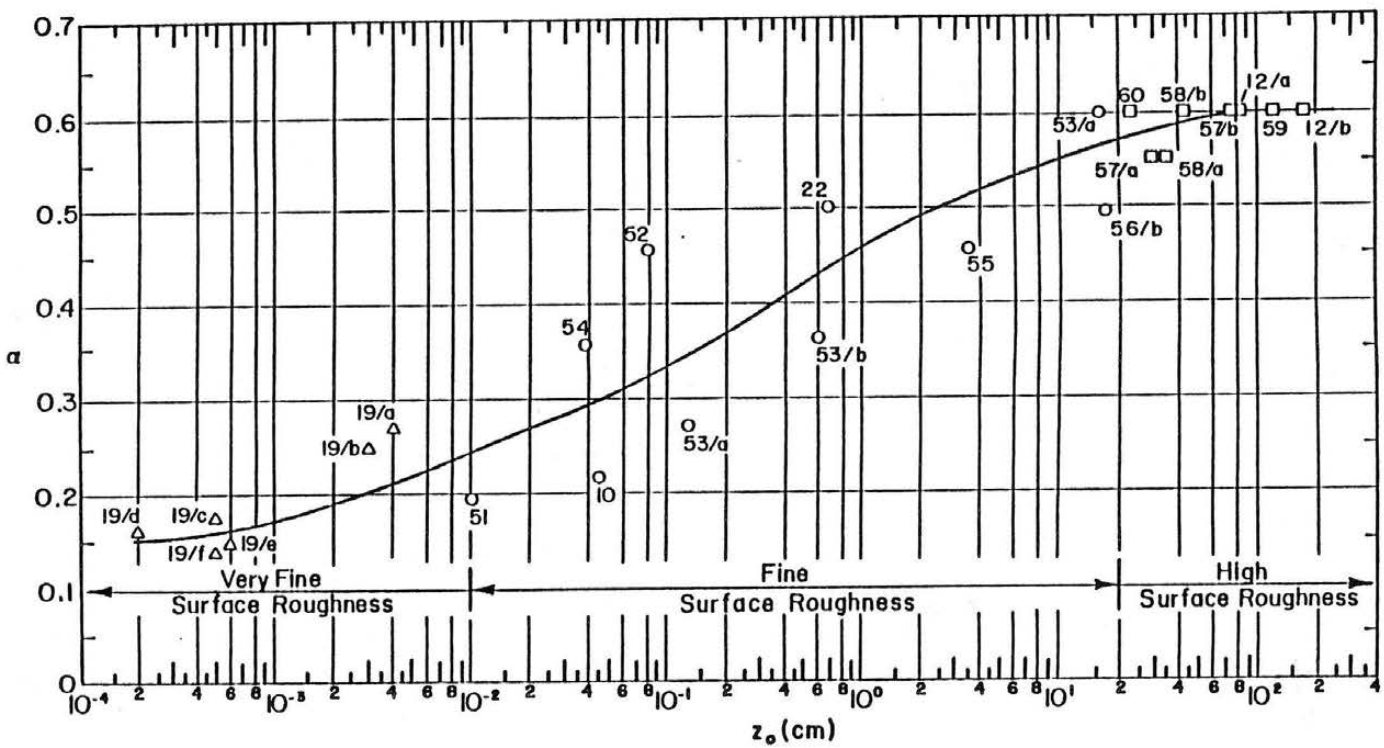

Figure 3.3.5 Variation of the power-law index with increasing roughness length. (Baron, 1981)

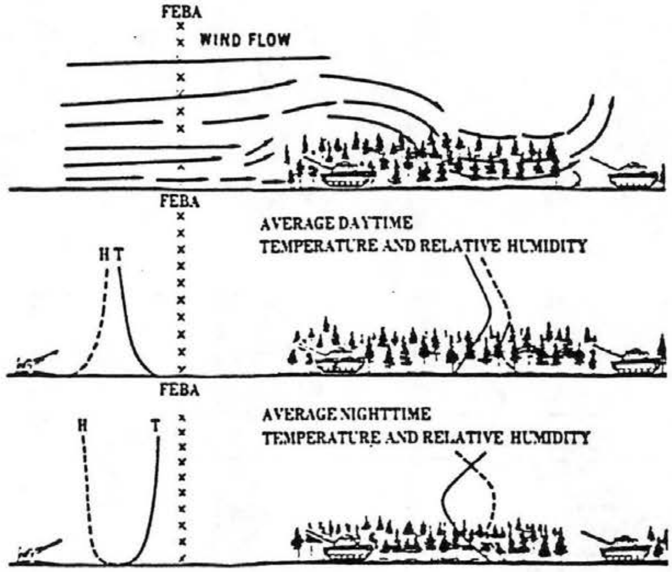

Figure 3.4.1 Windflow and vertical profiles of meteorological variables within and above a forest. (Cionco, 1982)

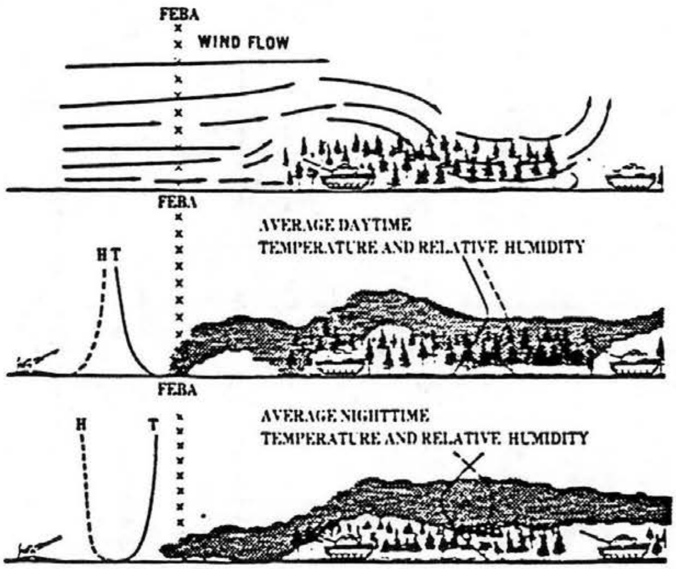

Figure 3.4.2 Figure 3.4.1 with smoke plumes deployed. (Cionco, 1982)

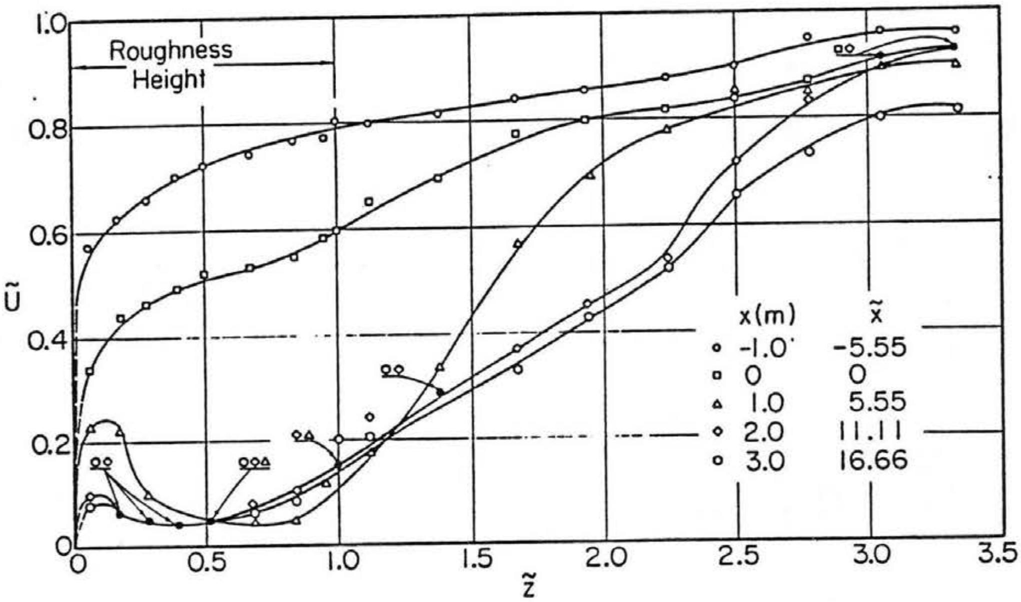

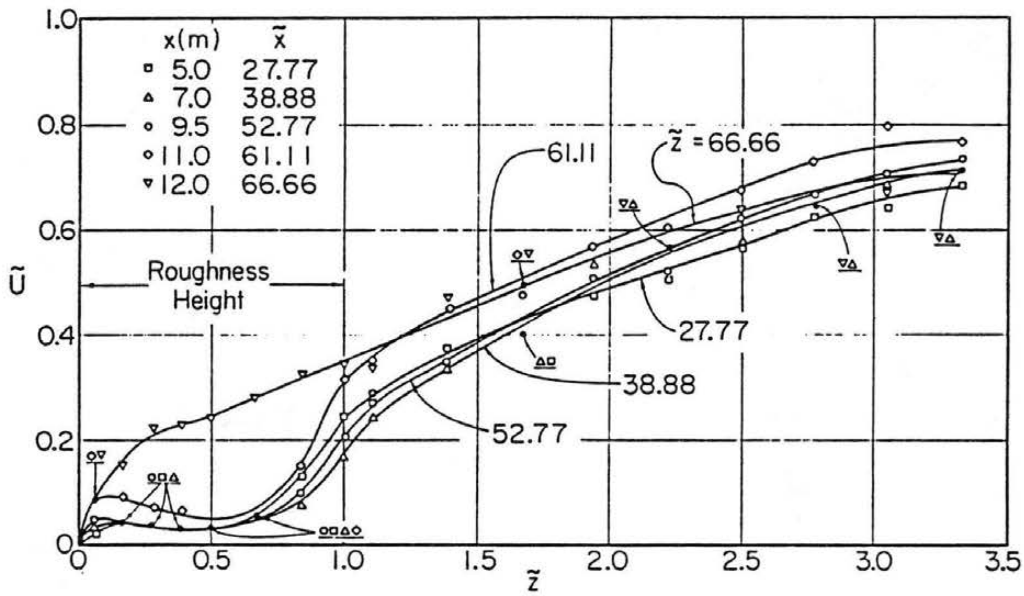

Figure 3.4.3 Mean velocity profiles within and above the roughness. (Kawatani, 1971)

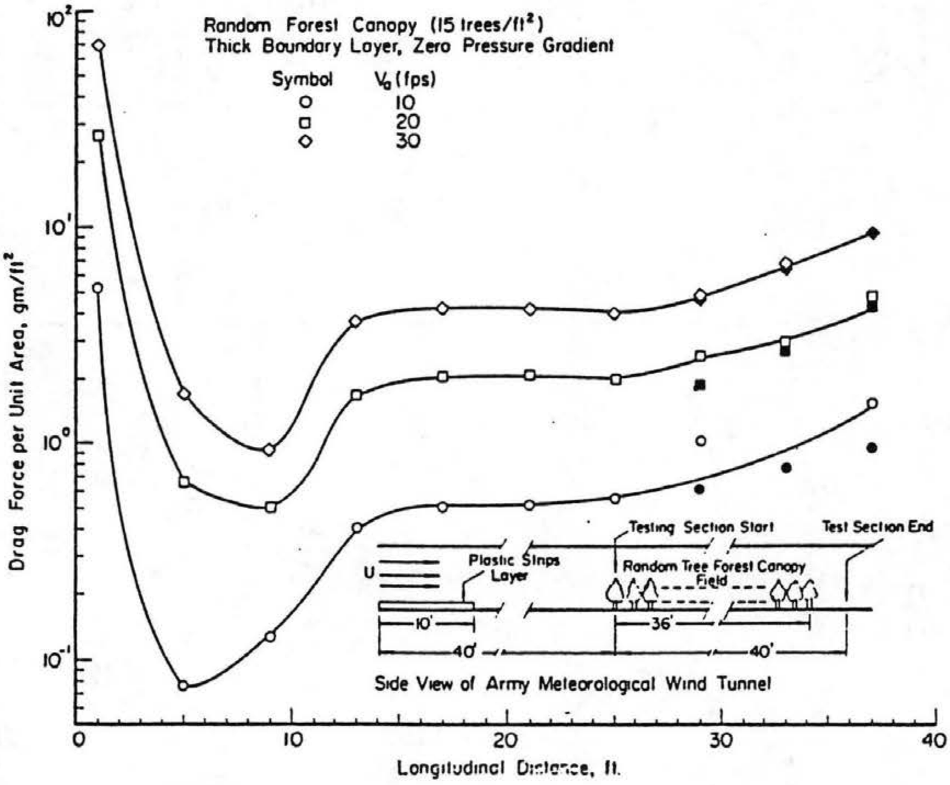

Figure 3.4.4 Shear plate drag for model forest canopy (Meroney, 1968)

Eimern (1964) considered the aerodynamics of shelterbelts and summarized the influence of density, shape, surface roughness, thermal stratification, wind angle and tree arrangement on downstream wind speed, turbulence, soil moisture, etc.. Simplified insights from this material were incorporated into **Table 3.4.1** by Meroney (1977). Behind porous objects the velocity defect generally persists twice as far downwind; however, the turbulence intensity excess is diminished. Maximum length of shelter will occur for long shelterbelts of near 50% permeability., 30% velocity defect may still exist at 0.5h for x/h > 50. The wind will return to its undisturbed condition in about half the distance if the shelter belt is only twice as long as it is high. Wind approaching a shelter belt at an angle increases its effective porosity, decreases the shelter, and increases turbulence excess.

The micrometeorology of shelter belts and forest edges are reviewed by McNaughton (1989). He notes that although extensive studies have been performed downstream of thin shelterbelts the effects of forest edges have received far less attention. Indeed with respect to wind flow downstream of forest edges he notes that "this discussion is more a summary of our ignorance than of our knowledge." There are similarities as well as differences between flow downstream of thin shelterbelts and forest edges. The foliage density of the forest canopy replaces the porosity used for narrow shelterbelts. Upwind profiles must be characterized by the upwind forest roughness, displacement height, forest friction velocity, and foliage density.

McNaughton sought a comparison to the flow over a forest canopy edge and the flow that occurs when a boundary layer passes over a solid backward facing step. For solid steps a recirculating eddy occurs of downwind extent of about 6 h. But permeability often allows the wind to penetrate the forest upwind of the forest edge. For example, wind tunnel experiments performed over plastic model trees (Meroney, 1968) notice winds increased above and within the canopy over the last 10 h. In coniferous forests researchers detect upwind penetration over several heights upwind, but in a denser foliage other researchers see little penetration at all. Nonetheless, little evidence exists to support the presence of a recirculating eddy downwind of the forest edge. The flow velocities and surface shear appear to adjust to the immediate absence of the forest edge by 20 h; however, the wind continues to accelerate over a longer distance as a deeper layer of the atmosphere adjusts to the change of surface roughness.

There appear to be very few measurements of actual winds made above and below forest canopies near clearings or forest edges. Leahey and Hansen (1987) report measurements made on meteorological tower located 60 m from a 0.5 km^2 in a forest in Alberta, Canada. Trees were primarily pine and aspen with heights ranging from 18 to 24 m growing on flat terrain. Measurements were taken at 10 and 20 m levels on a 24 m tower using a Gill U-V-W anemometer. They identified strong horizontal jets of air and large vertical velocities during unstable conditions, but rather normal conditions under stable stratification. Winds in excess of 6 ms^{-1} occurred about 15% of the time. Their measurements suggest that clearing a ridge may produce strong convergence toward ridge lines, which could modify ridge top conditions.

Table 3.4.1 Wake behavior of buildings, trees and shelterbelts (Meroney, 1977)

DISTANCE DOWNWIND $\frac{X}{H}$	5			10			20		
Flow Variable	-ΔV%	-ΔP%	T%	-ΔV%	-ΔP%	T%	-ΔV%	-ΔP%	T%
STRUCTURES (wind directed at face at 90°, measurement at H)									
W/H = 4	36	74	25	14	36	7	5	14	1
= 3	24	56	15	11	29	5	4	12	.5
= 1	11	29	4	5	14	1	2	6	-
= 0.33	2.5	7.3	2.5	1.3	4	.75	-	-	-
= 0.25	2.0	6.	2.5	1.0	3	.50	-	-	-
INDIVIDUAL TREE									
Dense Foilage (Colorado Blue Spruce)	20	49	-	9	17	-	4	13	-
Thin Foilage (Pines)	16	41	-	7	18	-	3	8	-
SHELTER BELTS (Wind measured at - H)									
Porosity 0%	40	78	18	15	39	18	3	9	15
Loose Foilage 20%	80	99	9	40	78	-	12	32	-
Dense Foilage 40%	70	97	34	55	90	-	20	49	-
Typical Height of Wake Flow Region	1.5			2.0			3.0		

$$\Delta V\% = \frac{U_o - U}{U_o} \times 100$$

$$\Delta T\% = \frac{\overline{U'}}{U} - \left(\frac{\overline{U'}}{U}\right)_o \times 100$$

$$\Delta P\% = \frac{U^3 - U_o^3}{U_o^3} \times 100$$

Fowler et. al. (1987) examined the effects of shelterwood cutting (30-percent canopy removal) and clearcutting clearings from 0.8 to 8.5 ha on climatic variables of the High Ridge Evaluation Area within the Umatilla National Forest in northeastern Oregon **(Figure 3.4.5).** Areas were harvested in 1976 after nine years of prelogging calibration.

The authors concluded that hydrological effects of the cuttings were surprisingly small, but wind passage and velocities increased dramatically with removal of the forest cover. **Figure 3.4.6** presents data from roughly equivalent 11-month periods during pretreatment and posttreatment. Data presented are for a height of 20 and 6 m above the grounds in watersheds 4 and 1. Little change was noted for the watershed 4, height 20 m case, but at all other locations the wind speeds increased substantially in all classes! One should note that the weather station in watershed 4 was within the uncut area; whereas the station in watershed 1 was in the middle of a clearcut region. Indeed winds at 6 m height in watershed 1 exceeded winds at 20 m height in watershed 4!

Elliott and Barnard (1990a, 1990b) discuss a field experiment to examine the effect of scattered groves of trees and grass on the variability of wind speed and turbulence at the Goodnoe Hills, WA, wind-power site. Two permanent towers and seven portable towers were used. The two permanent towers measured wind at heights from 15 to 107 m and 15 to 59 m above the ground. Wind speed measurements were taken from nine bivane anemometers sampled every second and averaged every minute. The site contains a broad ridge on which the MOD-2 turbines were installed. Terrain is gently sloping to the west and north, but drops abruptly off to the Columbia River Gorge to the south. Vegetation is mostly low sage brush and grass and scattered groves of scrub oak, western juniper and ponderosa pine.

Two towers were about 200-300 m downwind of a grove of 10-18 m high trees at which 20-30 percent reductions of wind speed and a 2-3 times increase in turbulence were measured at a height of 32 m. Wind gusts also increased at 30 m, but by heights of 60 m or distances of 500 m downwind tree effects were considerably reduced (25 to 50 h).

Wind-mill wake and non-wake data sets were created to determine effects of vegetation. Turbulence intensity was defined as the standard deviation of 1-s samples for a 1-min period referenced to a 1-min average speed. The relative arrangement of tree groves and meteorological towers are shown in **Figure 3.4.7**. Towers 6 and 7 evidenced the strongest forest induced wind effects as shown on **Figures 3.4.8 and 3.4.9.** These figures portray the relative wind behavior for different wind directions and associated grove fetch distances. The data set includes situations when the turbines were not operating (NO WAKE) as well as cases when the wind turbine wakes may also interact with the meteorological instruments for some orientations (WAKE). Smaller wake effects are noted for met towers 1, 2, and 9 which are further from the tree stands. Velocities decrease about 10% and turbulence increases no more than 20-30% at these towers.

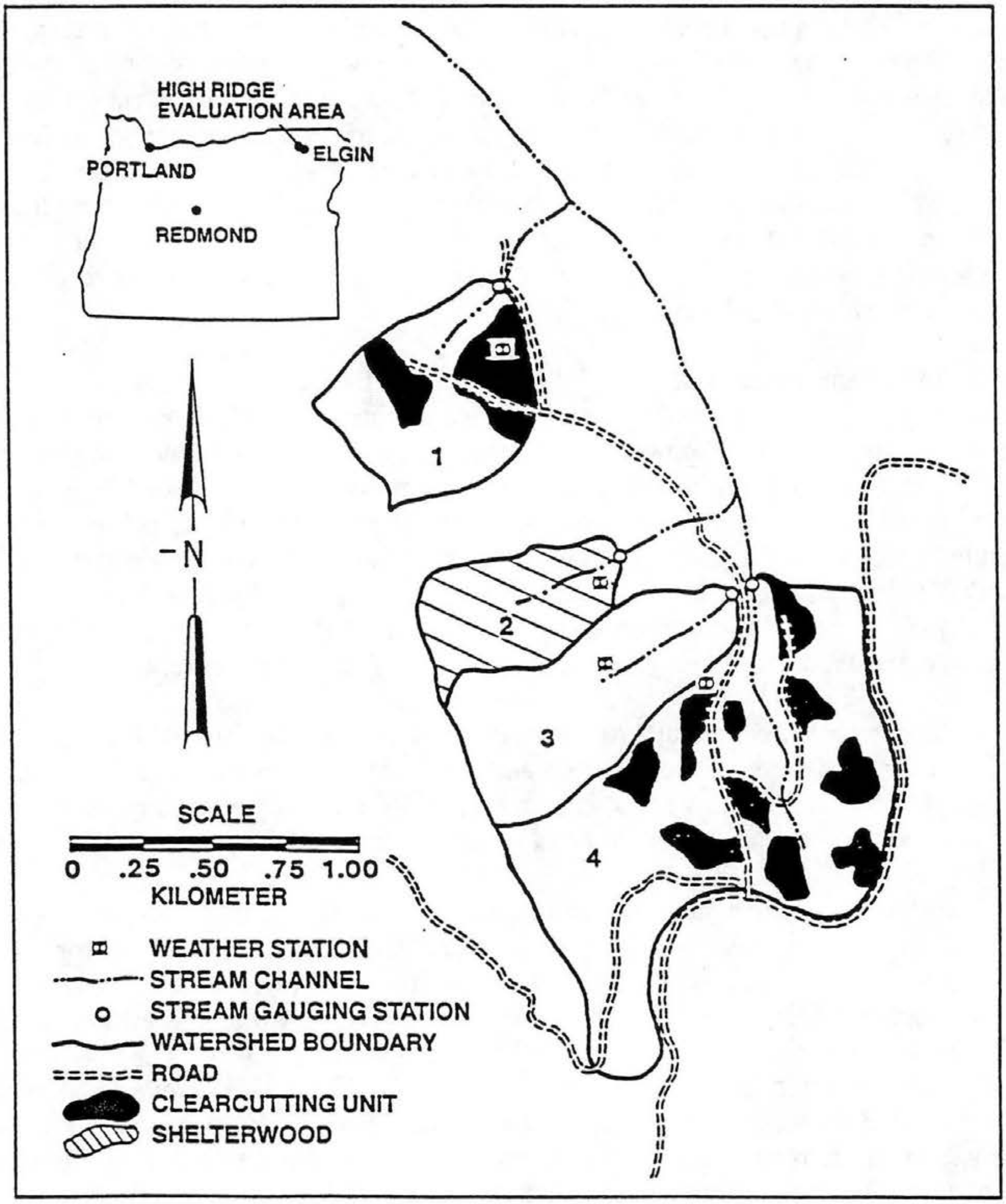

Figure 3.4.5 Study areas in the High Ridge Evaluation Area, Umatilla National Forest, Oregon. (Fowler, *et al.*, 1987)

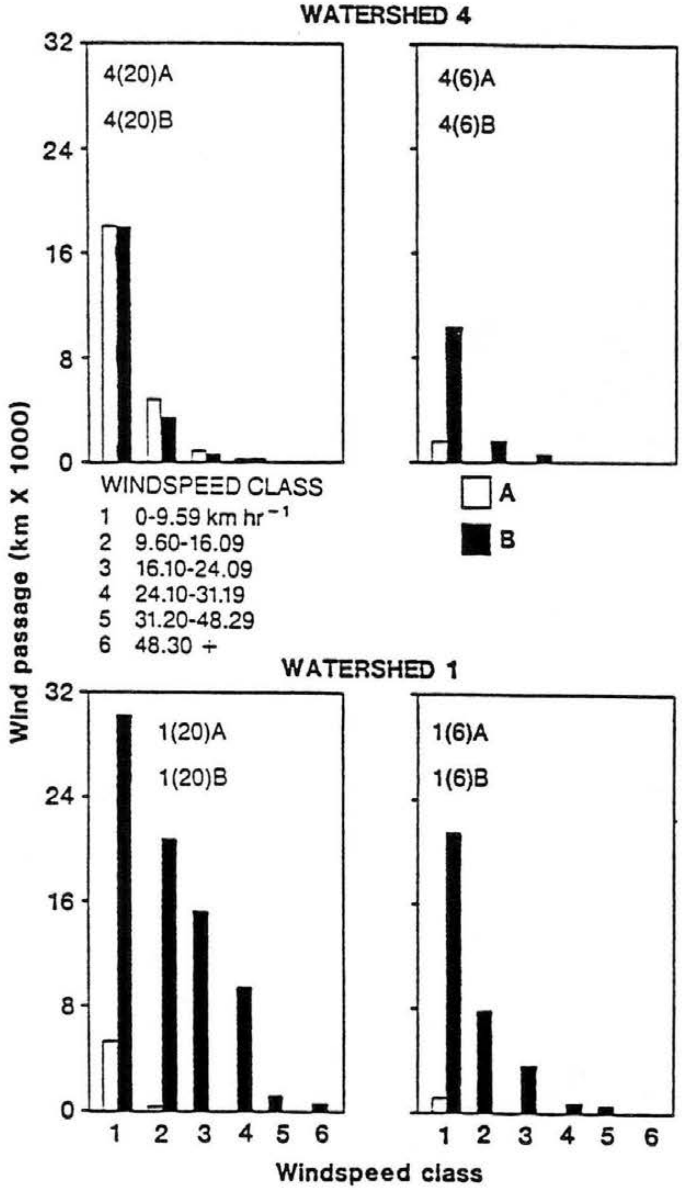

Figure 3.4.6 Wind passage at 6 and 20m in watersheds 4 and 1 during two 11 month periods--one before and one after treatment. (Fowler *et al.*, 1987)

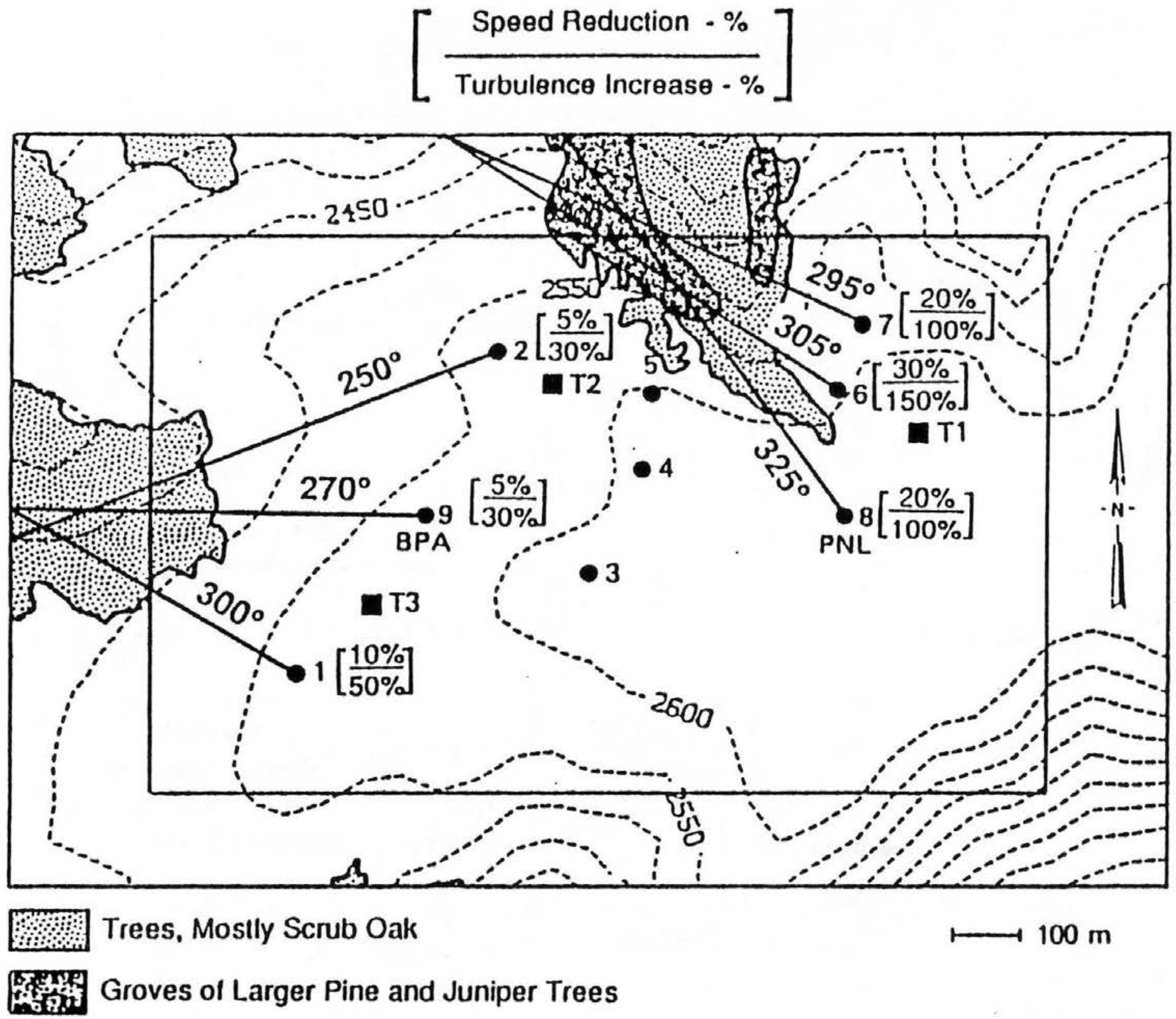

Figure 3.4.7 Goodnoe Hills, WA. Radials show directions to towers. Percent reduction in wind speed and increase in turbulence [ΔU%/Δu'%] (Elliott and Barnard, 1990)

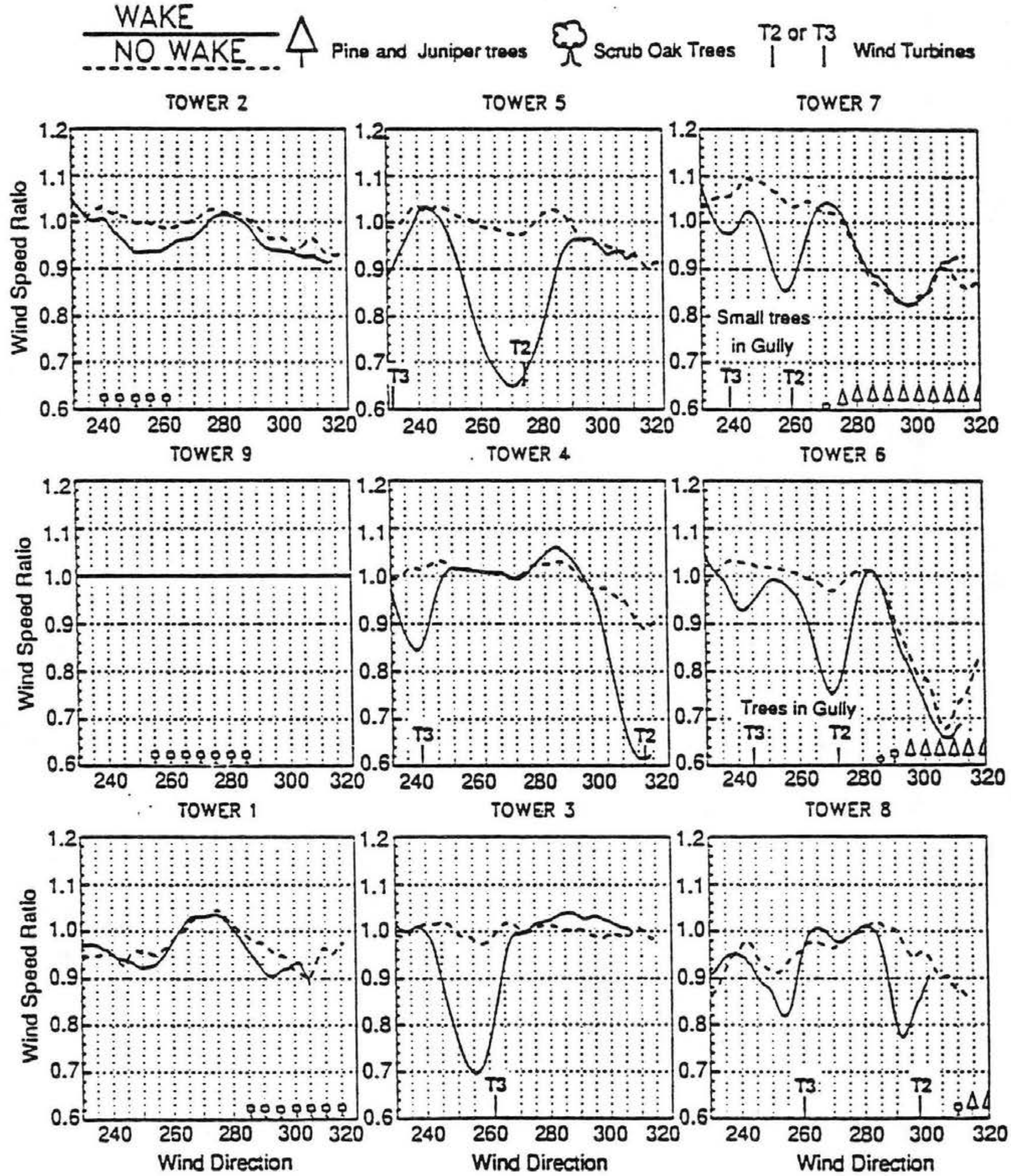

Figure 3.4.8 Wind speed ratios (to tower 9) versus tower 9 wind direction. Directions of major groves and wind turbines are indicated (Elliott and Barnard, 1990)

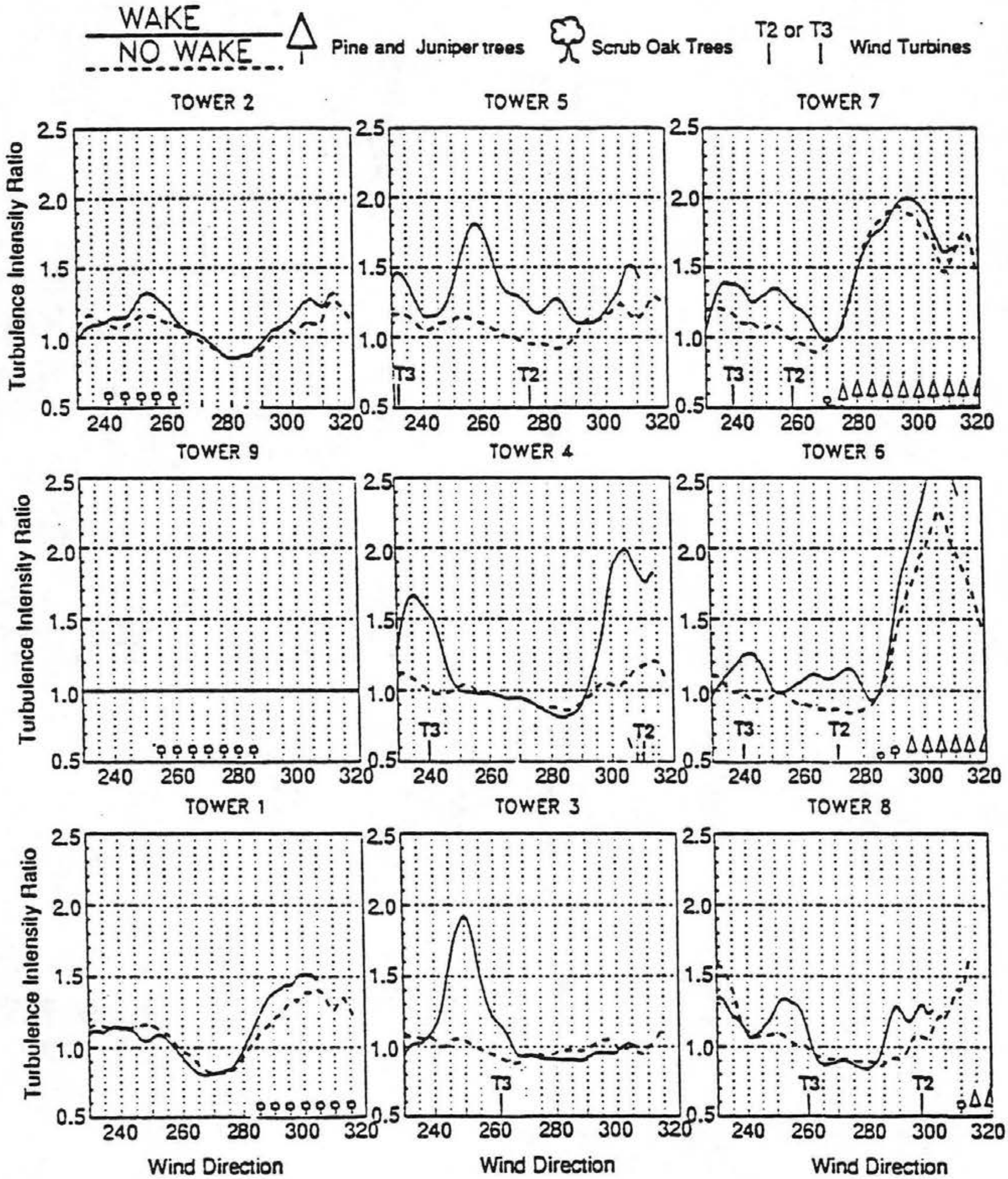

Figure 3.4.9 Turbulence intensity ratios (to tower 9) versus tower 9 wind direction. (Elliott and Barnard, 1990)

The taller towers permitted the authors to examine the effect of height on tree induced perturbations. Winds at the tower within 300 m of groves showed a change of power-law index from 0.14 to 0.28-0.29. The tower at 1000 m showed minimal effects.

3.5 Change of Surface Roughness

It has long been observed that when the wind flows from one surface texture to another a transition takes place in wind speed and turbulence within an inner-boundary-layer, l_z, that grows in depth with downstream distance from the surface change. When the surface change is associated with roughness height, and downstream wind profiles are plotted semilogarithmically with height, then a distinct "kink" in the slope of the plot is observed which can be associated with this inner-boundary-layer depth, l_z. The wind profile near the ground will adjust to surface roughness changes as it moves downwind from the ground cover transition. Above l_z the profiles will correspond to the wind profile for the roughness before the change in cover. Various field measurement programs over smooth-to-rough and rough-to-smooth roughness transitions provide justification for empirical plots of the sort proposed by Park and Schwind (1977). **Figure 3.5.1** consists of five curves that give the growth in transition height between the various profiles of **Figure 3.5.2.** Combining profile shape and transition growth information should permit estimation of a wind speeds below the layer l_z for different downwind distances. The wind speeds above and below the inner boundary layer are adjusted to match at their intersection at l_z.

3.5.1 *Change of Roughness Models*

A number of different analytic and numerical models exist to predict the resultant variation in wind profiles which exist at different fetch distances downstream of a transition of roughness. The subject is extensive enough that a literature review has been prepared on the topic by Hunt and Simpson (1982). They also provide a table summarizing field and laboratory change of roughness experiments used to verify various models. Unfortunately, little data exists for roughness variations as large as the abrupt change that occurs from a forest edge to a meadow or a clearcut region. Most models grew from the perturbation analysis originally proposed by Townsend (1966). Subsequent researchers have modified assumptions, boundary conditions, definition of perturbation variables and scaling lengths, but the basic concepts have remained the same. This same perturbation approach has subsequently been applied to predicting the effects of surface elevation, surface temperature, surface heating, surface humidity, and stratification on atmospheric boundary layer wind profiles and turbulence.

A presentation by Jensen (1978) is widely accepted. Given an upwind roughness, z_{o1}, a downwind roughness, z_{o2}, a corresponding up- and downwind surface friction velocity, u_{*1} and u_{*2}, and a distance downwind from the roughness change, x, then:

$$u(x) \approx (u_{*1}/\kappa)\ln[z/z_{o1}] + (u_{*1}/\kappa)\ln[z_{o2}/z_{o1}](\ln[z/z_{o2}]/\ln[l_z/z_{o2}]) - 1\} \quad [3.5.1]$$

$$u_{*}/u_{*1} \approx 1 + \ln[z_{o2}/z_{o1}]/\ln[l_z/z_{o2}] \quad [3.5.2]$$

$$l_z \ln[l_z/z_{o1}] = 2\,\kappa^2 x \quad [3.5.3]$$

TO:

FROM:	A	B	C	D	E	F
A	-	1	1	2	3	4
B	5	-	2	3	3	4
C	5	2	-	3	4	4
D	5	2	3	-	4	5
E	5	3	3	3	-	5
F	5	4	4	4	5	-

HOW TO READ THIS PLOT

1) SELECT UPWIND & DOWNWIND TERRAINS IN FIG. 10

2) ENTER TABLE ON LEFT WITH APPROPRIATE LETTERS, SELECT NUMBER

3) USE CURVE BELOW WITH NUMBER

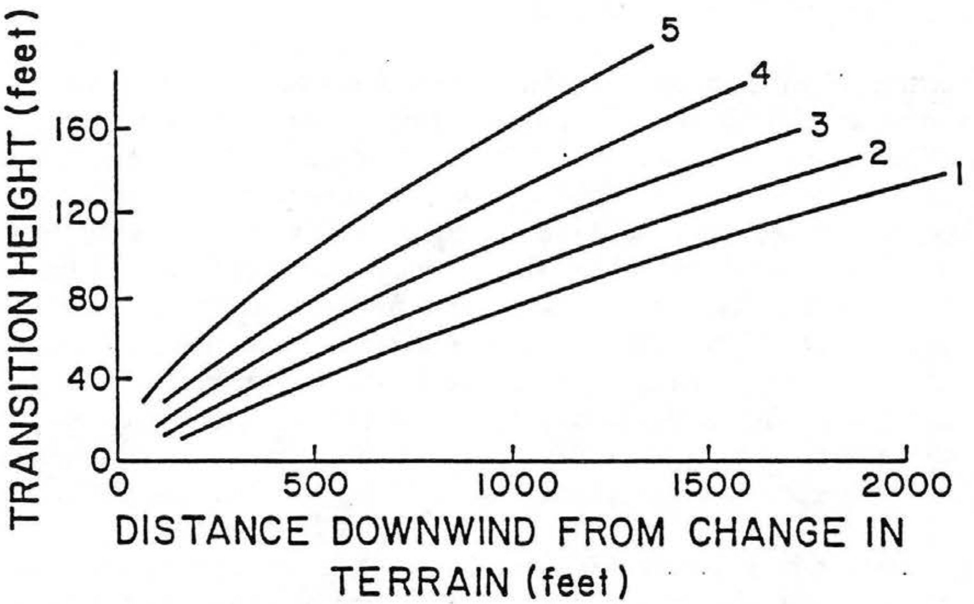

Figure 3.5.1 Wind profile transition height resulting from a change in surface roughness (Park Schwind, 1977, in Meroney, 1977)

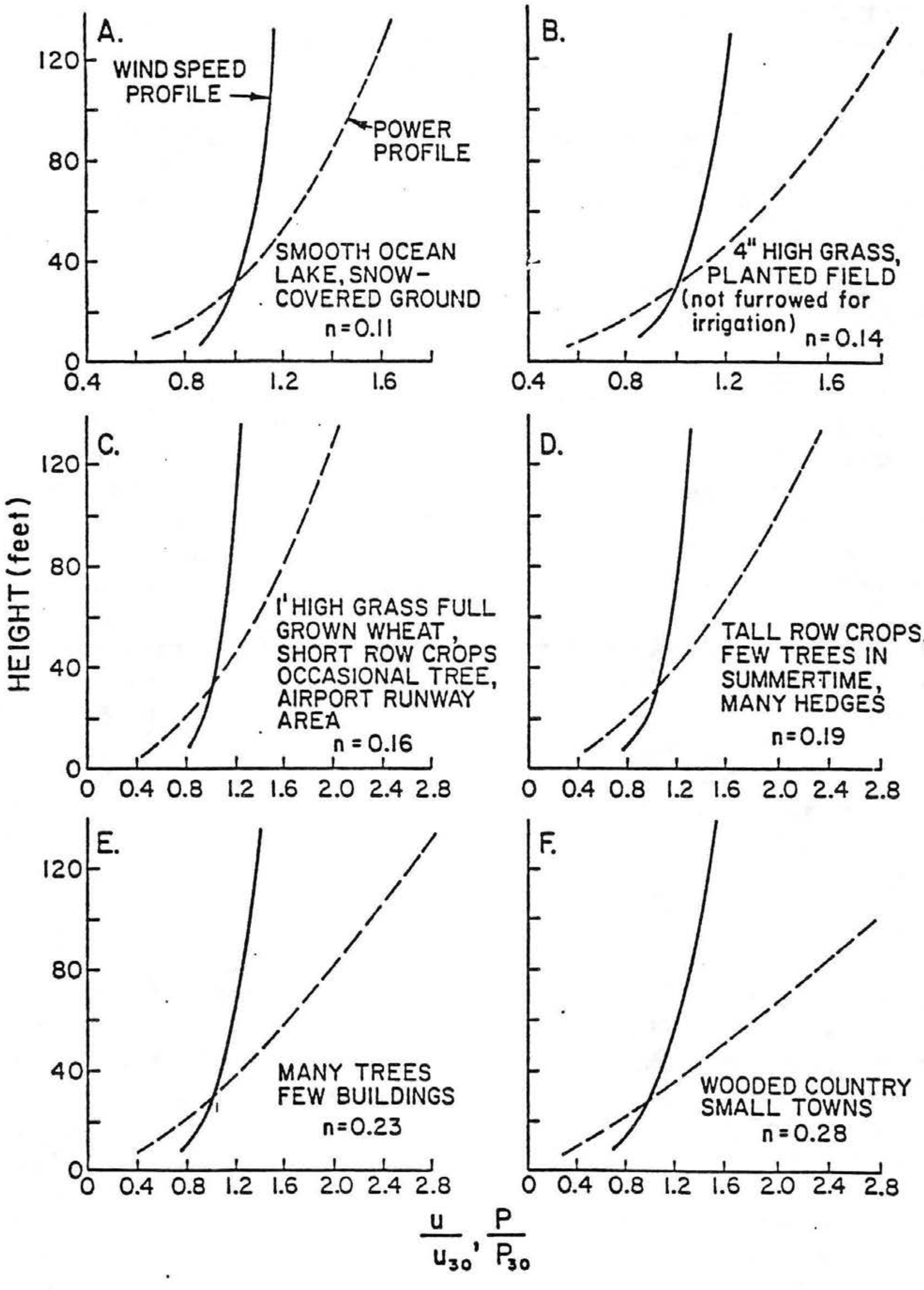

Figure 3.5.2 Wind profile shapes and wind power profile shapes for various types of flat terrain. (Park and Schwind, 1977)

where κ is the von Karman constant commonly set to 0.4. Hunt and Simpson (1982) point out that these expressions suggest that the perturbation shear stress and velocity decrease slowly and inversely with $\ln[l_z / z_{o2}]$ and are proportional to $\ln[z_{o2} / z_{o1}]$. By normalizing l_z and x on the larger of the up- or downwind roughness, z_o, an almost universal plot of inner boundary layer growth was prepared from field and model data. As shown in **Figure 3.5.3** the line produced by Equation [3.5.3] is found to lie within 25% of all data. An empirical fit to the nonhomogeneous Equation [3.5.3] might be

$$l_z / z_o = 0.3\ (x/z_o)^{0.8} \qquad [3.5.4].$$

3.5.2 *Multiple changes of roughness*

By superposition of the linear-perturbation solution for a one-dimensional change in surface roughness, one can create a method to predict the effect of arbitrarily distributed surface roughness on wind profiles. Belcher, Xu and Hunt (1990) propose such a model to predict the effect of non-homogeneous two-dimensional roughness on wind profiles and surface stress. Due to the lack of field or model data they compare their results to higher-order turbulence closure solutions of similar boundary conditions. The perturbation approach produces quite good correlation for roughness changes as large as $|\ln[z_{o2} / z_{o1}]|$ of order one.

Derickson and Peterka (1992) have also developed a method to correct anemometers for multiple changes of upwind roughness. Their ad hoc approach follows earlier work on roughness changes proposed by Deaves (1981) and Cook (1985). Whereas the Jensen approach is limited to correcting wind profiles in the lower regions of the boundary layer, this method corrects for the eventual adjustment of the gradient wind profile at all elevations to the change in surface conditions. This method is probably an over-kill for estimating the effects of forest clearings and clearcut regions of finite extent.

3.6 Summary

The development of wind profiles over different homogeneous surface roughness conditions can be predicted with fair accuracy. Measured profiles of wind speed both below and above vegetative canopies follow analytic models well. The actual values for surface shear and roughness length will depend upon the total area averaged, especially in areas where surface elevation varies. Surface roughness, z_o, and displacement height, d, can be related to canopy foliage density and average tree height. Surface shear can be predicted with somewhat less confidence.

The presence of openings, cleared areas, shelterwood clearings, and clearcut regions within forests produce motions which are qualitatively anticipated. Unfortunately, there are very little field data from forests available to verify any analytic or numerical models for such situations. The downwind effect of roughness change can be predicted by a linear-perturbation model. This model will be used with similar expressions for surface elevation effects to predict the joint effect of nonhomogeneous roughness and elevation in Section 5.4.

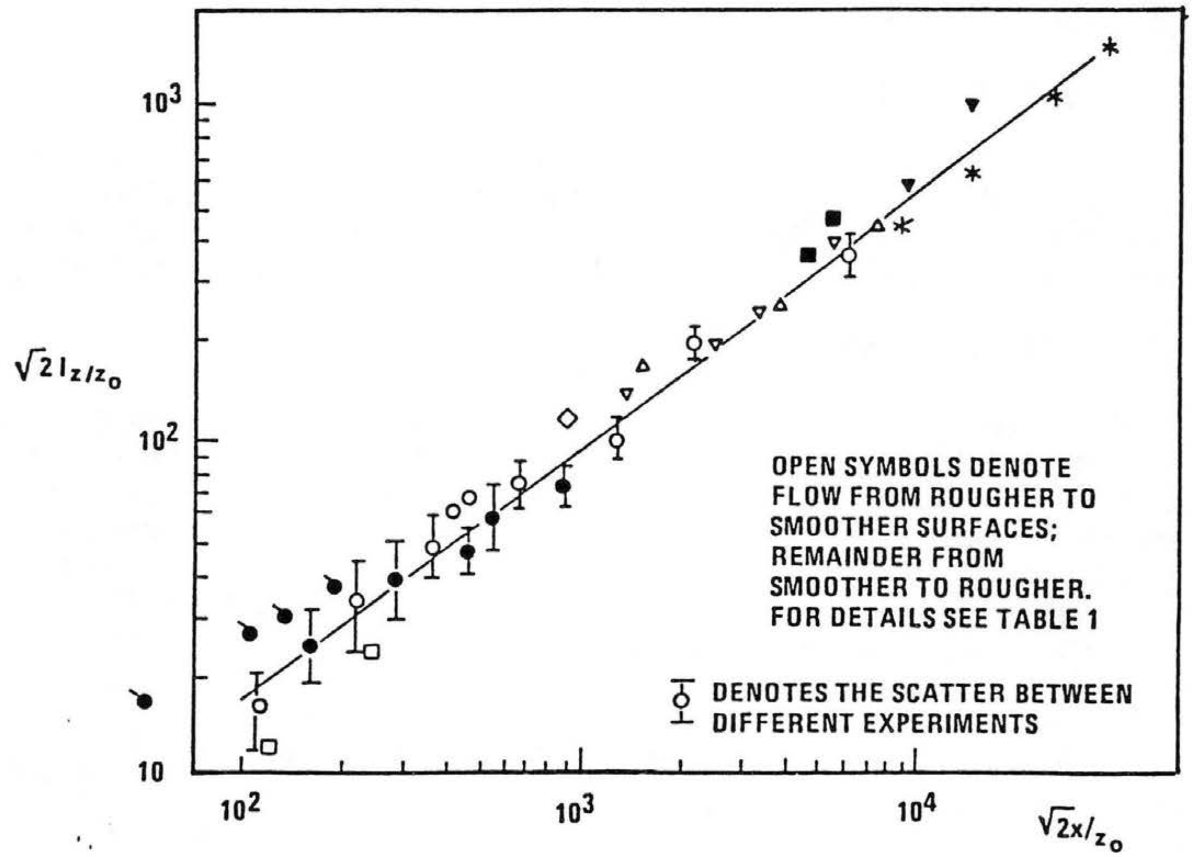

Figure 3.5.3 Internal boundary layer thickness versus normalized distance referenced to larger z_o. Line is best fit to points. (Hunt and Simpson, 1990)

IV. VEGETATIVE/SURFACE ROUGHNESS EFFECTS ON FLOW OVER HILLS /MOUNTAINS

Complex hilly terrain may exist with a variety of vegetative surface cover. For example the approach terrain and the hill itself may both be either bare or vegetation covered. Alternatively, the upwind surface may be smooth (farmed plains or meadows) and the hills may be rough (tree covered), or the upwind surface may be rough (tree covered) and the hill itself bare. In some cases only portions of the hill may be bare due to selective shelterwood cutting or clearcutting. The presence or absence of high roughness may lead to lower/higher wind speeds, higher/lower turbulence, or attached/separated streamline flow.

4.1 Homogeneous Surface Roughness Over Hills/Mountains

The upwind surface roughness induces different approach velocity profiles which can lead to variations in hill crest wind profiles **(Figure 4.1.1)**. The approximate effects of such profile changes on the fractional speedup have been examined using physical modeling, inviscid rotational numerical models, 2nd-order turbulent closure models and linear-perturbation analysis.

4.1.1 *Field and Laboratory Data*

Bouwmeester et al. (1978) performed wind tunnel measurements over triangular hill shapes, with equal hill heights and slope, but surface roughness varying between cases by a factor of ten (z_o/h_{hill} = 0.0013 versus 0.0178). The measured values of fractional speedup, ΔS, for smooth and rough hills are plotted in **Figure 4.1.2** as Test Case 5 and 14, respectively. The rough hill produced larger speedup values at all heights; however, since the reference wind speed at a given height is usually less for rough surface flows, the actual crest height wind speeds are less. Additional smooth surfaced hill measurements are also plotted for other hill slopes as Test Cases, I, 3 and 9.

In Section 2.2 it was noted that Bradley (1978) measured wind flows over a tree-covered ridge in Australia. The ridge height, h_{hill}, was 170m, the upwind ridge length was L_u = 550 m and the downwind length somewhat longer, L_d = 600 m.; hence, the average h_{hill} /L ratio equals about 0.29. The hill was covered with 10 m tall trees, and the associated surface roughness, z_o, and displacement height, d, were estimated to be 1.0 m and 7.0 m respectively; hence, z_o/h_{hill} = 0.006. The atmospheric boundary layer was estimated to be between 600 and 800 m. Bradley obtained wind data at various heights up to 100 m above the crest during neutral conditions. A separation region was believed to exist downwind of the crest. The fractional speedup for this hill is also plotted on **Figure 4.1.2.** where vertical heights have been correct for forest displacement above the ridge ground level. The roughened wind-tunnel model was relatively slightly rougher than the Bradley forested hill. Note that the inner-boundary-layer, l_z is noticeable at a dimensionless height of about 0.17. The magnitude of l_z during the model tests was believed to be considerably smaller than this due to relaminarization at low Reynolds numbers.

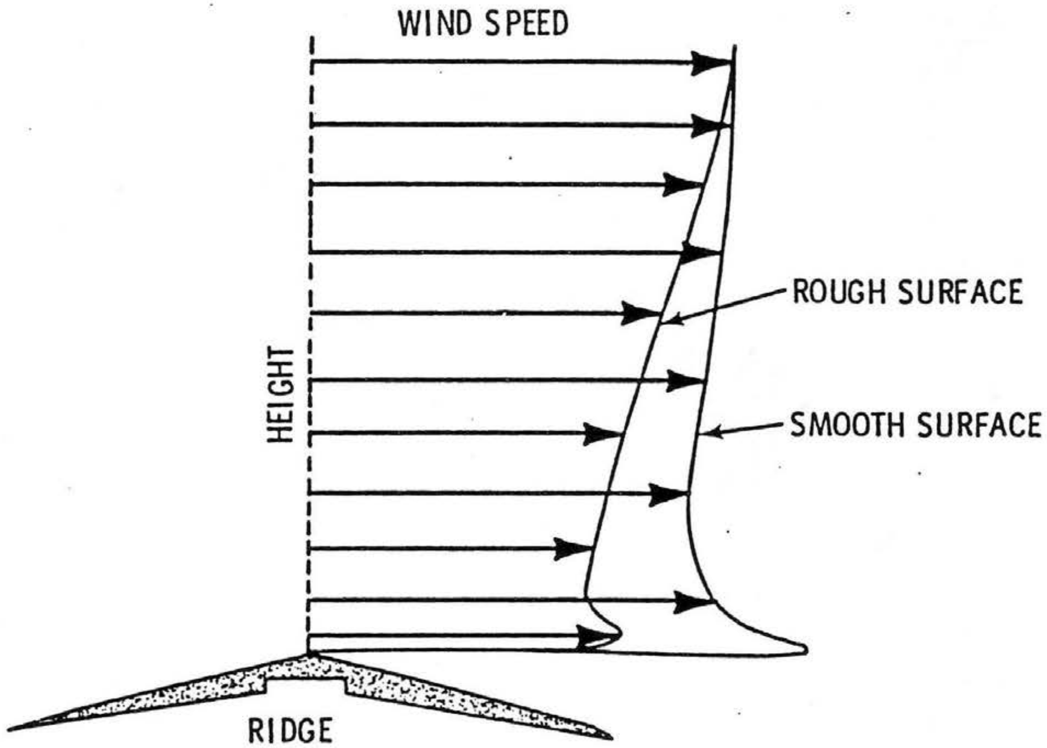

Figure 4.1.1 Effect of surface roughness on wind flow over a sharp-crested ridge. (Wegley, Orgill and Drake, 1978)

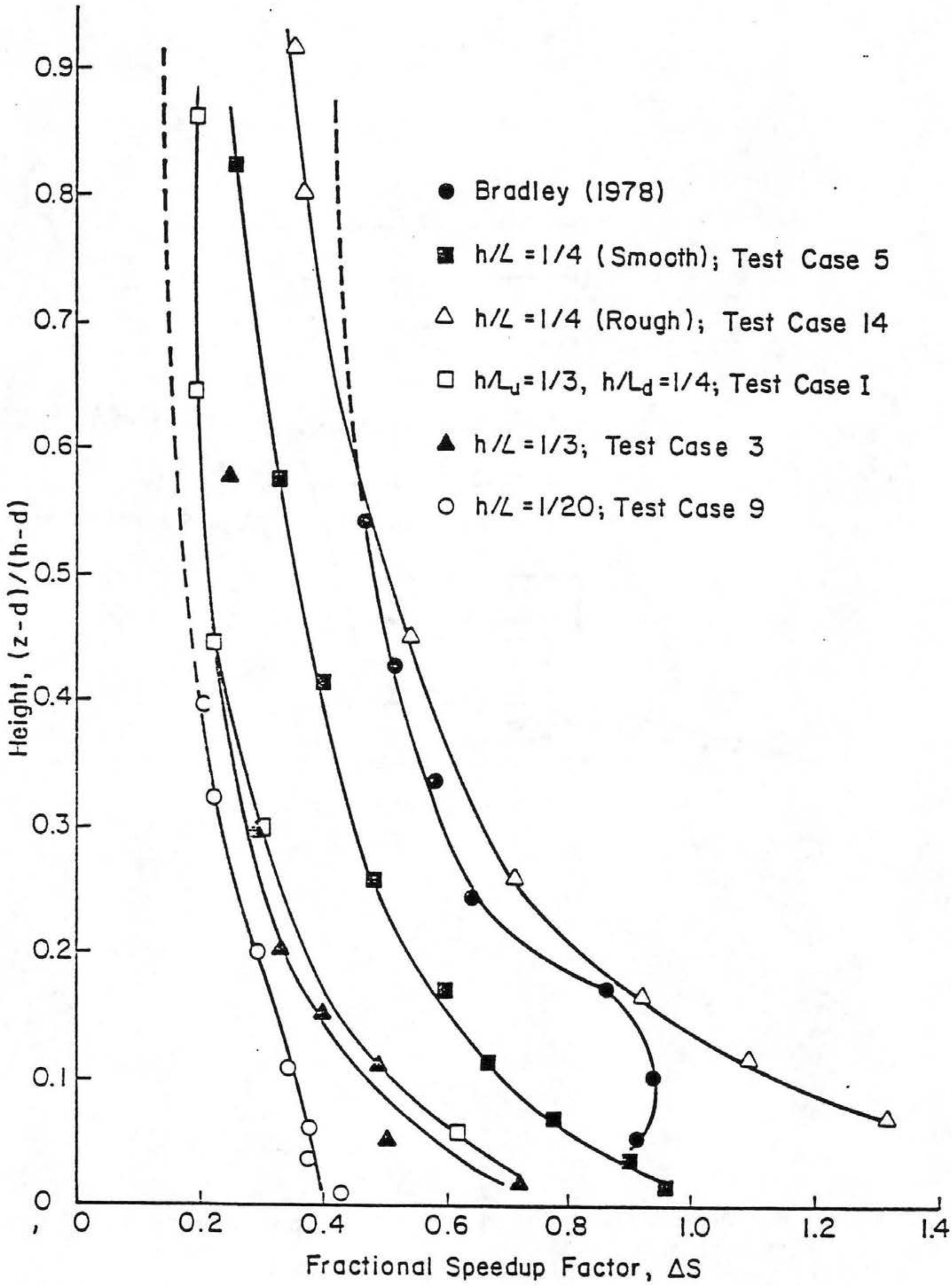

Figure 4.1.2 Fractional speedup ratio profiles at crest of triangular hills. Field data, Bradley (1978); Laboratory data, Bouwmeester *et al.* (1978)

4.1.2 *Inviscid -Rotational Numerical Model Results*

Bouwmeester et al. (1978) used the inviscid-rotational potential flow model proposed by Derickson and Meroney (1977) to predict fractional wind speed up over hills for different approach flow profiles. In **Figure 4.1.3** nine velocity distributions are plotted for different combinations of z_o/h_{hill} and h_{hill}/δ. Resultant fractional speedup ratios, ΔS, are shown in **Figure 4.1.4.** The fractional speedup ratios are essentially independent of roughness for $h_{hill}/\delta = 4$, and there is only a slight dependency on roughness for smaller h_{hill}/δ values. The upper flow perturbations proposed by Jackson and Hunt (1975) are also essentially inviscid potential flow solutions, and they also imply primary dependence on hill slope and no variation with surface roughness, that is $\Delta S = (h_{hill}/L)\sigma(x,y)$. These results seem inconsistent with the measurements reported in Section 4.1.1. One reason might be that despite the range of roughnesses specified for the upwind profiles, the absolute roughness magnitudes were less than $z_o/h_{hill} = 10^{-4}$. The differences might also result because the inviscid model does not correct for the inner-boundary layer which increases as $l_{z1}/l_{z2} = (z_{o1}/z_{o2})^{0.2}$. Thus, if the roughness length increases by a factor of ten the inner-boundary-layer increases by almost two..

4.1.3 *Turbulence Model Insights*

Frost, Maus and Fichtl (1974) solved the turbulent boundary layer equations over a plane surface using mixing-length closure for a horizontal pressure distribution equal to that along the $\psi = 0.6$ streamline of inviscid potential flow around an elliptical cylinder. Numerical solutions were carried out for aspect ratios 2:1 and 4:1 and for various surface roughness lengths. **Figure 4.1.5** shows the resulting wind profile directly over the crest of the ellipse with alternate roughness lengths and aspect ratios. Notice that the inner-boundary-layer length, l_z (or in this case shown as δ) increases with larger roughness such that $\delta_1/\delta_2 \approx 1.33$, which agrees well with the value $(z_{o1}/z_{o2})^{0.2} = 1.38$ suggested by manipulation of Equation [3.5.4]. Fractional speed up at inner-boundary-layer height appears to remain nearly constant as roughness increases.

Taylor and Gent (1974) solved for flow over a hypothetical hill using second-order turbulence closure methods. Bouwmeester et al. (1978) determined that surface shear stress predicted by inviscid models underestimated the Taylor-Gent nonlinear model values by up to 300%.

4.1.4 *Linear-perturbation Model Insights*

Linear-perturbation models of the sort used by Jackson and Hunt (1975), Jensen (1978), and Jensen and Petersen (1978) provide for the influence of surface roughness in an inner layer, l_z, such that the fractional speed up becomes:

$$\Delta S(z) = (h_{hill}/L)\sigma(x)\,(\ln[L/z_o]/\ln[l_z/z_o])^2, \qquad [4.1.1]$$

where $\sigma(x)$ adjusts for dimensionless hill shape, f(x/L). The factor is maximum at hill crest, $\sigma_{max} = \sigma(0) = \Delta u_{max}/[(h_{hill}/L)u_o]$. Typical values of σ_{max} are displayed in **Table 4.1.4** .

Table 4.1.4 Maximum increase of velocity in potential flow over various two-dimensional hills with low slopes.

$$\sigma_{max} = \frac{\Delta u_{max}}{(h_{hill}/L) * u_o}$$

Hill Shape		**Max slope/(h_{hill} /L) u_o**	σ_{max}
Inverse Polynomial	$f = 1/[1 + (x/L)^2]$	0.56	1.0
Unsymmetric Inverse Polynomial	$f = 1/[1 + (x/L_1)^2]$, $x < 0$ $f = 1/[1 + (x/L_2)^2]$, $x > 0$	0.56, $x < 0$ $0.56(L_1/L_2)$, $x > 0$	$1/2(1 + L_1/L_2)$
Gaussian	$f = \exp[-(x/L)^2 \ln 2]$	0.71	1.13
Ramp	$f = 1/2\ 1 + \tanh(x/L)]$	0.5	0.29
Sin	$f = 1/2\ \{1 + \cos[\pi/2\ (x/L)]\}$	0.79	0.93

Note that L is chosen so that $f(x/L = 1) = 1/2$ in all cases.

If the hill is in the form of an ellipsoid, a useful approximation to many hill shapes, then Δu_{max} may also be calculated by hydrodynamic methods as shown by Hunt and Simpson (1982).

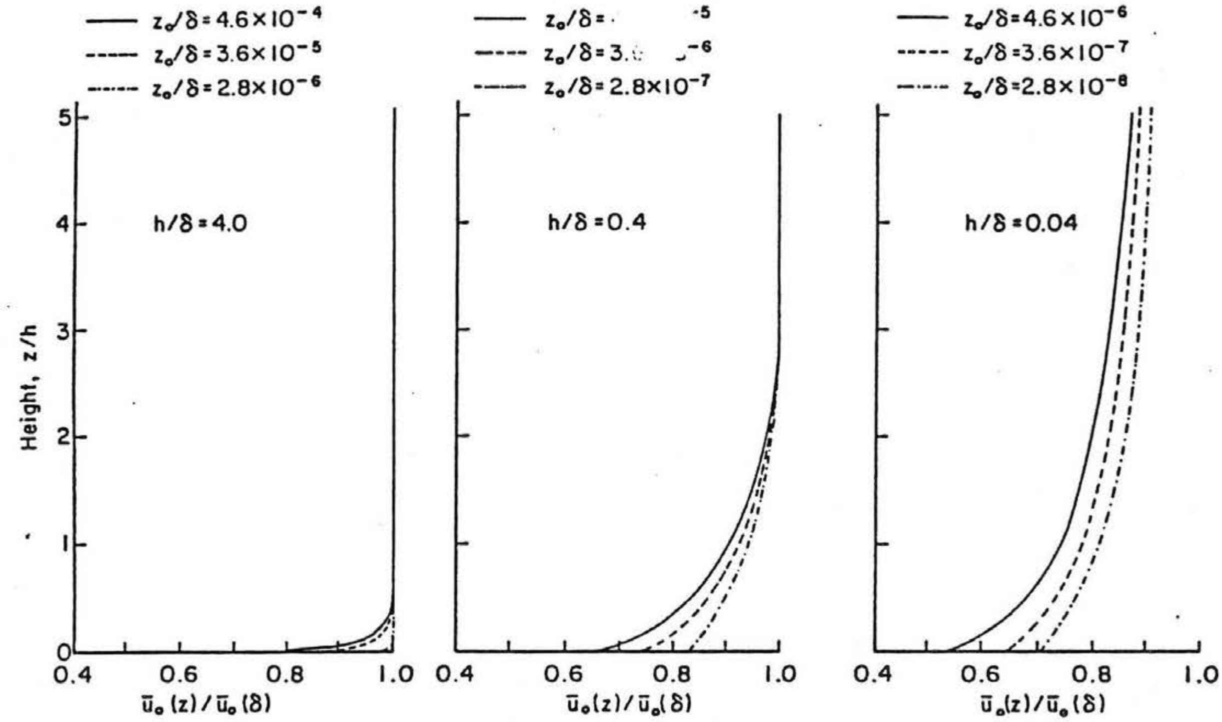

Figure 4.1.3 Approach flow velocity profiles for numerical inviscid flow calculations. (Bouwmeester *et al.*, 1978)

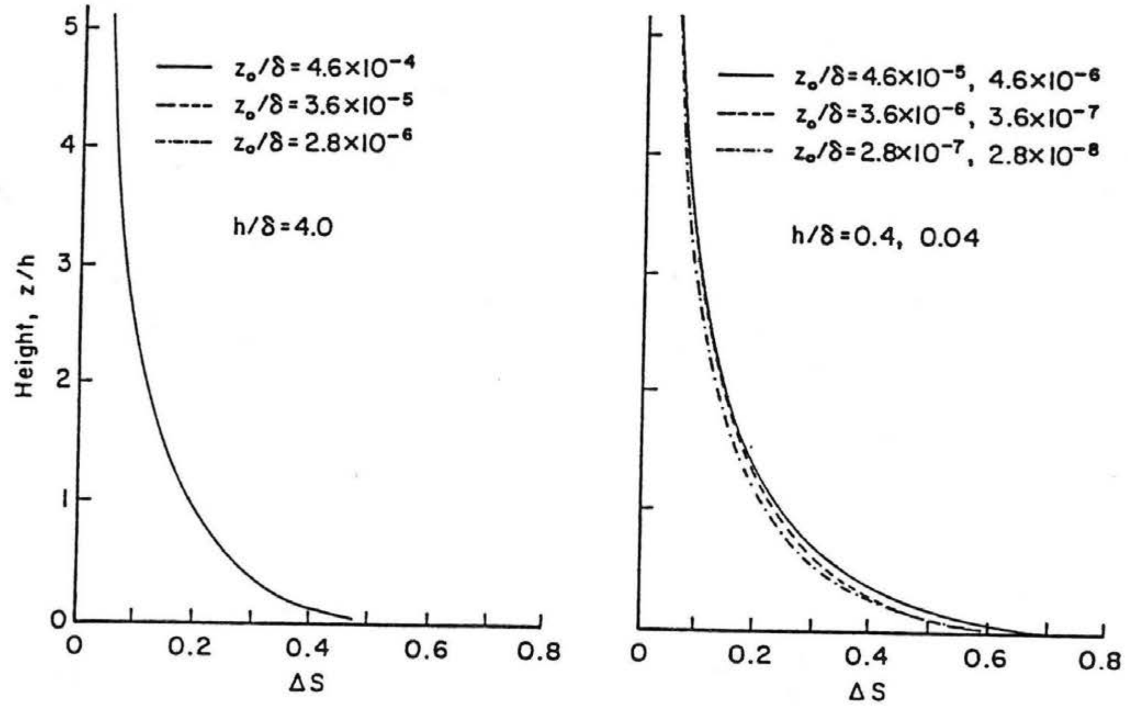

Figure 4.1.4 Fractional speedup ratios predicted from numerical inviscid flow calculations (Bouwmeester *et al.*, 1978)

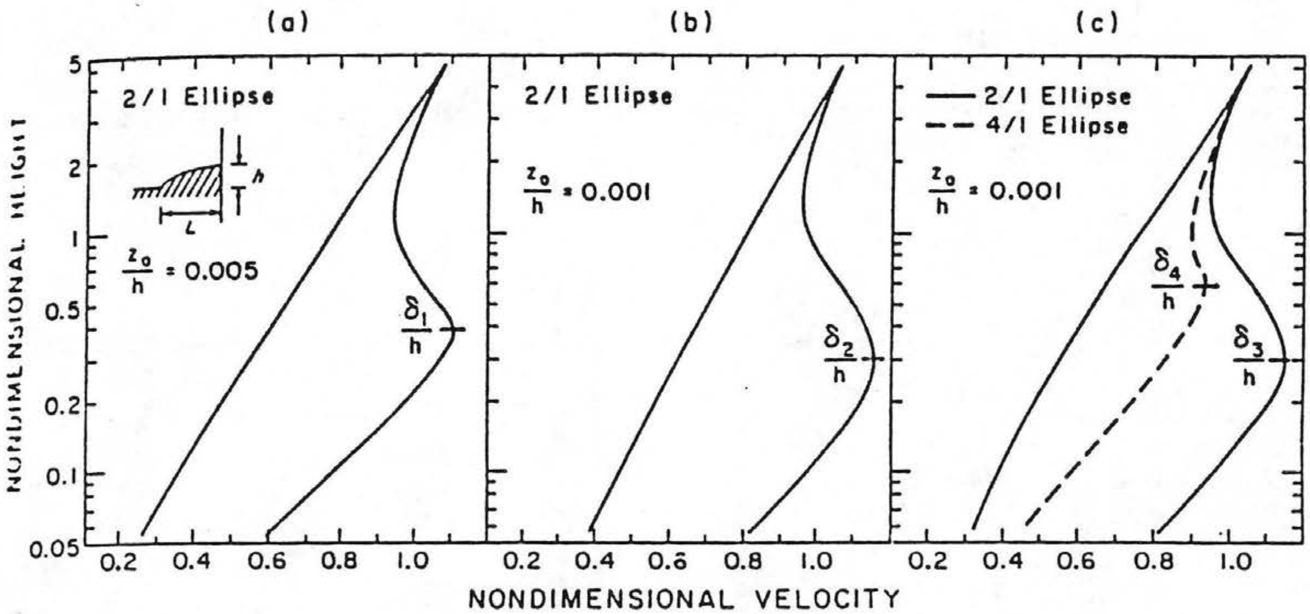

Figure 4.1.5 Flow over elliptical obstacles. Heights are scaled by object height. Velocities are scaled by upstream velocity at z/h = 3. (Jensen and Petersen, 1978)

but from Equation [3.5.4] we can argue $l_z / z_o \approx (L/z_o)^{0.8}$, so

$$\Delta S(z) = (h_{hill} / L)\sigma(x) (\ln[L/z_o]/(0.8 \ln[L/z_o]))^2 \neq f(z_o). \qquad [4.1.2]$$

Thus, most analysis predicts that variation in homogeneous surface roughness upwind and over the hill will produce only small changes in the fractional speedup, but consequently large variations in the actual mean profiles.

4.2 Change in Roughness Effects on Flow Over Hills/Mountains

An early observation made during wind-tunnel measurements was that when surface roughness was reduced over the steeper models the mean velocity on the lee side actually increased, and the flow did not separate, even intermittently, though the flow remained turbulent. Conventional wisdom for flow around bluff bodies usually proposes the addition of surface roughness to inhibit separation not its removal. Britter et. al. (1981) explained this paradox by arguing that the delay of separation is induced because the surface velocity near the separation point is increased as the flow accelerates over the smoother hill surface. Thus the boundary layer can penetrate further into the adverse pressure gradient on the lee side of the hill. (The boundary layer is energized by the descent of streamlines toward the wall after a decrease in surface roughness.)

4.2.1 *Linear-perturbation Model Insights*

Jensen and Petersen (1978) discussed the possibility of adding the linear-perturbation solutions for boundary layer response to changes in surface roughness and elevation. Since the solutions are separately linear their perturbations should be additive; thus

$$u(z)_{hill\ \&\ roughness} = u_o(z) + \Delta u(z)_{roughness} + \Delta u(z)_{hill}. \qquad [4.2.1]$$

Hunt (1978) applauded this step, and he concluded that the maximum perturbation induced by change of roughness would occur at height z_{o2} whereas the maximum perturbation induced by the hill would occur at height l_z. Consequently, it is not really possible to cancel out the changes induced by one effect by the other. Hunt proposed the ratio:

$$\frac{|\Delta u(l_z)_{hill}|}{|\Delta u(z_{o2})_{rough}|} = \frac{(h_{hill}/L)(\ln[L/z_{o1}])^2}{\ln[l_z / z_{o2}]\ln[z_{o2} / z_{o1}]} \qquad [4.2.2]$$

Thus, where there is a large change in roughness of say 1 m to 10 cm at the hill half-width, if it is accompanied by a change in slope say 1 in 4 over a hill width of 1000 m, the maximum hill slope effect is comparable to the change in roughness effect! On the other hand, if the change of roughness is from 2 m to 2 cm under otherwise similar conditions, then the maximum hill slope effect is five times less than the maximum roughness effect!

4.2.2 *Field and Fluid Model Data*

Britter et al. (1981) performed wind-tunnel experiments over a polynomial shaped hill for which $h = 0.1$ m, $L = 0.25$ m, $z_o = 0.002$ m, and $u_* / U_\delta = 0.0685$. The authors suggested that at a model scale of 1: 500 the surface roughness corresponded to a value of about 1 m (forest canopy). A second experiment was performed where the roughness ended 1 m upwind of the hill crest. This resulted in significant acceleration in the lower part of the boundary layer as a direct result of the change in roughness as shown in **Figure 4.2.1.** Finally, velocity profiles were also measured at the equivalent location of the hill crest downwind of the roughness change after the hill was removed. Examination of the figure reveals that the increase in wind speed of the smooth hill over the rough hill is almost exactly equal to the perturbation induced by the change in roughness alone.

4.3 Laboratory Measurements of Vegetation Covered Terrain

Extensive tree shelter belts were planted over the Rakaia Gorge, NZ, terminal moraine and river plain studied by Meroney et al. (1978). These 10 m high dense tree belts were planted by farmers to protect sheep paddocks. Comparison of field and physical model measurements revealed that the shelter belts played a dominant role in determining near surface winds. Measurements made over vegetation free models of the Rakaia Gorge over-estimated wind speeds and under-estimated turbulence levels at a 10 m measurement height **(Compare Figures 4.2.2, 4.2.3, 4.2.4 and 4.2.5)**. When vegetation was modeled field and laboratory wind speeds agreed at sample correlation coefficient levels from 0.68 to 0.78 and rank correlation coefficient levels from 0.78 to 0.95. (Sample correlation coefficient levels for field measurements at the same sites taken on independent days was only 0.68. This suggests that there is an inherent limitation to the paired replication of any single realization of a wind flow pattern by an model whether physical or numerical.

Recently Gong and Ibbetson (1989) reported physical model measurements made over cosine shaped hills and ridges of slope 15°. They added a uniform roughness to the hills made of a rubber sheet having flat-topped circular cylinders 3 mm high and 2 mm diameter at a uniform spacing of 3.6 mm between centers. The surface Reynolds number, Re_* , was about 5 ,which implies a rough model surface during simulations. Hill height was 31 mm and half hill width was 100 mm. The effective surface roughness, z_o, was determined to be 0.17 mm. If we assume a scale ratio of 1:10,000 then field scale hill height would be 310 m, roughness height would be 30 m, and surface roughness, z_o, equals 1.7 m. This would be typical of many forest covered hills/mountains found in nature. Gong and Ibbetson recorded extensive mean velocity, shear, and turbulence information. Comparisons of their data against linear-perturbation models was excellent on upwind hillsides and higher levels. Measurements over the two-dimensional ridge and the circular hill suggests that the mean flow and turbulence over a circular hill resembles those over two-dimensional ridges of similar cross-section, but with reduced perturbation amplitudes.

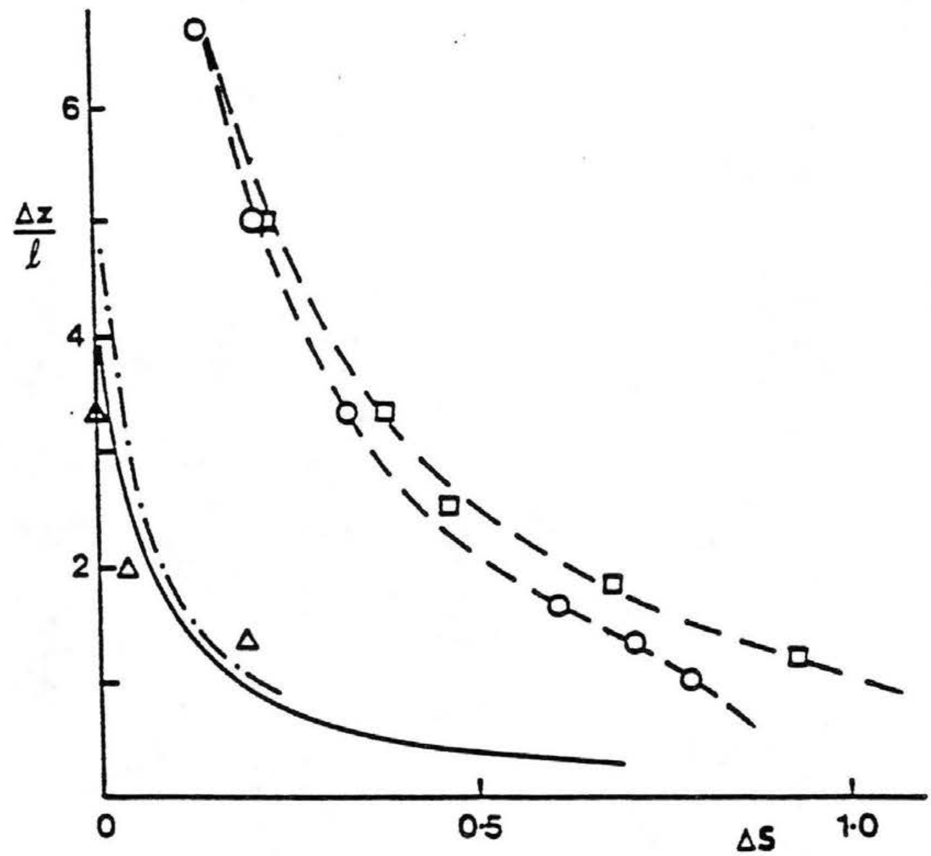

Measured fractional speed-up ΔS ($= \Delta u / U_0$) at top of the smooth and rough hills.

△	roughness change, no hill
—○—	rough hill
—□—	smooth hill
— · —	(smooth) – (rough) hill
———	Townsend roughness change theory

Figure 4.2.1 Measured fractional speed-up at top of the smooth and rough hills. (Britter *et al.*, 1981)

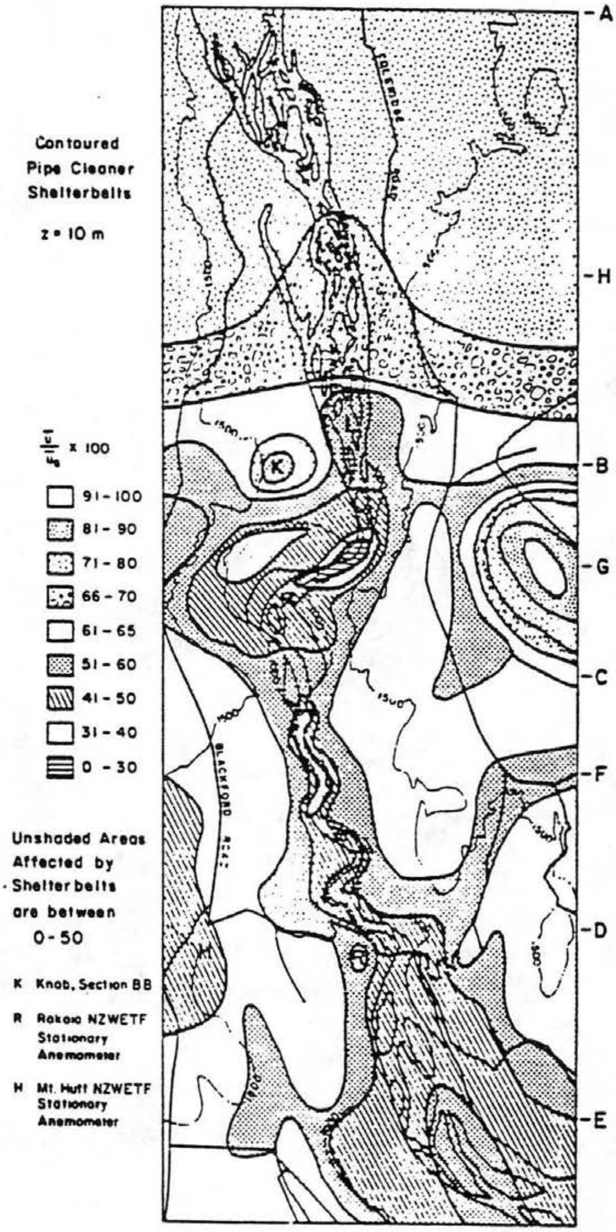

Figure 4.2.2 Horizontal isotachs over Rakaia Gorge, N.Z. z_p = 10 m. (Meroney *et al.*, 1978)

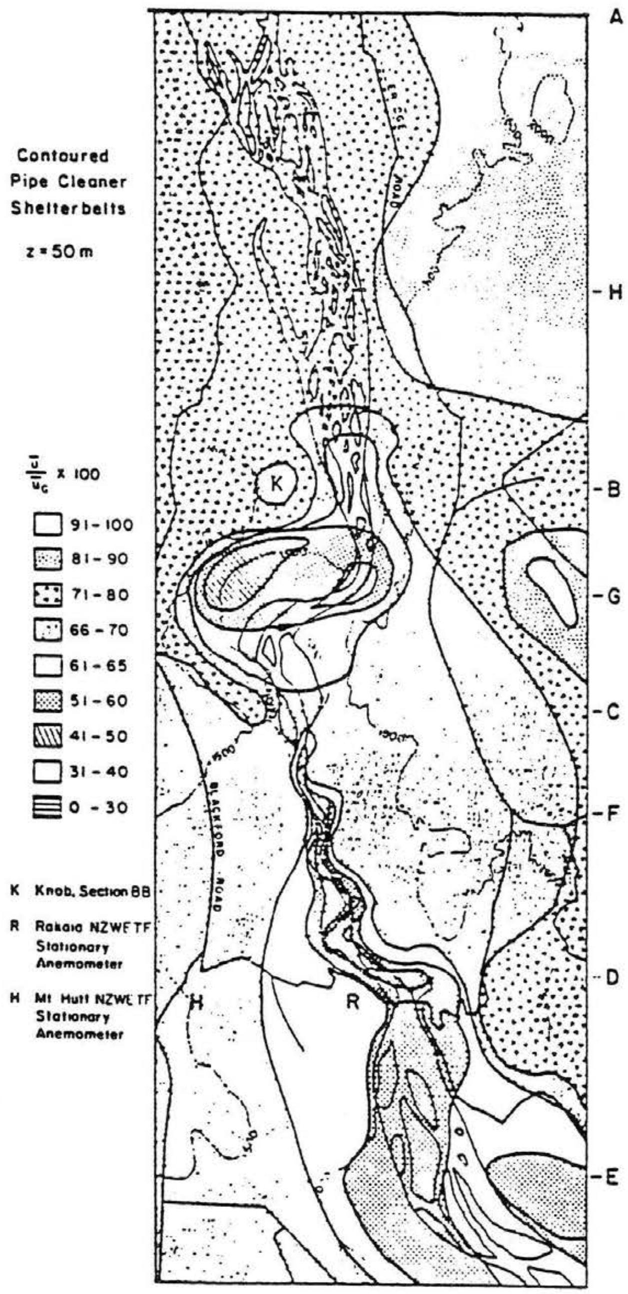

Figure 4.2.3 Horizontal isotachs over Rakaia Gorge, N.Z., $z_p = 50$ m. (Meroney *et al.*, 1978)

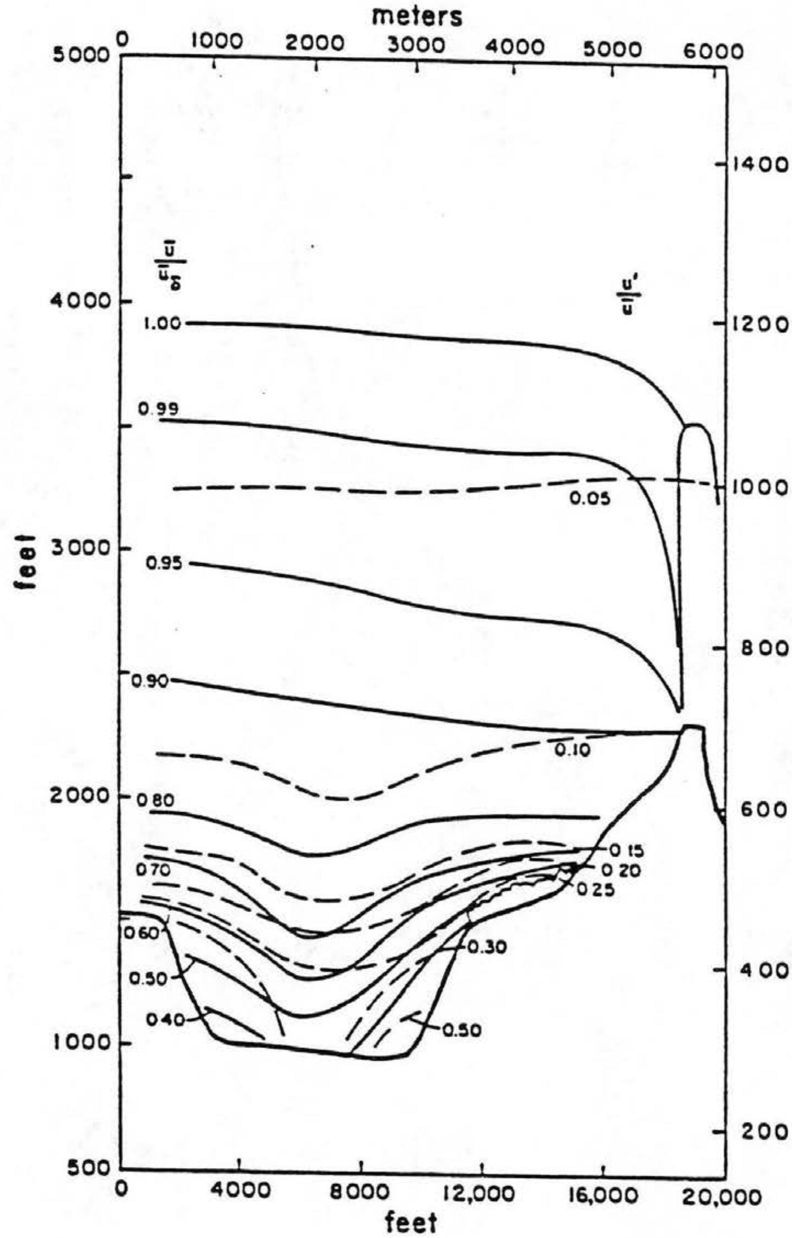

Figure 4.2.4 Vertical section G-G isotachs at Rakaia Gorge, N.Z. (Meroney *et al.*, 1978)

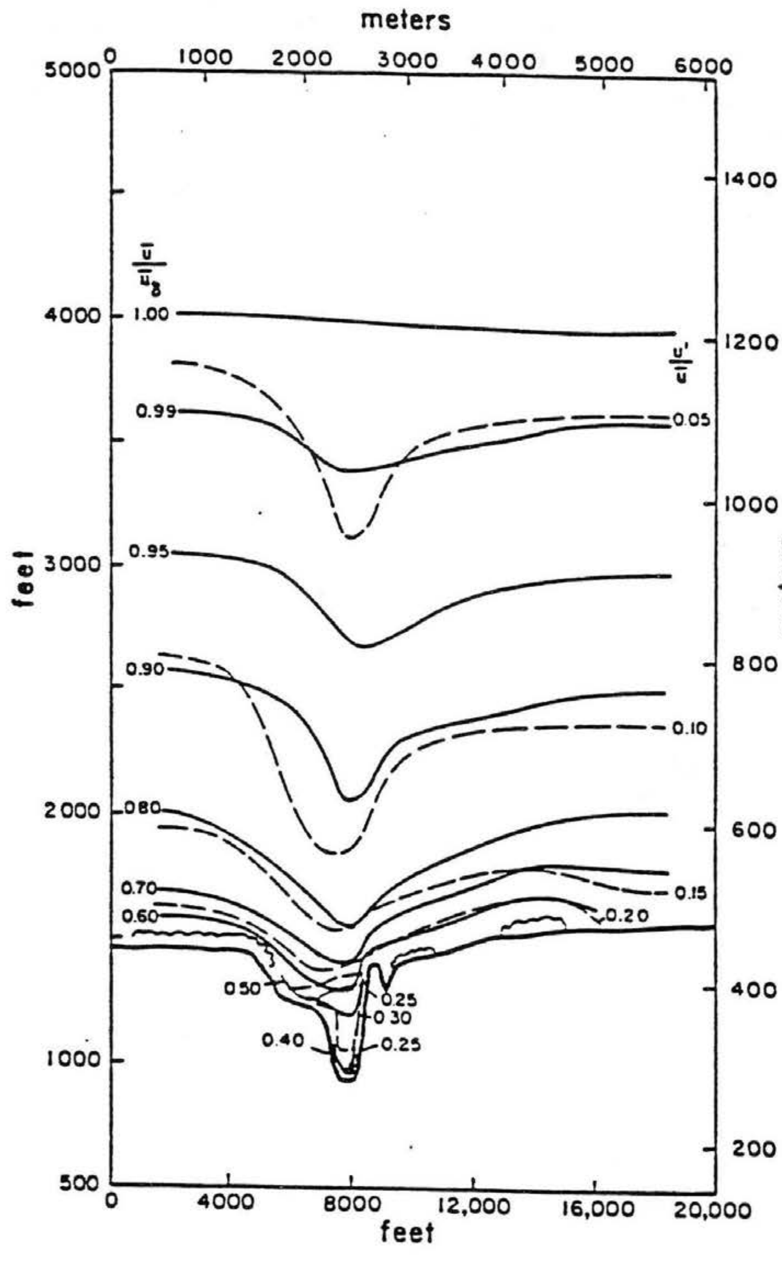

Figure 4.2.5 Vertical section F-F isotachs at Rakaia Gorge, N.Z. (Meroney *et al.*, 1978)

4.4 Summary

The removal of vegetation upwind of the crests of hills has been shown to substantially increase hill-top winds and reduce the probability of separation and consequent gustiness. Most evidence available from fluid model studies. Models based on linear-perturbation principles appear to predict correctly the order of magnitude of combined elevation and roughness change effects on wind speed profiles. Inviscid flow models are not expected to account for the effects of roughness change over hilly terrain.

V. ANALYTIC AND NUMERICAL MODELS

Today there are literally dozens of numerical models available to predict various aspects of flow over complex terrain. Both the use of linear and primitive equation models for flows over complex terrain are discussed in Blumen (1990). A review and classification of complex terrain models was prepared by Meroney (1990) for the Forest Service. Prediction codes or algorithms for flow over complex terrain can grouped into those designed to describe situations where a) stratification causes flow to divert around or over hills and mountains, b) flows which are diverted, accelerated or decelerated due to variations in surface contours, temperature, and roughness in the absence of separation or recirculation, or c) flows where backflows and recirculation may occur as a result of obstacle separation, valley drainage circulations, land/water recirculations, etc. Parallel with these flow categories one can identify at least six categories of numerical modeling:

- i) Dividing streamline models,
- ii) Phenomenalogical models,
- iii) Mass-consistent or objective analysis models,
- iv) Depth integrated models,
- v) Linear-perturbation models, and
- vi) Full primitive equation models.

It would not be appropriate to review all complex terrain models here. A comprehensive list of models by name, type and author will be provided in Appendix tables. Prominent members of each that have been applied to the vegetated terrain problem will be described to identify the advantages and disadvantages of each approach. Copies of almost all model source codes are available by request or purchase. Dividing streamline, depth integrated (shallow layer), and phenomenalogical models have primarily been used to predict plume dispersion in stratified flow situations associated with hill/plume interaction or valley drainage flows. Hence, they will not be considered further here.

5.1 Mass-consistent or Objective Analysis Models Applied to Vegetation Covered Terrain

This class of models combines some objective (regression or maximizing or minimizing some variable) analysis of available wind data to form a wind field. The wind field analysis typically forces the resulting flow to satisfy air mass continuity by constraining the flow between the ground surface and some elevated inversion height. Such models may either produce a fully three-dimensional wind field, or they may solve the depth integrated continuity equation in a horizontal plain, and then recreated a vertical field assuming certain similarity profiles. Comments about specific numerical characteristics of different mass-consistent models are reserved for Appendix Section 2.0. Appendix Table A.1 lists several objective analysis models potentially suitable for wind energy analysis.

5.1.1 *NOABL Predictions for Clearcut Effects Over Cape Blanco, Oregon*

Lin, Veenhuizen, and Qualmann (1985) ran hybrid 2-D and 3-D numerical models for estimating wind flow in Cape Blanco area of Oregon. The effects of terrain height and vegetation were examined. Model was calibrated against kite anemometers. Winter and summer seasonal flows were simulated using long-term wind data at eight fixed height anemometers. The authors report that the variance between measured and predicted winds was only 10%. Results of simulation show that presence of forest in wind turbine site area could cause substantial vertical and horizontal wind shear. Computer simulations were used to assess the impact of tree removal, and they found typical increases of 6 mph at 40 feet and 4 mph at 100 feet above ground.

Veenhuizen and Lin (1982) looked at a 2-dimensional model for flow over a simulated clearing. Subsequently, Veenhuizen and Lin (1983) examined the Goodnoe Hills, WA, area by using a surface roughness length smoothing scheme. They adjusted for the presence of trees by using a virtual origin shift associated with the height of the tree canopy where $d = 0.6$ h and a specified roughness length, $z_o = 0.25$ (h-D) where $u/u^* = 5.75 \log[(z-d)/z_o)]$. Note that this gives $u/u^* = 5.75 \log[10(z-0.6h)/h]$; hence, the equation is oversimplified because it does not allow for atmospheric stability and tree density. Roughness lengths were specified over test area for forest, scrub, town, swamp, cleared forest, prairie and beach such that z_o varied from 1.52 m to 0.005 m. A system was used to smooth between the forest and cleared areas as noted in **Figure 5.1.1** Basically the method produces a weighted average of roughness lengths based on examining specified roughness lengths from aerial maps around the point of interest. A similar smoothing was used for the displacement lengths.

Horizontal wind fields at a specified height were initially estimated from a 2-dimensional program , then these winds were distributed in the vertical using power law formulae which results in profile predictions shown in **Figure 5.1.2 and 5.1.3.** Once initialized from the estimated profiles NOABL was then used to calculate the final wind fields! Up to 50 iterations were permitted to occur, after which it was assumed wind field was divergence free. Authors provide validation comparisons between short-term measurements and calculations; then they provide comparisons between long-term seasonal measurements and calculations.

Areal distributions of wind speed were calculated for heights of 50, 100 and 200 feet above the ground with isotach plots. Calculations were also made after an assumption of tree removal over potential wind power sites. The authors plotted wind speed difference isotachs for same regions after tree removal. (Unfortunately, the report figures are difficult to read; hence, no example is reproduced here.) Tree removal caused a maximum of +6 mph at 50 feet, but at 200 feet zero wind speed increase occurred.

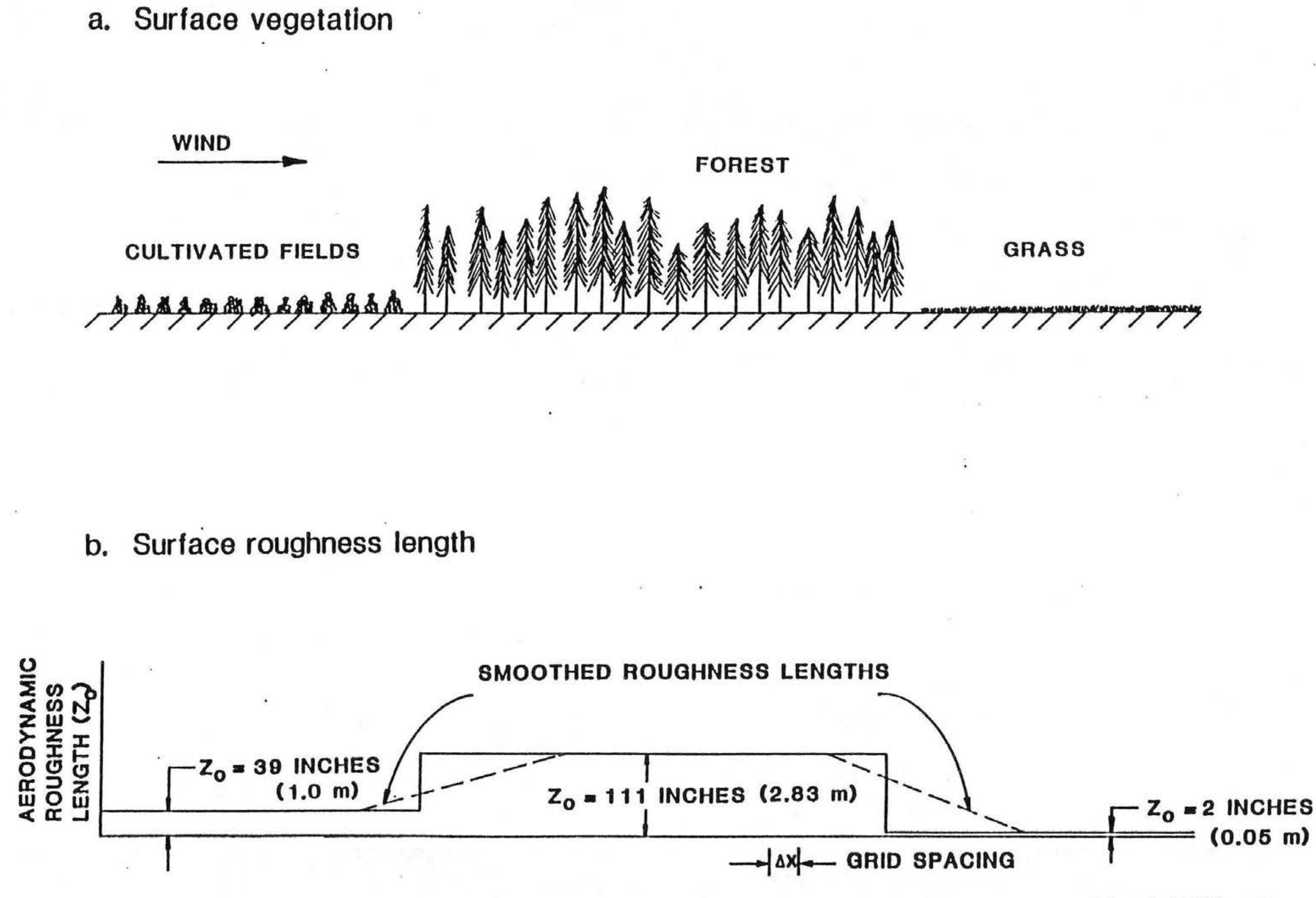

Figure 5.1.1 Smoothing scheme for aerodynamic roughness length (Lin *et al.*, 1985)

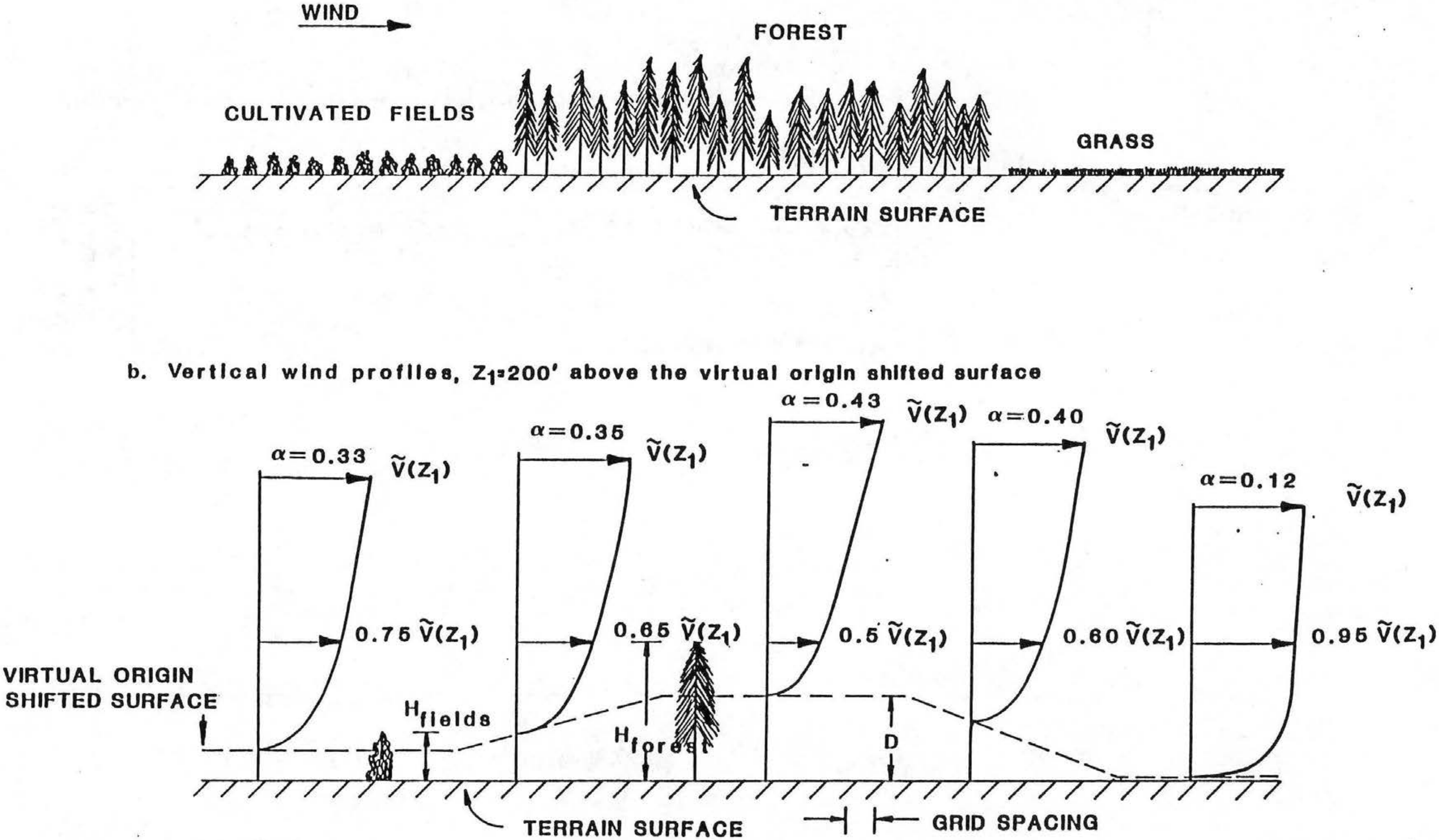

Figure 5.1.2 Vertical wind profiles over a surface of smoothed surface roughness (Lin *et al.*, 1985)

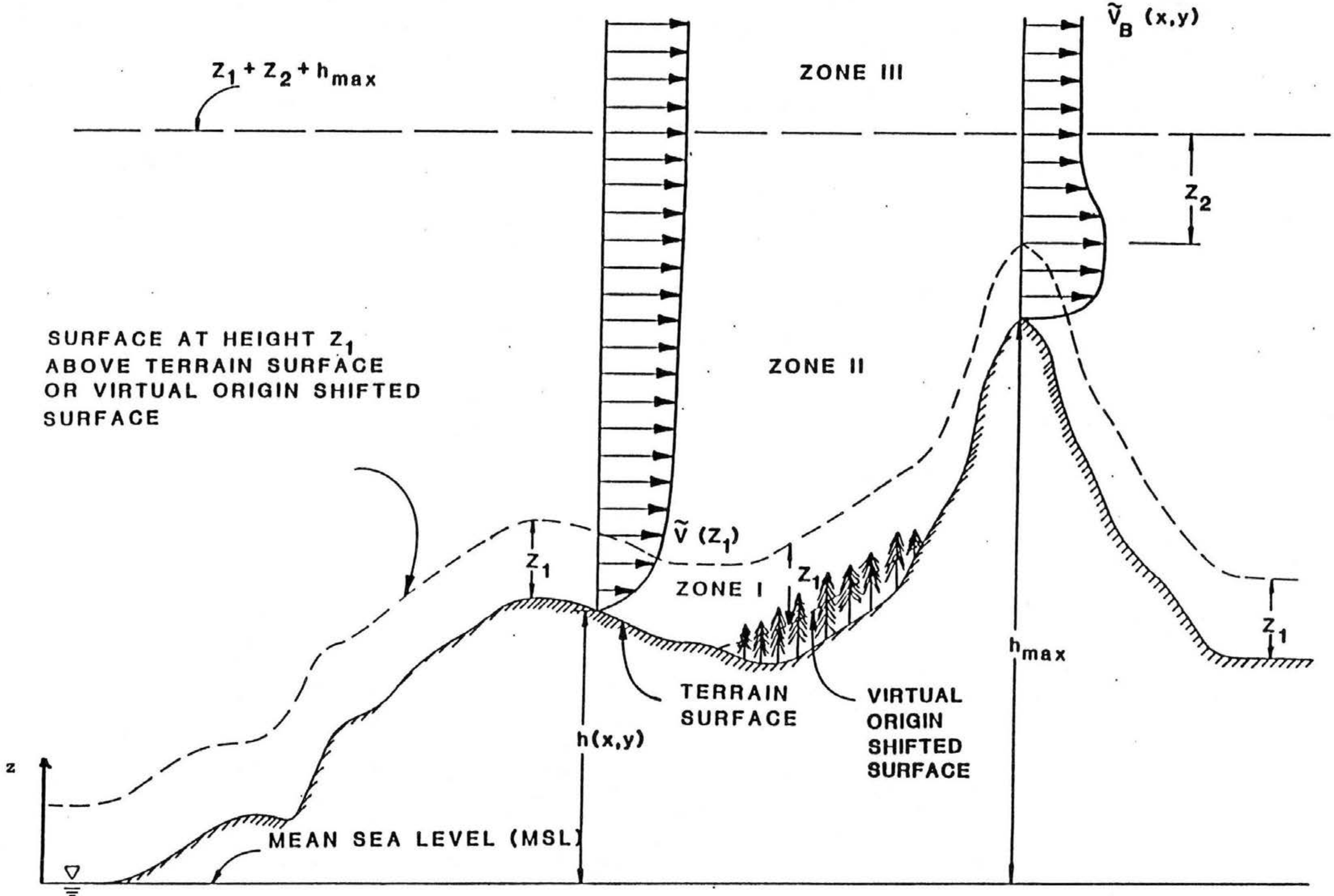

Figure 5.1.3 Initialization of vertical wind profiles for 3-D wind flow computations. (Lin *et al.*, 1985)

Lin (1989) reports the use of the same program to predict the reduction of fugitive dust over coal piles near a power station using wind shelterbelts and wind turbines to reduce surface wind speeds. A wind break model and a turbine wake model was added to the NOABL model. Lin (1990) combined the modified NOABL program, turbine wake model and a turbine performance model to estimate total energy availability for a complex site and distribution of wind turbines. Validation runs were made against field data available for actual wind farms for which wind energy performance was available.

(United Industries Corporation is no longer in business. They turned over their programs and data to R. Lynette and Associates, a consultant firm located in Redmond, Washington. This firm uses program to evaluate complex terrain for wind farm operators, investors, and insurance carriers concerned about low-wind regions used to promote wind energy investments.)

5.1.2 *Atmospheric Science Laboratory (ASL) Model Predictions*

Cionco (1982) and Lanicci (1985) report calculations using the ASL objective analysis model modified to include vegetation. **Figures 5.1.4** and **5.1.5** present a typical complex terrain scenario with grass, forest and villages and the resultant surface-layer wind field produced by the ASL model, respectively. The model appears to account for downslope and vegetation which results in convergence and divergence at a specified height. Cionco combined ASL diagnostic predictions with his own above- and under-canopy algebraic models which allow for specification of vegetative indexes and coupling ratios for different types of cover, **Figure 5.1.6**. The effect of a flow passing from a ten cm tall grass into a 15 m tall forest on a hillside is displayed in **Figure 5.1.7**. The model reproduced subcanopy jetting, lofting of the flow over the canopy wall and subsequent streamline penetration some 10 to 20 tree heights downwind.

Later Lancini used a 3-dimensional extension of the 2-dimensional ASL model to examine a 5 km x 5 km section of Fort Polk Military Reservation in Louisiana. The model was modified to handle the effects of stratification, streamline displacement and variable surface roughness associated with vegetation. The author assumed $d = 0.7\ h_{veget.}$ and $z_o = 0.14\ (h_{veget.} + 0.1)$. The model was used to calculate the effects of vegetation on drainage flows, but no field verification of the predictions were presented.

5.1.3 *NUATMOS Predictions of Complex Terrain Flows*

Ross et al. (1988) describe the mass-consistent model jointly developed by the Chisholm Institute of Technology, Australia, and the Rocky Mountain Forest and Range Experiment Station, Fort Collins, CO. Grandfather of this model is MATHEW and the father is ATMOS1, but the new model has better terrain following boundary conditions, parameters to separately adjust vertical and horizontal wind components, and versions can be run on PC-486 size computers. The RMFRS is currently adapting the model to include vegetative canopies, but the modifications are not yet available. NUATMOS has been "extensively" tested against field data from the CTMD and ASCOT programs. The model appears to correctly predict streamline splitting, plume impaction, and nocturnal drainage flows.

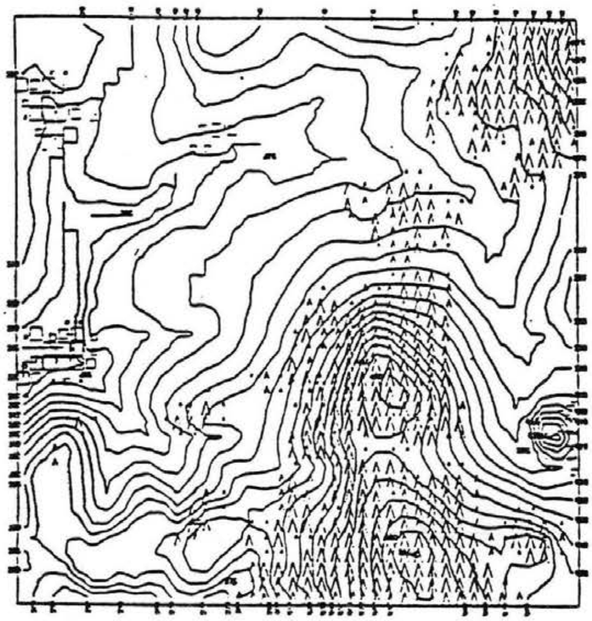

Figure 5.1.4 Typical complex terrain scenario with grass and forest (∧)vegetation and villages (□). (Cionco, 1982)

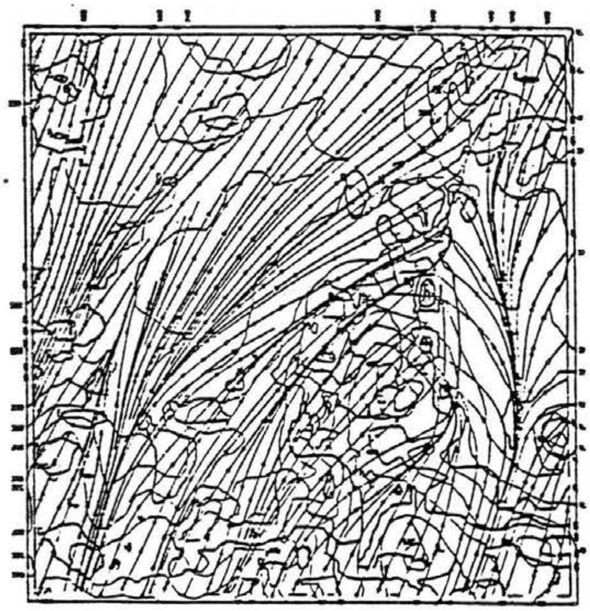

Figure 5.1.5 Surface layer windfield solution for Figure 5.1.4. (Cionco, 1982)

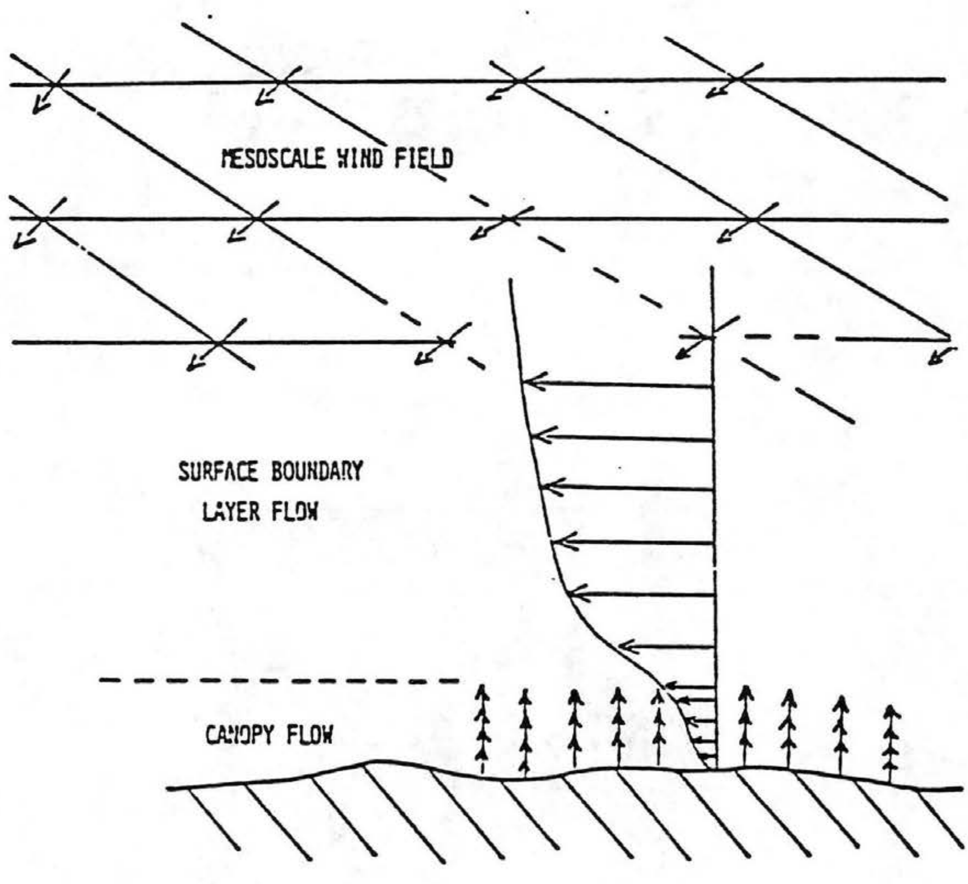

Figure 5.1.6 Schematic of 3-dimensional coupled wind model (Cionco, 1982)

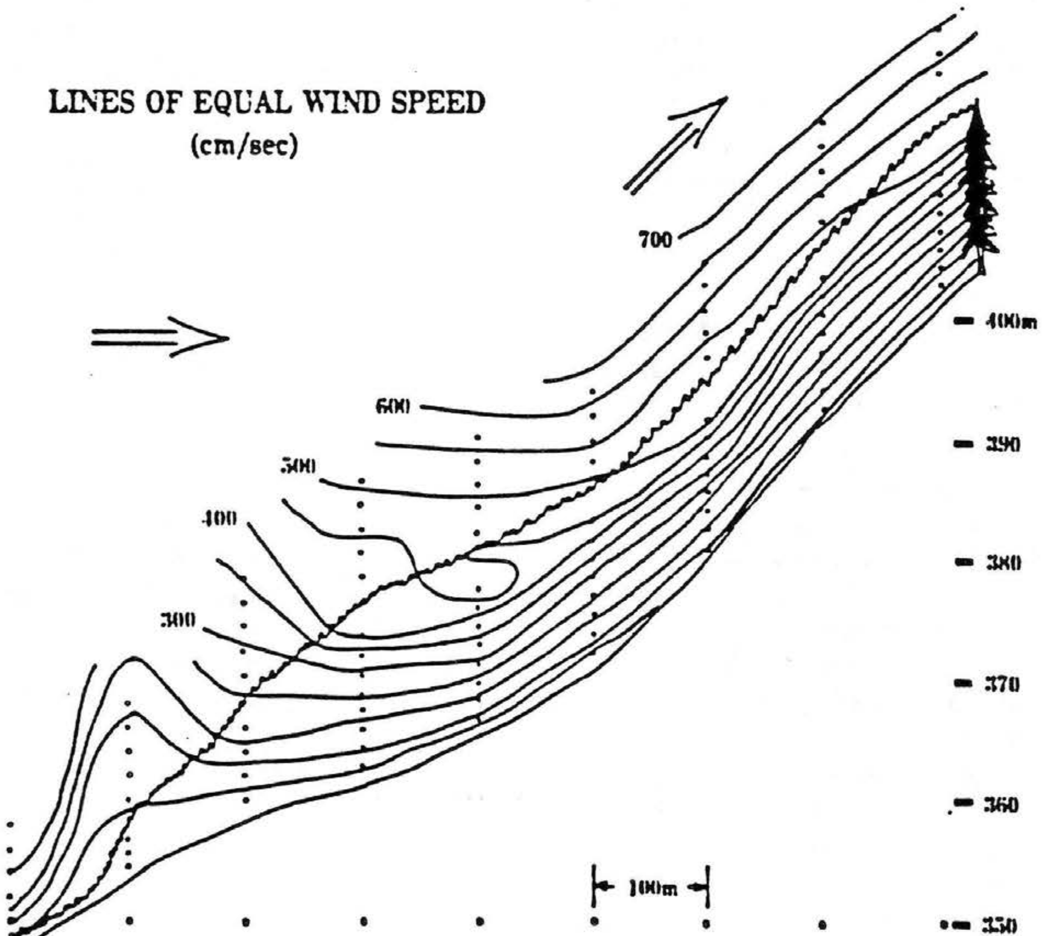

Figure 5.1.7 Cross-section analysis of adjacent grid point wind profiles. (Cionco, 1982)

5.2 Linear-perturbation Models Applied to Vegetation Covered Terrain

The linear-perturbation analysis approach originates with Townsend's (1966) analysis of roughness changes and the inviscid and laminar flow theories of perturbed shear flow and stratified flow. Jackson and Hunt (1975) developed algebraic equations which predicted the development of wind and turbulence over moderate slope two-dimensional hills and ridges. The advantage of the linear theory is that it enables formulae for the flow to be derived analytically. Independent effects of elevation variation, roughness, surface temperature variation, and atmospheric stratification are superimposed through addition of the individual perturbations calculated for each effect. Of course linear theories *cannot* describe large nonlinear-perturbations to the flow or nonlinear interactions where two or more effects combine such as roughness change and flow separation. Subsequently, it was recognized that if the surface elevations in arbitrary terrain were converted through Fourier transform into its component waves perturbation solutions could be obtained to the individual waves, and the resultant velocities can be re-transformed and summed into actual flow velocities (Carrruthers and Hunt, 1990). In contrast to numerical models that solve the equations of motion on a grid, there is no iteration involved and no doubt about the solution once the algorithms and their assumptions have been established. The resultant program is quite appropriate for use on small personal computers. The conditions on terrain and meteorology which must be satisfied for realistic solutions are mentioned in Appendix Section 3.0. Table A.2 lists several linear-perturbation models suitable for wind energy analysis.

5.2.1 *FLOWSTAR Model Predictions*

FLOWSTAR is designed to predict velocity fields over complex terrain in the presence of elevation variation, roughness variation, and stratification. The program is packaged with post processing graphics that can produce a streamline, flow vector, or profile graphs. The program is commercially distributed by Cambridge Environmental Research Consultants, Cambridge, U.K. Carruthers and Hunt (1990) report examples of output of the model applied to flow over isolated hills Brent Knoll and Great Dun Fell in England. No public literature references were found for the application of the program to forested terrain, and most subsequent publications relate to using the program to provide velocity fields to predict pollutant dispersion or the modification of temperature and humidity fields.

5.2.2 *MS3DJH and MS-MICRO Model Predictions*

The MS3DJH series of models are primarily intended to predict neutrally stratified wind flows over surfaces with variations of elevation and surface roughness. The model predicts velocities on one surface plain at a time. The wind data can then be exported for evaluation on commercial graphics software such as SURFER. A PC-version of MS3DJH designated MS-MICRO has also been coded. The programs are available at nominal cost directly from the Atmospheric Environment Service, Canada.

Walmsley, Taylor and Keith (1986) considered sinusoidal variations of roughness, predicted their influence with the MS3DJH program, and compared them to finite difference solutions over the same roughness variations. At values of $\lambda/z_o < 10^3$ phase errors appeared in the surface shear distribution probably due to advection errors. Also under the same limitations the lower level perturbation velocities were under predicted **(Figures 5.2.1 and 5.2.2)** . The model dealt with the step change in roughness problem quite well.. A series of 2-dimensional idealized terrain cases were examined with surface roughness variations. Gaussian shape hills were specified and both rough approach surfaces with smooth hills and smooth approach surfaces with rough hills were considered. Test cases were calculated for $h_{hill} = 100$ m, $\beta = 500$ m, $z_{ou} = 0.01$ m and $z_{0d} = 0.1$ m at the crest. for the rough-crested hill. The opposite roughness sequence was specified for the smooth crested hill. **Table 5.2.1** summarizes the predictions of MS3DJH and a finite difference model. The model appears to perform rather better with roughness or topography alone and tends to underestimate the surface stress perturbations at the crest in the combined case, **Figures 5.2.3, 5.2.4, and 5.2.5**. The neglect of nonlinear interactions must be partially responsible for this. The lee regions where non-linear effects become important are not predicted as well as the crest and upwind parts of the hill.

Finally two 3-D idealized hills with and without roughness were studied: (i) a 'Coastal Hill', an idealized circular coastal hill of cosine-squared section and (ii) an 'Island', a rough-crested cosine-squared hill with a cosine-squared distribution of $\ln[z_o]$. **Figure 5.2.6** shows cross-sections of normalized with speed (S/u_o) along the x-axis at $z = 2$ m. The contribution of the roughness change alone are quite different between the two experiments. When elevation effects are added, the shapes of the curves in the two cases appear similar, although the wind recovers to within 97% of the upwind values in the Coastal Island case. **Figure 5.2.7** illustrates the normalized wind speed at the crest of the hill. Above $z = 20$ m, the differences between the two cases are small. At lower levels the different roughness patterns produce larger velocities over the Coastal Island.

Walmsley and Taylor (1987) proposed to use the AES Regional Finite element Model (EFR) to predict areal averaged winds over 100 km squares. Then within a 256 square km region with a 128 square km central region finely represented the MS3DJH model could be used to interpolate the EFR data. Subsequently, a second interpolation could be made for a 15 square km region within which an 8 square km area can be finely represented for terrain as well as roughness variation. Demonstration runs were provided for several areas in Nova Scotia, Canada where meteorological observations were available for comparison. Land cover is mostly pine forest ($z_o = 1$ m), but main valley areas are cleared for farming ($z_o = 0.05$ m). The calculated wind velocities predicted up to 50% variations over high resolution areas. An algorithm was proposed to combine the various predictions into a forecast wind:

$$U(z = 10\text{ m}) = U_R(10) S_\Pi S(x,y),$$

where $U_R(10)$ = forecast FEM wind speed as average of 9 values at a 10 m height,
S_Π = is normalized average of nine values in coarse resolution model, and
$S(x,y)$ = is the prediction from the fine resolution run.

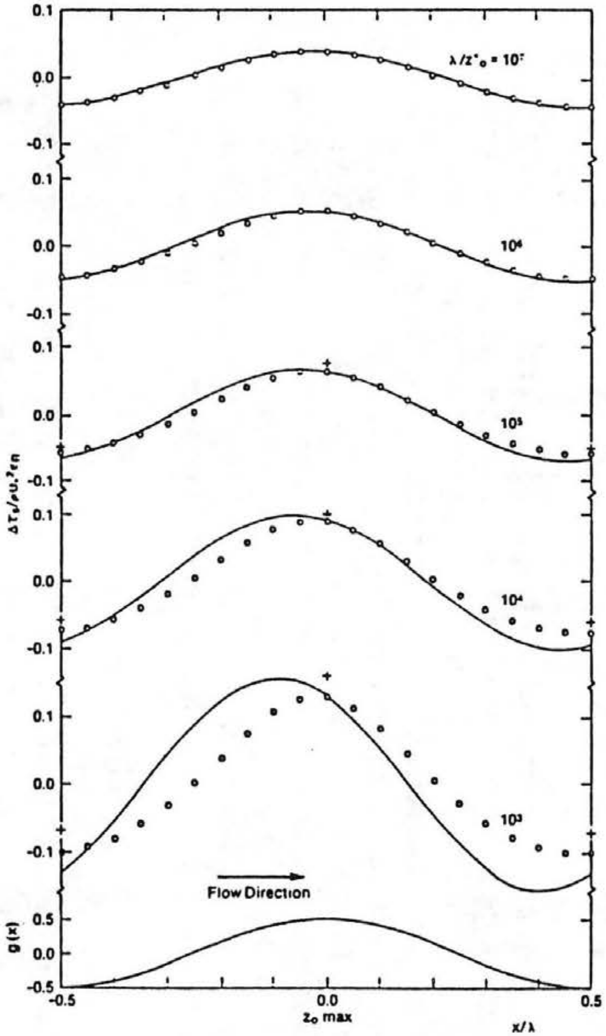

Figure 5.2.1 Sinusoidal hill & ln{z_o].———— MS3DJH/3R, finite diff. model, m_r = 4; + , m_r = 100. (Walmsley *et al.* 1987)

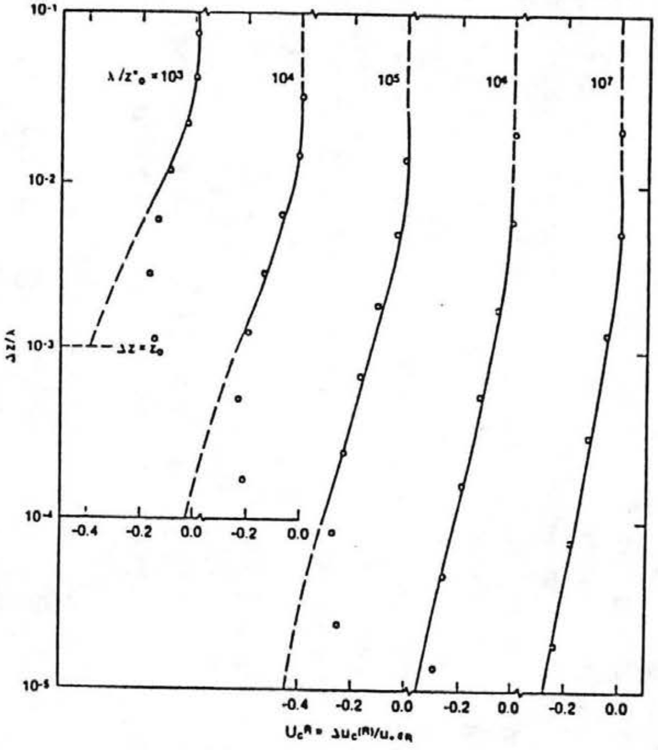

Figure 5.2.2 Crest velocities for sinusoidal hill and ln[z_o], ————MS3DJH/3R; Finite diff. m_r= 4. (Walmsley *et al.*, 1986)

Table 5.2.1 MS3DJH/3R and finite-difference model predictions for flow over Gaussian hills with roughness modulation. (Walmsley *et al.*, 1986)

MS3DJH/3R and finite-difference model predictions for flow over Gaussian hills with roughness modulation.

Terrain $z_s = h \exp[-(x/\beta)^2]$: h = 100 m, 2β = 1000 m.
Domain length XR = 12.8 km for MS3DJH/3R computations. Underlined values indicate the choices of z_0^* giving best agreement with the finite-difference model at Δz = 10 m.

(i) Rough-crested hill
$\ln(z_0/z_{0u}) = M \exp[-(x/\beta)^2]$: z_{0u} = 0.01 m, $M = \ln 10$ (m_r = 10)

	Surface pressure $p_c/\rho u_*^2$	Velocity perturbation, $\Delta u/u_*$ at $x = 0$								
		Δz = 1 m			Δz = 10 m			Δz = 100 m		
		(1)	(2)	(3)	(1)	(2)	(3)	(1)	(2)	(3)
MS3DJH/3R										
(a)	−117	$\underline{5.19}$	−2.08	3.11	$\underline{6.88}$	−0.51	6.37	$\underline{4.59}$	+0.01	4.60
(b)	−117	4.67	−2.48	2.19	6.79	−0.63	6.17	4.59	+0.01	4.60
(c)	−117	3.96	$\underline{-3.02}$	$\underline{0.94}$	6.65	$\underline{-0.80}$	$\underline{5.85}$	4.59	$\underline{+0.01}$	$\underline{4.61}$
Finite-difference										
model (1)	−142	4.62	−3.12	−0.35	6.86	−0.97	5.16	4.76	+0.01	4.75
(3)	−141									

(a) z_0^* = 0.01 m (upstream value).
(b) z_0^* = 0.03162 m.
(c) z_0^* = 0.1 m (crest value).

(1) Topography only.
(2) Roughness modulation only.
(3) Topography plus roughness modulation.

(ii) Smooth-crested hill
$\ln(z_0/z_{0u}) = -M \exp[-(x/\beta)^2]$: z_{0u} = 0.1 m, $M = \ln 10$ (m_r = 10)

	Surface pressure $p_c/\rho u_*^2$	Velocity perturbation, $\Delta u/u_*$ at $x = 0$								
		Δz = 1 m			Δz = 10 m			Δz = 100 m		
		(1)	(2)	(3)	(1)	(2)	(3)	(1)	(2)	(3)
MS3DJH/3R										
(a)	−65.5	$\underline{2.99}$	3.19	$\underline{6.18}$	$\underline{5.22}$	1.01	$\underline{6.23}$	$\underline{3.98}$	−0.01	$\underline{3.97}$
(b)	−65.5	4.00	$\underline{2.24}$	6.24	5.48	$\underline{0.68}$	6.16	3.97	$\underline{-0.01}$	$\underline{3.96}$
Finite-difference										
model (1)	−80.5									
(3)	−79.3	2.10	2.24	5.97	4.75	0.76	6.24	3.75	0.02	3.80

(a) z_0^* = 0.1 m (upstream value).
(b) z_0^* = 0.01 m (crest value).

(1) Topography only (z_0 = 0.1 m).
(2) Roughness modulation only.
(3) Topography plus roughness modulation.

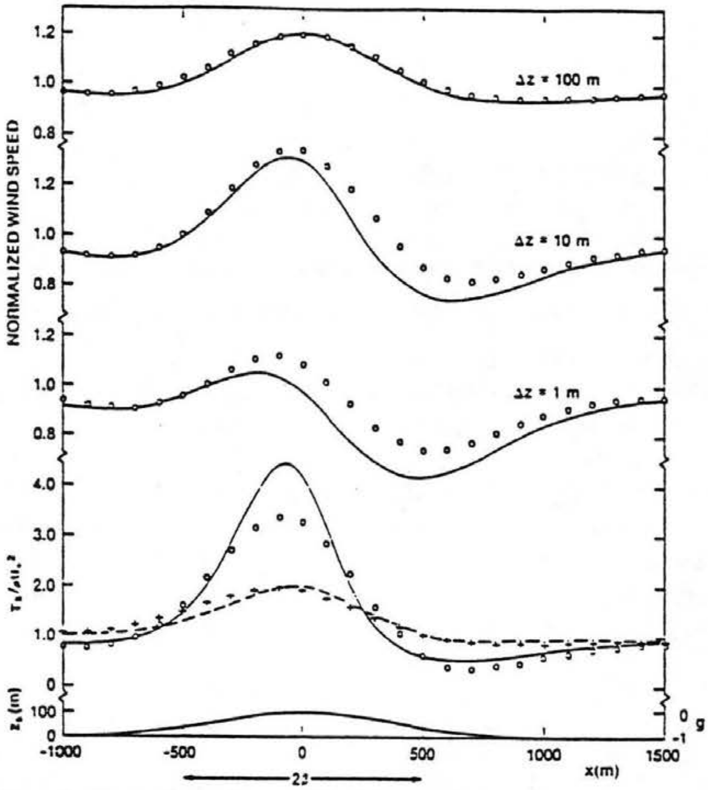

Figure 5.2.3 Rough-crested 2-D Gaussian hill,($2\beta=1000$m, h=100m, $m_r=10$)———u,--- roughness only fd model;○, + roughness only MS3DJH/3R model,

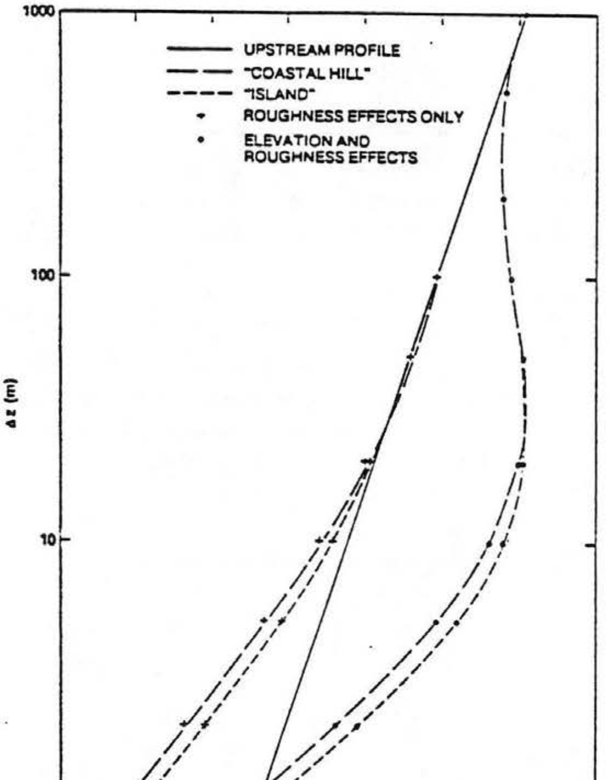

Figure 5.2.4 Crest velocities over rough-crested 2-D Gaussian hill (See Figure 5.2.3 for notation) (Walmsley *et al.*, 1986)

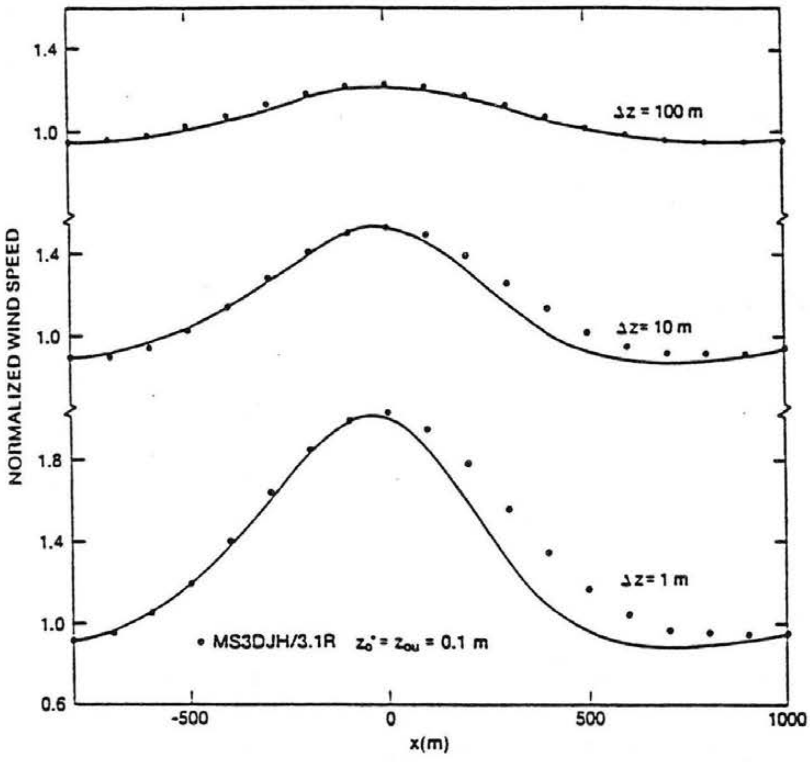

Figure 5.2.6 Wind speed at z = 2m for Coastal and Island experiments. Dashed curves are roughness change alone. (Walmsley *et al.*, 1986)

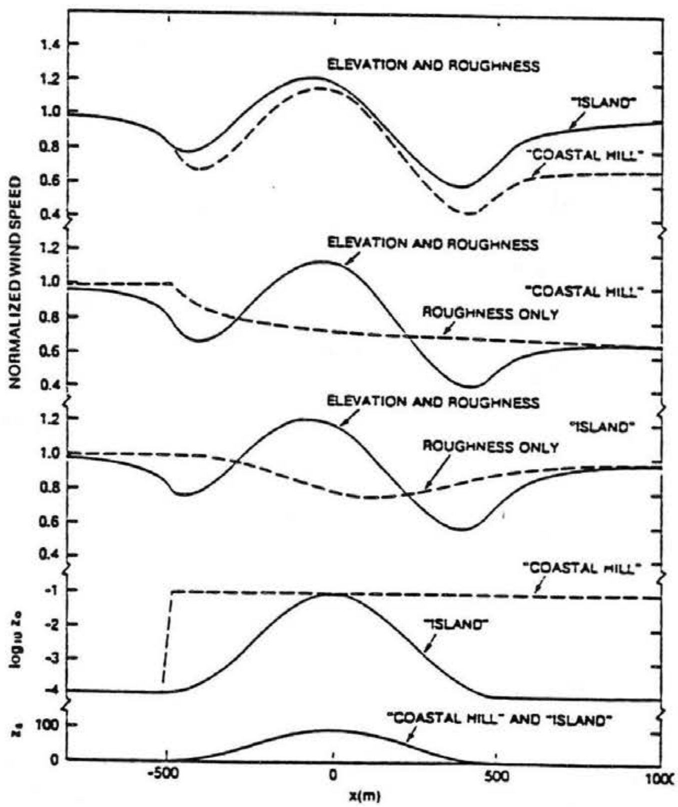

Figure 5.2.7 Cresttop velocities for the Coastal Hill and Island experiments. (Walmsley *et al.*, 1986)

For one case tested a 1 hr forecast of wind speed resulted in U(10) = 13.0 m/s but the actual observed average was 8.4 m/s. But corrections in roughness specified in the S_{II} level model to allow for roughness over the nearby ocean produced a revised estimate U(10) = 9.2 m/s. .

5.2.3 *Mass-consistent and Linear-perturbation Model Comparisons*

Lalas, Tombrou and Petrakis (1988) ran three numerical codes for wind-energy siting, WAsP of the Danish National Laboratory, MS-MICRO of the Atmospheric Environment Service of Canada, and NOABL* of Science Application Inc. for two sites on Limnos, an island in the norther Aegean sea with strong topography. WAsP and MS-MICRO are both based on linear-perturbation concepts. NOBAL* is a modified mass-consistent algorithm which includes initialization by logarithmic velocity profiles, the specification of different surface roughness at grid point, and variable transmissivity coefficient in the vertical direction.

Since most previous comparisons looked at hills that were rather isolated and simply shaped the intent of this study was to compare results in a more complex (and more realistic) environment. The island of Limnos has hills rising to 420 m and wind data have been taken at five sites on the island for some years. Three sites were selected for numerical simulation, two are in relatively smooth terrain and the third in a hillier region. **Figure 5.2.8** displays the winds predicted at the hilly site by the three codes. The mass-consistent model NOABL* was easy enough to use, but it took more computer resources and generally under-predicted wind speeds. WAsP produced the best combination of accuracy, ease of operation and computing power requirements. The version of MS-MICRO available was not easy to use and overpredicted wind speeds.

5.3 Primitive Equation Models Applied to Vegetation Covered Terrain

Primitive equation models compute all meteorological variables directly given appropriate initial and boundary conditions. The model codes can vary widely depending upon discretization, turbulence closure, initialization, and solution algorithms (FDM, FEM, FVM, etc.). Appendix Section 3.0 summarizes some features of such codes, and Appendix Table A.3 documents some of the major primitive equation codes. Because of the grid sizes generally treated in meso-scale models, the details of local or under-forest canopy flows are not always resolved. Since forest features are typically sub-grid scale their presence are accounted for by incorporation of appropriate drag terms.

5.3.1 *HOTMAC Predictions of Forest and Vegetation Effects*

Yamada (1982) used a simplified second-moment turbulence closure model to calculate the effects of a homogeneous infinite extent tree canopy on surface fluxes, wind speeds and turbulence. Yamada stipulated the normal 2.5-turbulence closure model that solves turbulent kinetic energy and length scale transport equations; however, terms were added in mean motion equations, turbulence energy equations, and length-scale equations for a form drag associated with the trees.

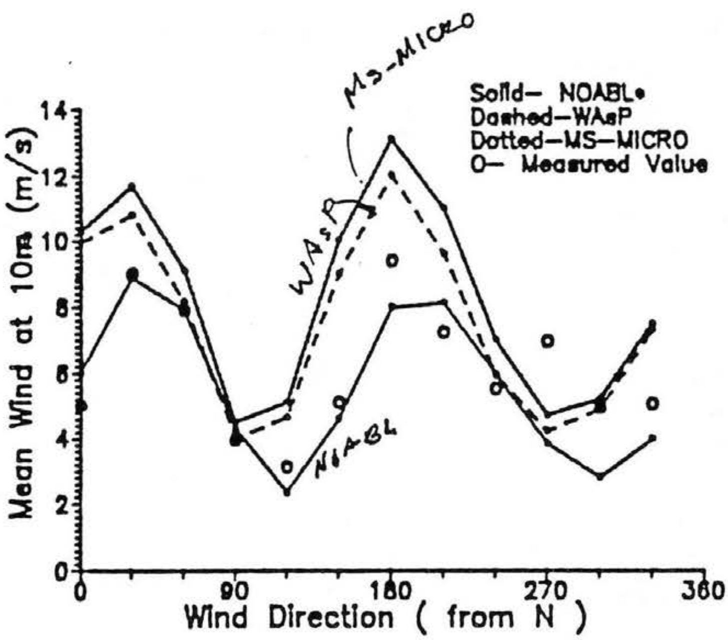

Figure 5.2.8 Mean wind speeds for each of 12 directions computed by WAsP, NOABL*, and MS-MICRO and measured values at Vounaros. (Lalas *et al.*, 1988)

The approach is based on idea that:

$$dp/dx = C_d a(z)\ U_i\ |U_i|,$$

where C_d is drag coefficient, a(z) is the plant area density, and the absolute sign insures that the direction of the drag force is always opposite to the wind direction. Corrections to the thermal energy equation were also proposed to adjust for radiation absorption and emission from the vegetation. Yamada calculated diurnal variation of potential temperatures, wind speeds, kinetic energy, eddy viscosity, and length scale for various assumed levels of vegetation coverage. As expected trees slow down the wind near the surface significantly.

Yamada and Bunker (1989) incorporated the tested drag and radiation relations into a three-dimensional mesoscale model HOTMAC. They applied this model with its vegetation adjustments to predict nocturnal drainage flows which develop during the evening in the Brush Creek valley in Colorado. Nudging was used to follow flow above the ridge top from observed (ASCOT 1984 field program) wind directions. Deviations from horizontally averaged temperatures and wind speeds were computed. **Figure 5.3.1** displays the horizontal distribution of tree canopies in the nested grid, and **Figure 5.3.2** shows typical horizontal wind vectors at 24 m above the ground a about 2 a.m. The tall tree canopy was believed to explain the inhomogeneous wind distributions, especially in levels below the canopy top. Notice that down valley flow vectors are reduced in forested regions.

5.3.2 *FITNAH Vegetation Modifications to Predict Deforestation Effects on Drainage Flows and Local Climate*

Gross (1987) modified a 3-d mesoscale model FITNAH to include the effects of a tall tree canopy on airflow in complex terrain. Specifically he examined a nighttime situation for cases with and without a canopy. He found surface wind speed will increase after deforestation. Tree effects were included by using the distributed drag system suggested by Yamada (1982). Terrain following coordinates were introduced such that η = (z-h)/(H-h), where h is the height of the topography and H is the height of the model domain. Stratification effects were also included through gravity terms. Perturbation pressures and temperatures were used to reduce errors. Fluxes were replaced by flux gradient transport expressions using total turbulent kinetic energy solved by a transport equation and a mixing length relation for eddy size.

A specific area in Finkenbach valley, Germany, was simulated and compared to field measurements. Effects of surface vegetation were included through two parameters; (i) the leaf surface area density and (i) a drag coefficient caused by leaves, stems and branches. Finkenbach valley trees are conifers mostly about 20 m tall. A drag coefficient $c_d = 0.2\ n_c^2$ was used where n_c is the fraction of area covered with trees. The author compared the current situation with complete deforestation. Computed results showed that when one compares points that were already deforested before and afterwards the surface temperature are very similar, but when a region was covered by trees before deforestation, then at night surface temperatures are significantly lowered whereas temperatures aloft may increase. After deforestation calculated

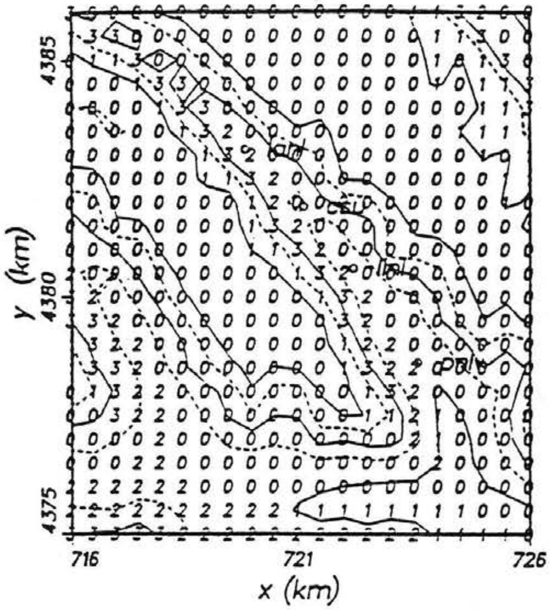

Figure 5.3.1 Distribution of tree canopies. Units are in decimal, *i.e.*, 3 indicates 0.3, 2 for 0.2, and 0 for no trees. (Yamada and Bunker, 1989)

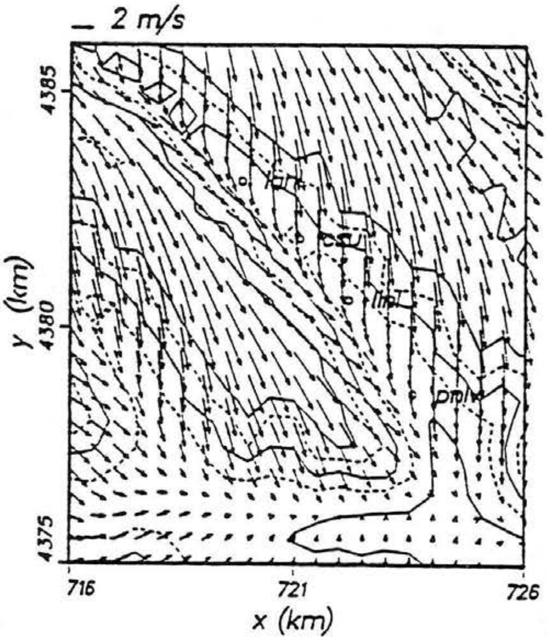

Figure 5.3.2 HOTMAC modeling of horizontal wind vectors at z = 24 m at 0200 LST. (Yamada and Bunker, 1989)

drainage winds were more intense, and the surface jet lies closer to the ground, **Figure 5.3.3**. Gross concluded after deforestation wind speed near the ground increases, depth of drainage flow decreases, surface temperatures decrease, but air aloft warms.

5.4 Spread-sheet Predictions of Wind Effects of Clearcutting

The linear-perturbation theory approach to predict effects of sudden roughness changes of airflow over 2-dimensional hills can be reduced to a few simple algebraic algorithms. These equations can be used to estimate the effect of forest clearcutting on ridge crest winds. These equations have been incorporated into a LOTUS spreadsheet, and the resultant predictions are discussed below.

5.4.1 *Linear-perturbation Expressions for Combined Changes in Roughness and Elevation*

As noted in Section 3.5.1: *Change of Roughness Models*, Jensen (1978) proposed that perturbations in mean wind velocities induced by surface roughness change could be calculated from:

$$Du(z)_{roughness} = (u_{*1}/j)\ \ln[z_{o2}/z_{o1}]\{(\ln[z/z_{o2}]/\ln[l_{zr}/z_{o2}]) - 1\}, \qquad [5.4.1]$$

where $l_{zr} \ln[l_{zr}/z_{o1}] = 2\, j^2\, x.$ [5.4.2]

Jensen and Petersen (1978) recommended perturbations induced by surface elevation change for triangular shaped hills could be calculated from:

$$Du(z)_{hill} = (u_{*1}/j)\ [1 + (h_{hill}/L)(\ln[L/z_{o1}]/\ln[l_{zh}/z_{o1}])^2]\ \ln[z/z_{o1}], \qquad [5.4.3]$$

where $l_{zh} \ln[l_{zh}/z_{o1}] = 2\, j^2\, L$ [5.4.4]

Since the solutions are separately linear their perturbations should be additive; thus

$$u(z)_{hill\ \&\ roughness} = u_o(z) + Du(z)_{roughness} + Du(z)_{hill}. \qquad [5.4.5]$$

These expressions are sufficient to calculate estimates of ridge crest wind speeds for different clearcut options over alternative slope triangular hills.

5.4.2 *Results of Spreadsheet Calculations*

Calculations were performed for a typical 300 m hill and an upwind forest with canopy height of 20 m ($d = 12.6$ m and $z_{o1} = 3.71$ m) over a range of hill slopes, (h_{hill}/L), varying from 0.05 to 1.0, clearcut to an average surface roughness, $z_{o2} = 10$ cm for distances upwind of the crest ranging from 0.2 L to 2 L. Data were prepared into figures that displayed resultant cresttop velocity profiles and cresttop fractional speedup factors.

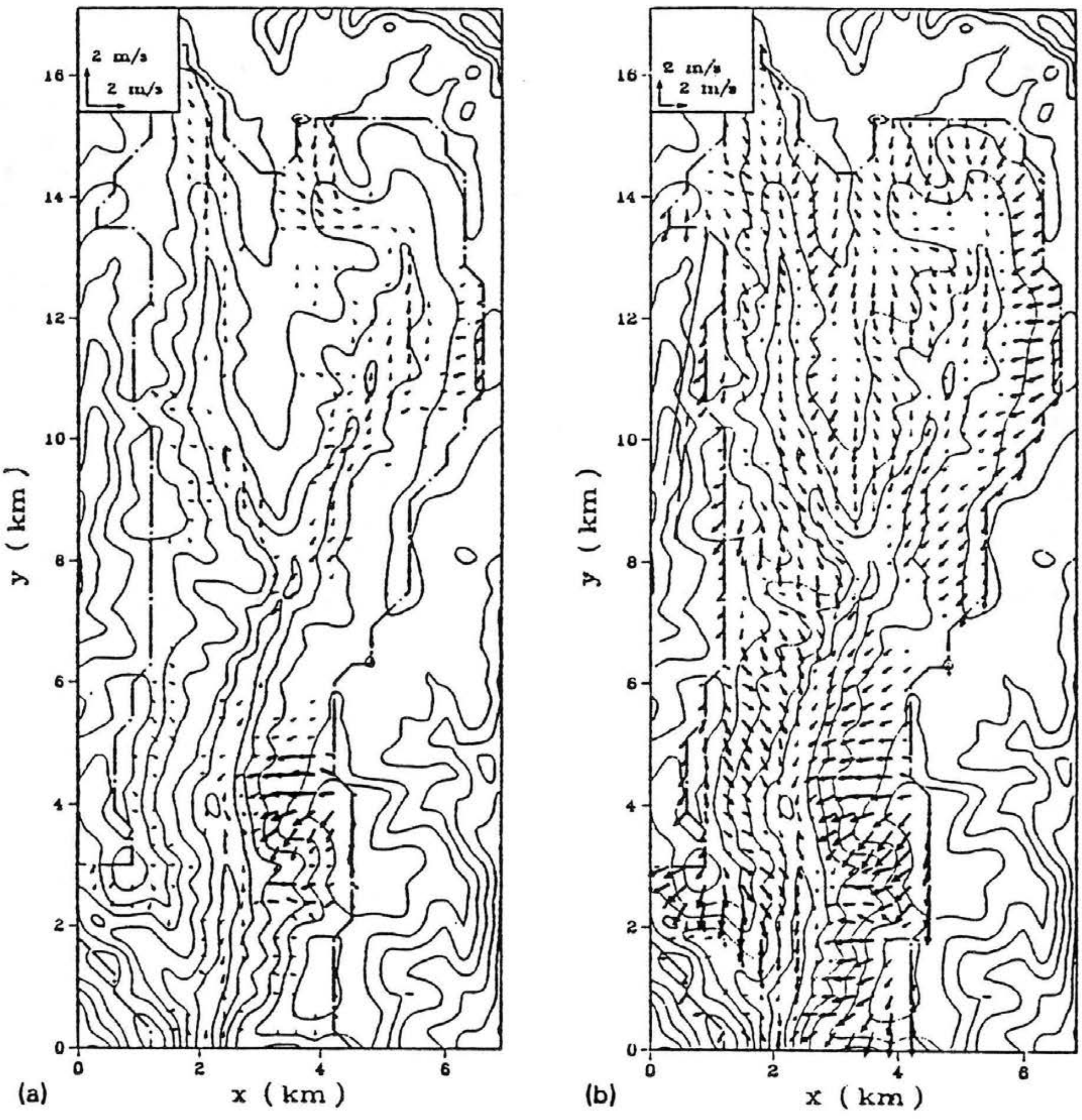

Figure 5.3.3 Computed wind vectors at 2 m above Finkenbach valley terrain: (a) with canopy, (b) after deforestation. (Gross, 1987)

Figure 5.4.1 displays inner- and outer-layer predictions of cresttop velocity profiles for a $h_{hill}/L = 0.1$ slope hill with and without clearcutting upwind to the half-height distance from the crest. Notice that the outer solution reflects the influence of the hill, but is not influenced by the change in surface roughness. Near the ground clearcutting will dominate the change in windspeed for shallow slope hills.

Figure 5.4.2 depicts the effect within the inner layer, l_z, of clearcutting upwind to the hill half-height, $x = L$, for various hill slopes. The relative improvement in windspeed decreases as hill slope increases. Since the maximum perturbation produced by roughness occurs at the ground level, the effects of tree removal on cresttop winds are most noticeable at the surface.

Figures 5.4.3 to 5.4.5 show the influence of clearcutting different distance upwind of hills with slopes, h_{hill}/L, ranging from 0.1 to 0.4. Since the inner-boundary-layer for the roughness change, l_{zr}, is now different than the characteristic inner-boundary-layer depth due to change in hill elevation, l_{zh}, the resultant wind profiles exhibit kinks where the effects of roughness and hill elevation on wind profile intersect.

Figures 5.4.6 to 5.4.8 show the same effects as **Figures 5.4.3 to 5.4.5,** but in this case the upstream roughness which characterizes the 20 m tall trees has been reduced to $z_{o1} = 1.85$ m. This roughness reflects the difference caused by using a different roughness height algorithm proposed by Lin et al. (1985) as opposed to the roughness algorithm proposed by Jaeger (1985).

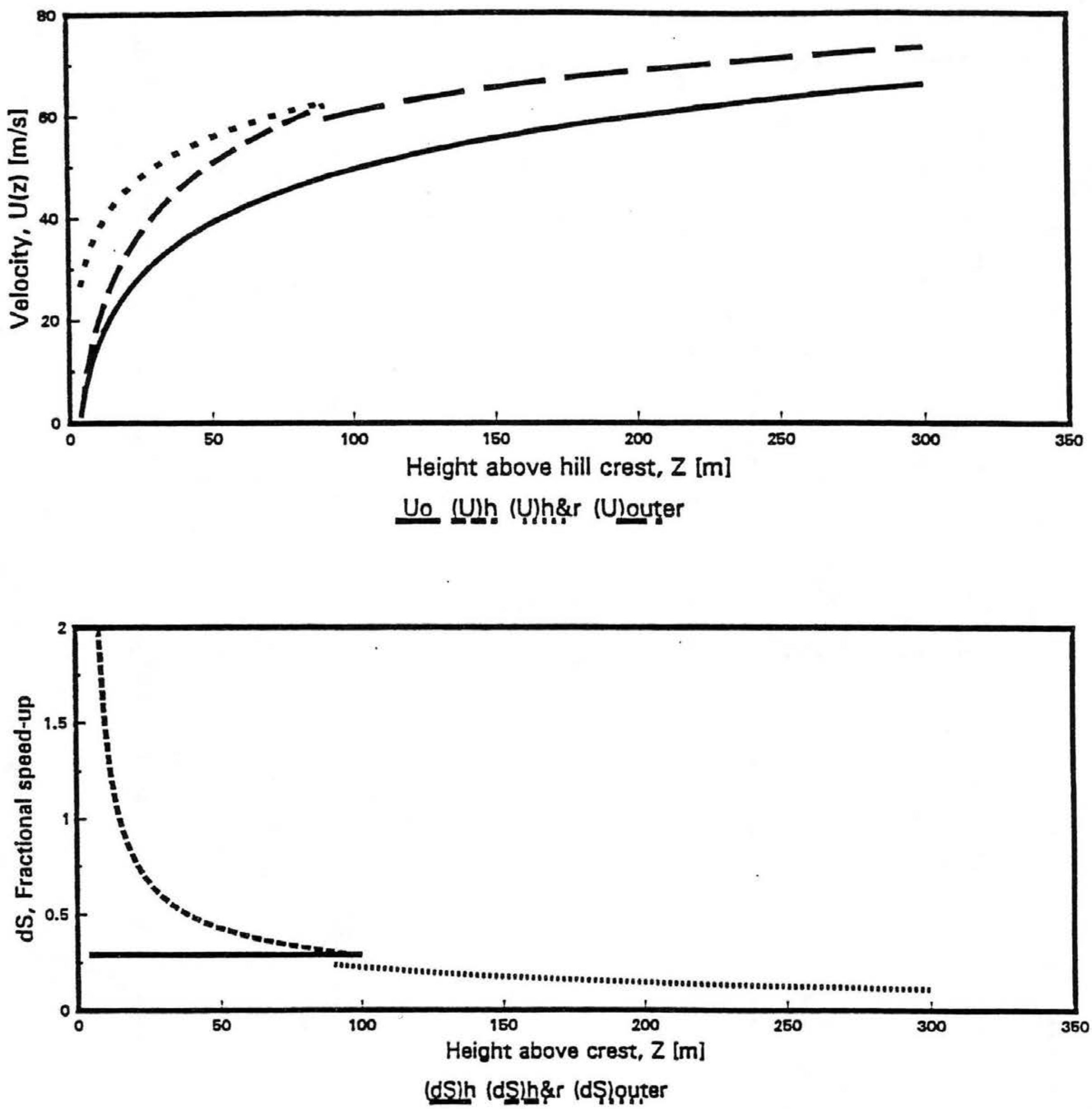

Figure 5.4.1 Linear-perturbation. Inverse-polynomial hill. h_{hill} = 100 m, L = 1000 m, z_{o1} = 3.71 m, z_{o2} = 0.1 m. U_{10m} = 10 m/s.

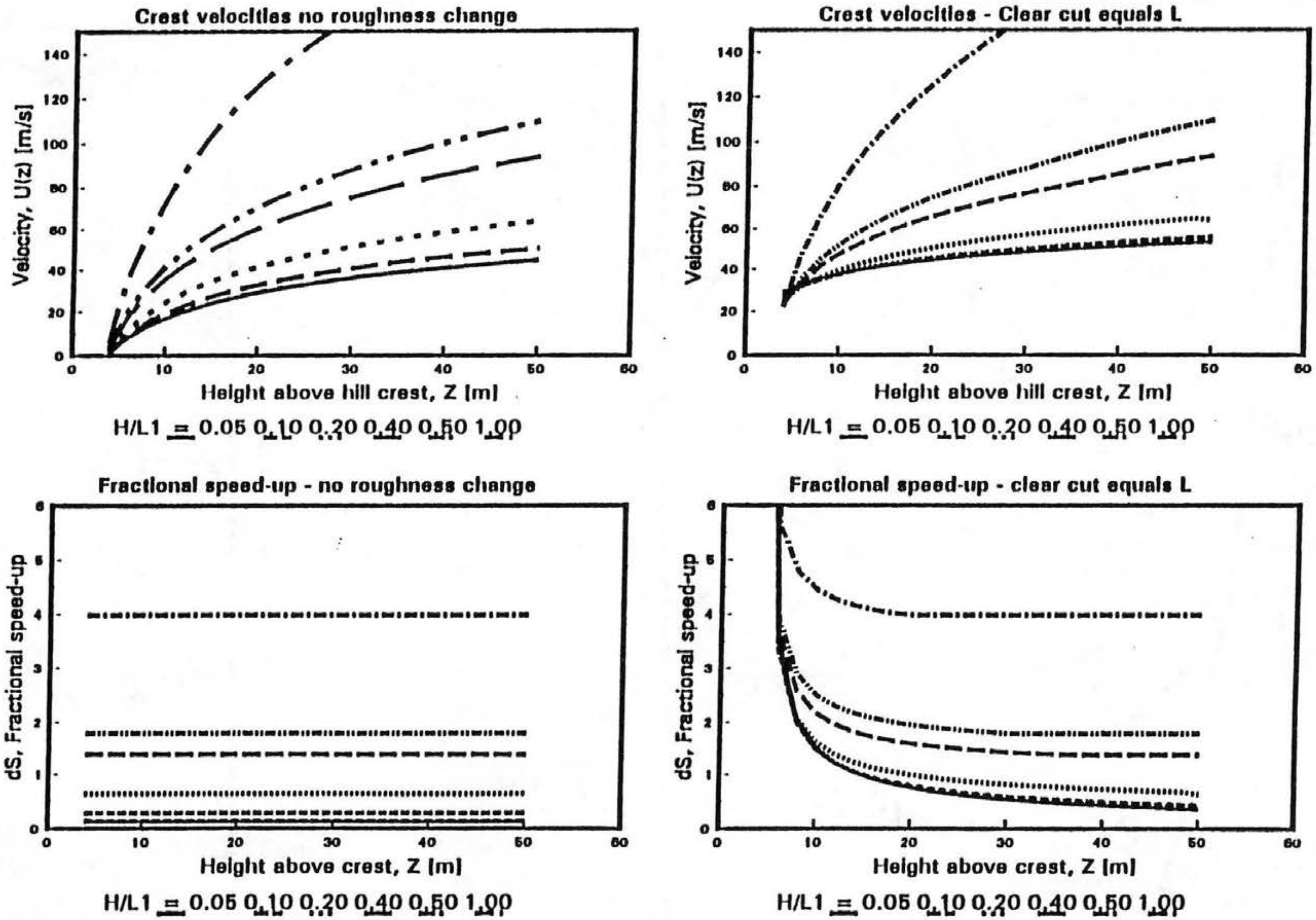

Figure 5.4.2 Effects of clearcutting upwind to the hill half-height, h_{hill} /L = L for various hill slopes. z_{o1} = 3.71 m.

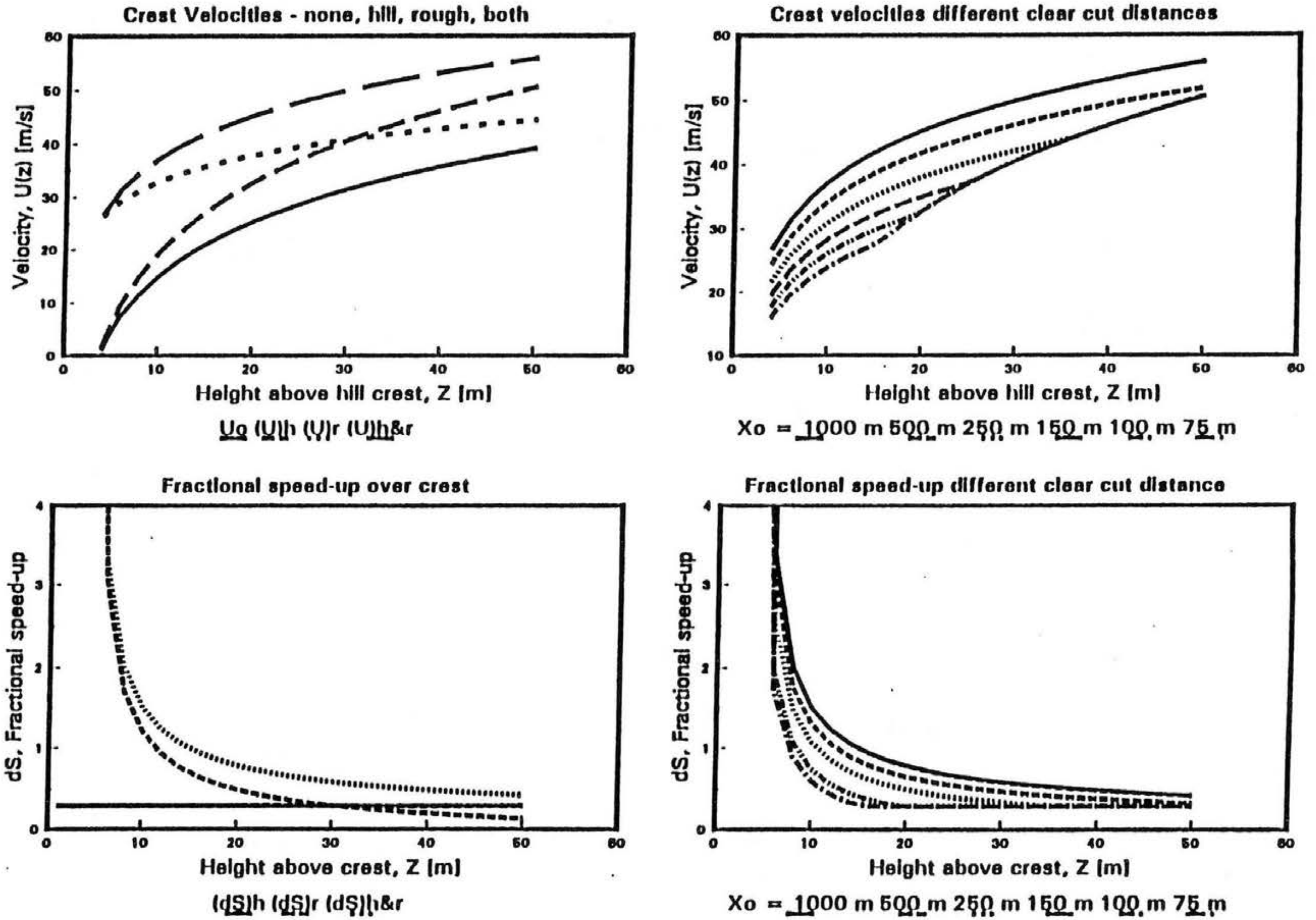

Figure 5.4.3 Influence on windspeed of clearcutting different distances upwind for a hill slope $h_{hill}/L = 0.10$. $z_{o1} = 3.71$ m.

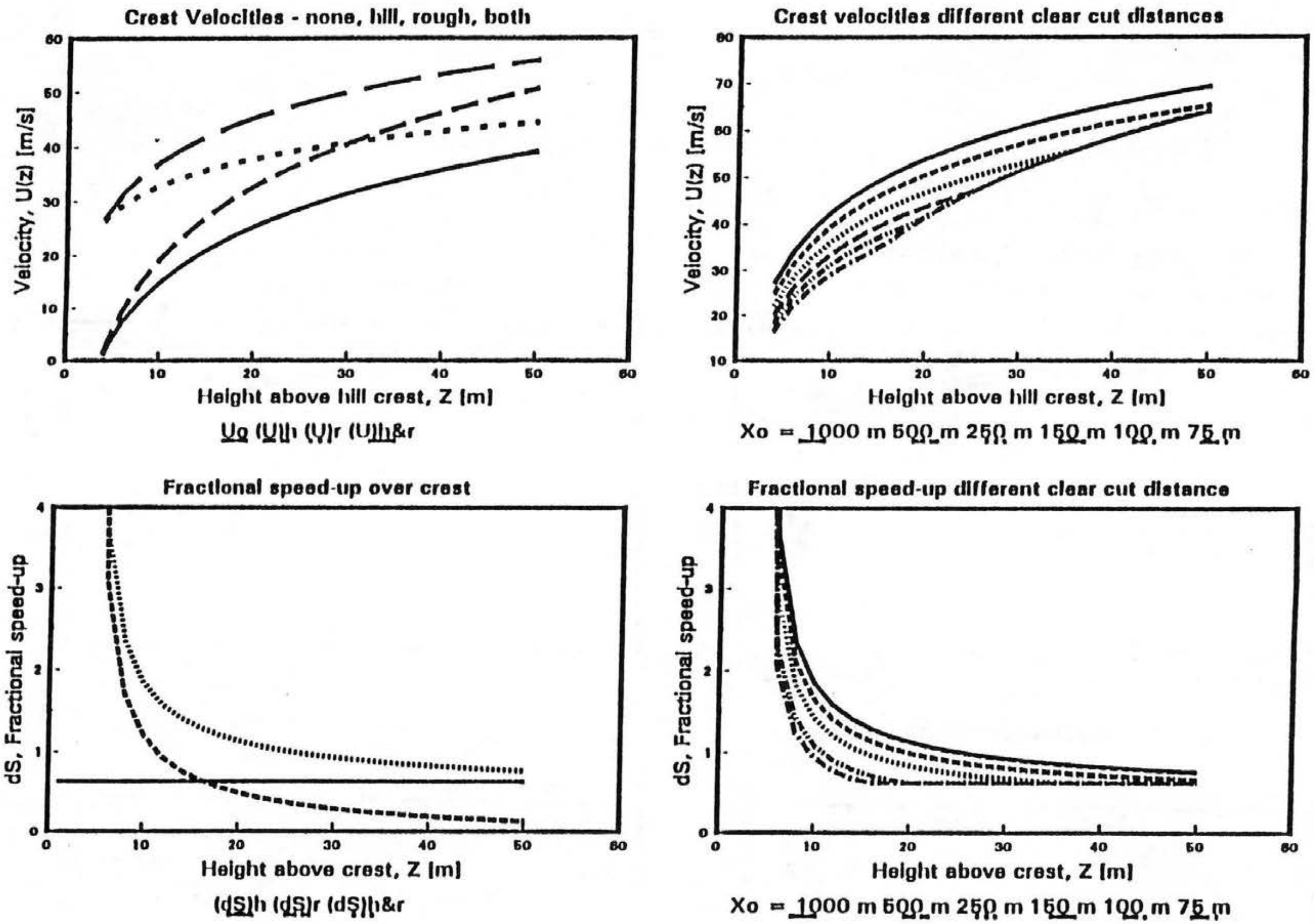

Figure 5.4.4 Influence on wind speed of clearcutting different distances upwind for a hill slope $h_{hill}/L = 0.20$. $z_{ol} = 3.71$ m.

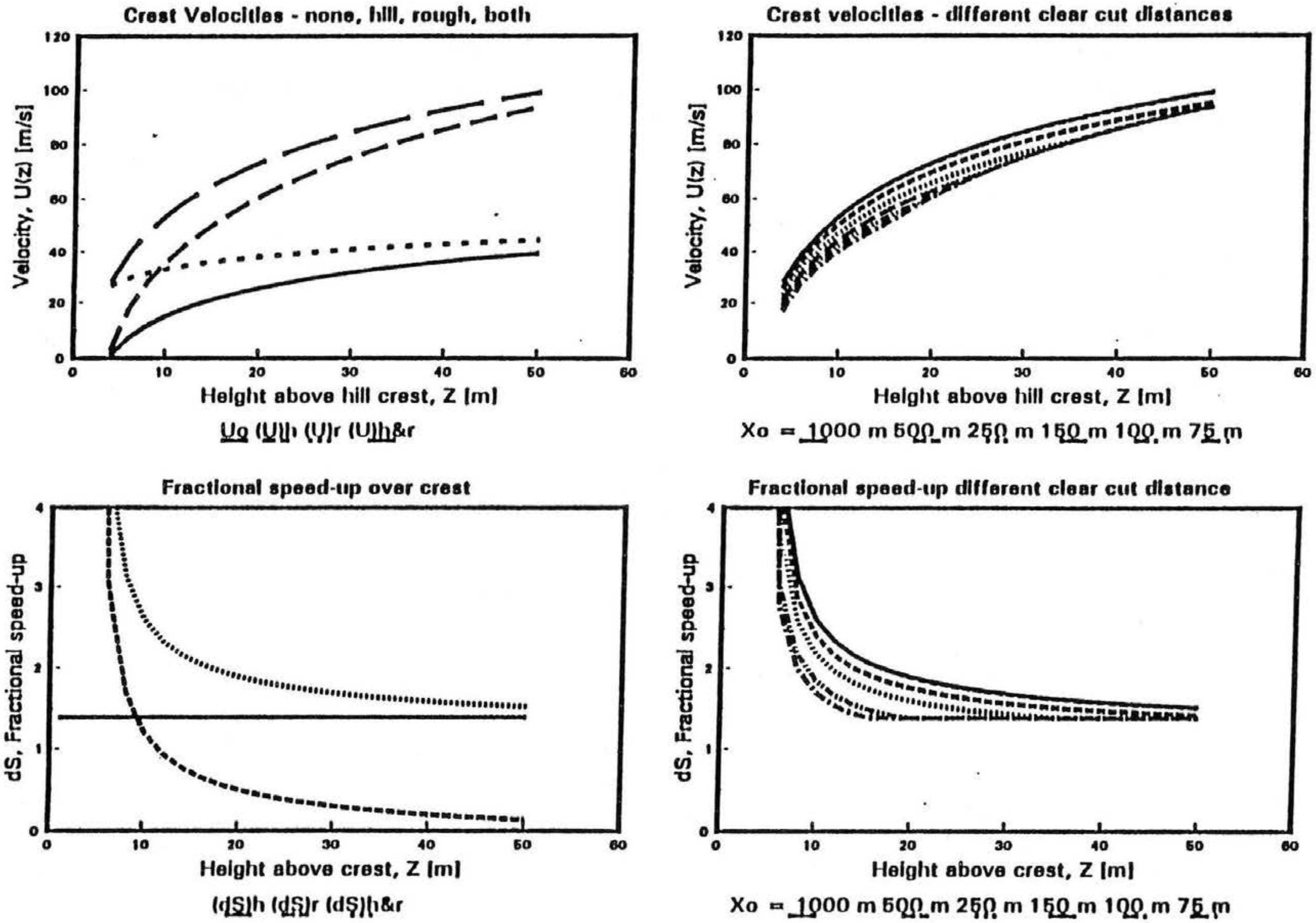

Figure 5.4.5 Influence on windspeed of clearcutting different distances upwind for a hill slope $h_{hill}/L = 0.40$. $z_{o1} = 3.71$ m.

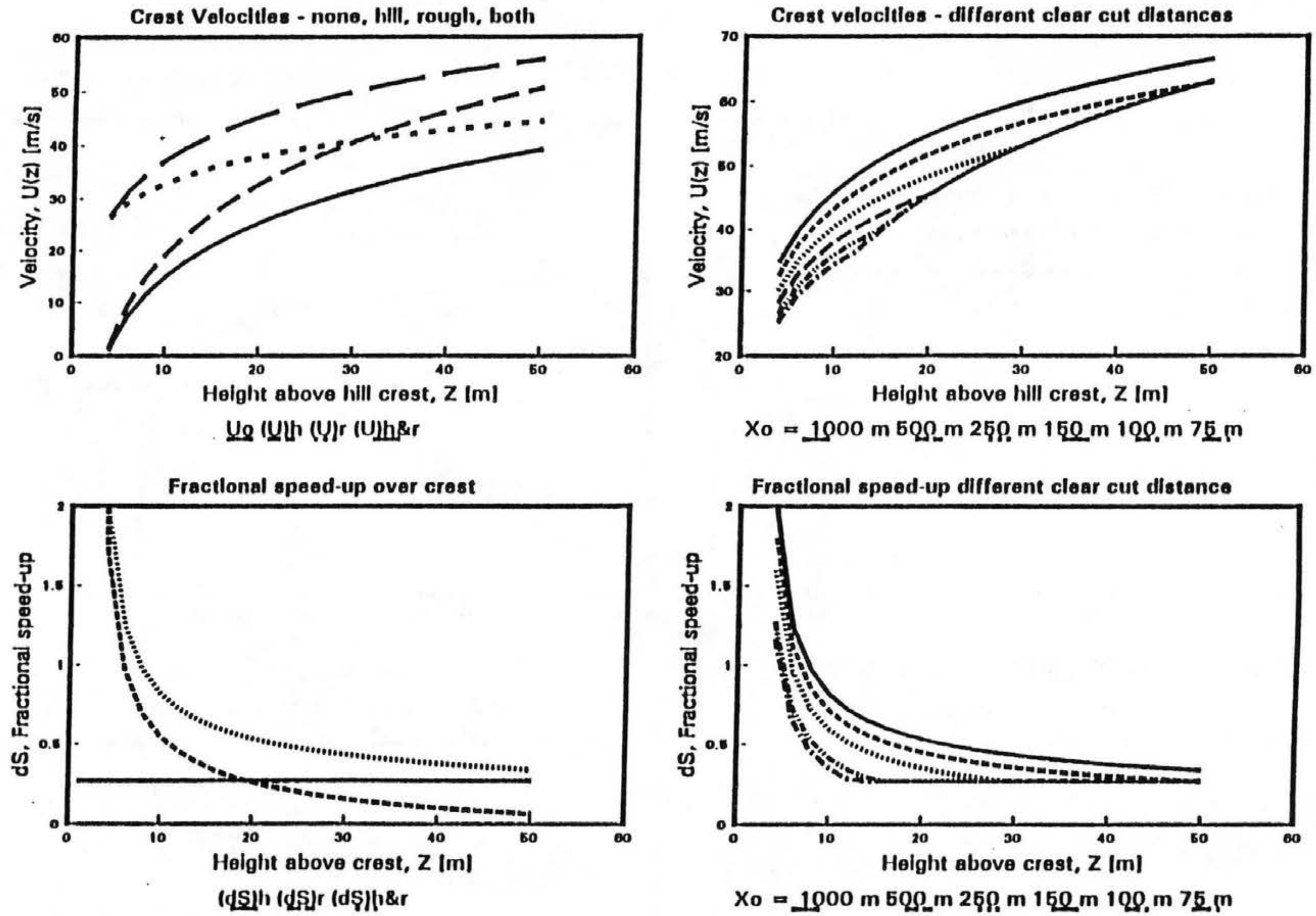

Figure 5.4.6 Influence on windspeed of clearcutting various distances upwind for hill slope $h_{hill}/L = 0.10$, $z_{o1} = 1.85$ m.

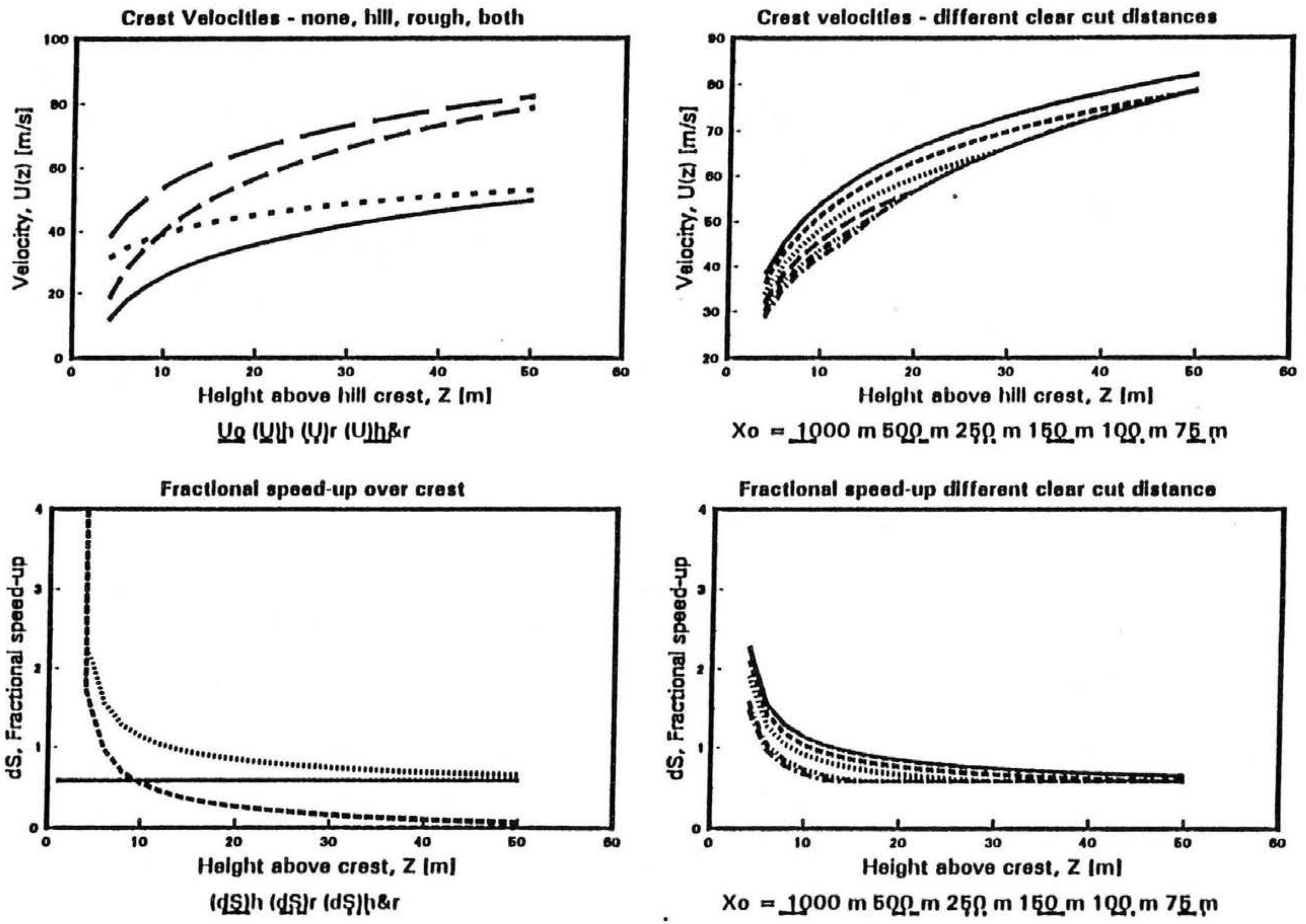

Figure 5.4.7 Influence on windspeed of clearcutting different distances upwind for hill slope $h_{hill} / L = 0.20$, $z_{ol} = 1.85$ m.

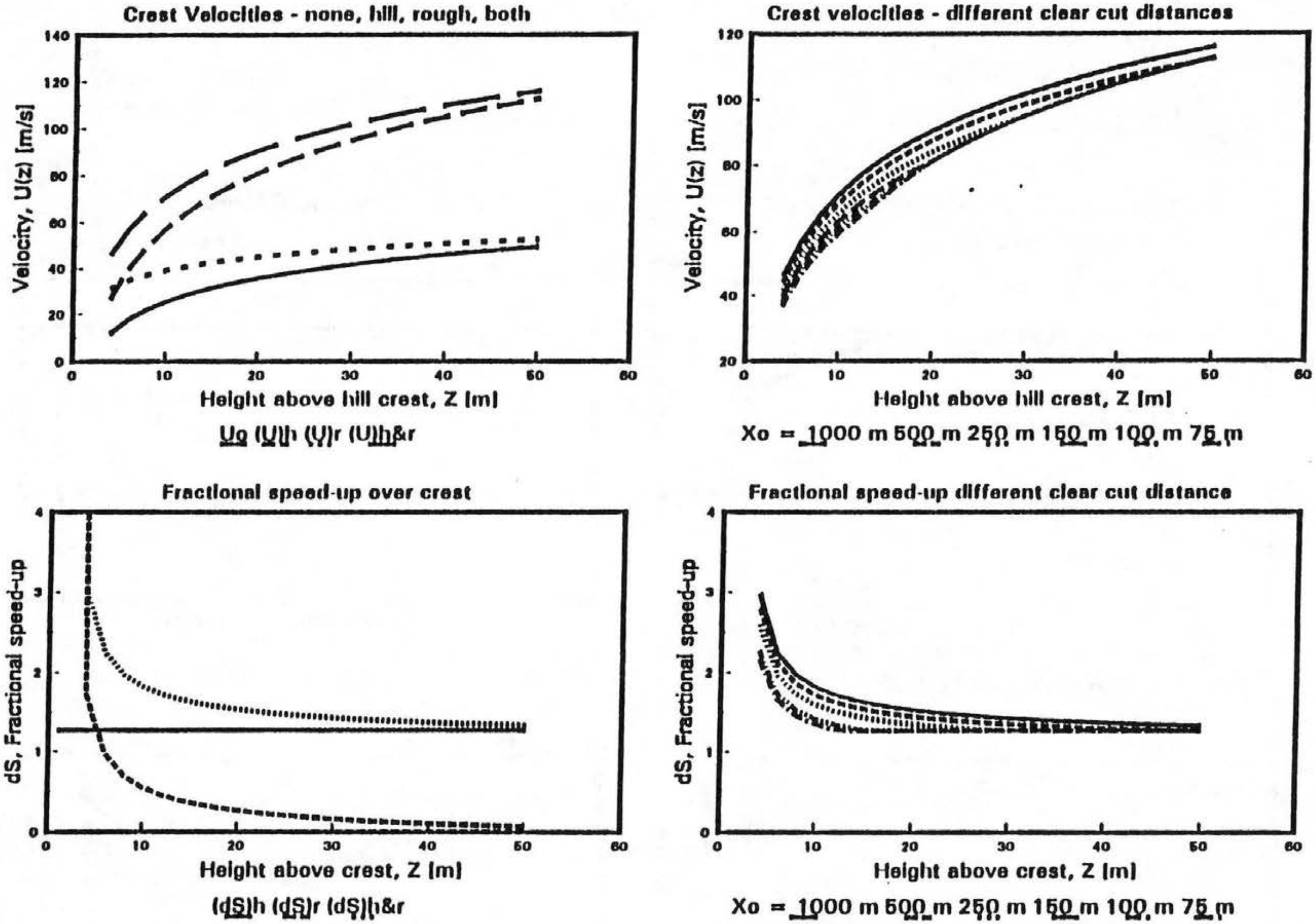

Figure 5.4.8 Influence on windspeed of clearcutting different distances upwind for hill slope $h_{hill}/L = 0.40$, $z_{ol} = 1.85$ m.

5.5 Summary

Numerical and analytic models now exist which can be used to predict wind behavior over complex terrain including roughness, elevation variation and stratification. These models have been validated against a number of isolated hills and ridges, most of which are covered with short homogeneous roughness. In the absence of flow separation and convective heating both the mass-consistent and linear-perturbation models predict wind speeds within 10-20%. The more versatile primitive models (but generally more expensive and cumbersome) reliably predict the same flowfields, but they also are believed to adjust for flow separation, convective heating, and non-linear interactions of flow variables and boundary conditions. Unfortunately, complete validation of all of these models in real complex terrain is not possible because of the varied limited extent of wind data taken over complex terrain combining variations in both elevation and roughness. In particular wind data downwind and over forest clearcuts are nonexistent.

Estimates have been prepared using linear-perturbation algorithm to predict probable effects of forest clearcuts for flow normal to ridges. The actual effect of such clearcut operations may vary significantly depending upon local variations in hill slope, the influence of terrain upwind of the ridge, the presence of atmospheric stratification, differences in upwind versus downwind hill slope, the presence of flow separation, and wind direction.

VI. CONCLUSIONS

This review set out to examine the effects of vegetation variation on wind fields over complex hilly or mountainous terrain. The character of wind over hills, wind over homogeneous vegetation, and wind over combinations of the two were considered. Both field and laboratory data on these topics were accumulated. Finally, numerical and analytic models were critiqued to determine if the state of mathematical calculations were adequate to predict such flows. Spreadsheet calculations based on linear-perturbation algorithms were then demonstrated.

Summary statements are appended at the end of each chapter. Succinct conclusions have been reduced to the following bulleted remarks:

- Qualitatively, the general behavior of flow over simple and complex terrain is well understood. Measurements in field and laboratory have been made over a wide range of conditions.

- Actual measurements in the field or laboratory of wind flow over vegetative cover which include edge transitions such as forest edges, clearings, or clearcuts are minimal.

- Wind profiles which develop under and above vegetative canopies can be predicted with fair accuracy. Measured profiles of wind speed follow analytic models closely. Wind profiles can be characterized by surface roughness, displacement height, and wind shear which correlate with canopy height and foliage distribution.

- Analytic linear-perturbation models exist which can predict the effect of roughness variation on wind profiles.

- The removal of vegetation upwind of the crests of hills has been shown to substantially increase hill-top winds and reduce the probability of separation and consequent gustiness.

- A variety of numerical programs exists which purport to predict wind flow over complex terrain even in the presence of roughness (vegetation) variation. These range from PC compatible mass-consistent and linear-perturbation programs which can be run in the order of minutes, to primitive equation models which require super or mini-super computers or large workstations to produce results in the order of hours.

- No numerical estimator is yet available which can forecast wind speeds over complex terrain in real time.

- Linear-perturbation algorithms predict that tree removal from ridge tops back to half-hill width will result in increases in ridge-top winds of the order of 929/421%, 390/162%, 150/54%, 53/14%, 37/8%, and 11/0% at heights of 10/20 m above 100 m hills as the hill slopes, h_{hill}/L, varies from 0.05, 0.10, 0.20, 0.40, 0.50 to 1.0, respectively.

- Linear-perturbation algorithms predict that tree removal from upwind distances of 2L, L, 0.5L, and 0.20L produce increases in ridge-top winds of the order of 179/75%, 150/54%, 116/32%, and 66/0% at heights of 10/20 m above a typical 100 m high hill of slope $h_{hill}/L = 0.2$.

APPENDIX: REVIEW AND CLASSIFICATION OF COMPLEX TERRAIN MODELS

REVIEW AND CLASSIFICATION OF COMPLEX TERRAIN MODELS

INTRODUCTION

A review of currently available complex terrain models is provided to select software which might provide wind energy siting in complex terrain information. The review does not propose to identify new computational research areas but to determine which models are ready for incorporation into a wind-energy management program. The review document contains:

a) An examination of the relative merits of phenomenilogical models, objective analysis models, linearized models, shallow layer models, or primitive equation models,

b) Examples of appropriate models in each category together with appropriate references and availability of source code, and

c) A critique of the various models, together with recommendations concerning model development or revisions necessary.

BRIEF HISTORY OF PREDICTION OF DISPERSION IN COMPLEX TERRAIN

The need to estimate reliably the impact of pertubed boundary-layer winds in regions of complex terrain for decision-making purposes remains a "key challenge" to the meteorological community (Egan and Schiermeir, 1985). For example, no adjustments for terrain influence on pollutant concentrations were made until the 1970s, when it became necessary to use diffusion models as a requirement of the U.S./ Clean Air Act and its amendments. Increased concentrations in rugged terrain can result from plume impingement on high terrain, pooling in valleys, drainage towards population centers, or persistence due to channeling. AMS, EPA, DOE, and EPRI have all supported workshops and research programs dedicated to a better understanding of air movements in rugged terrain. Prominent among the coordinated analytic, field and numerical studies have been EPA's Complex Terrain Model Development (CTMD) Program, EPRI's Plume Model Validation and Development (PMV&D) study, and DOE's Atmospheric Studies in Complex Terrain (ASCOT). These field studies have added substantially to the understanding of drainage and slope flows, stratified flow over and around isolated hills or ridges, and narrow valley circulations.

An excellent review of meteorological processes over complex terrain and the state-of-the-art of analytical, physical and numerical modeling was provided during the AMS Workshop on Current Directions in Atmospheric Processes Over Complex Terrain, October 1988 in Utah. The results of this workshop now appear in an AMS Monograph of the same name, and frequent reference to chapters were made during this review.

MODEL CLASSIFICATION

Prediction codes or algorithms for flow over terrain can be grouped into four flow categories of increasing flow complexity. These are a) flows for steady-state, straight line winds over homogeneous flat terrain, b) flows where flow impact or contact with the face of hills or ridges occurs due to terrain rising to intercept the approaching streamlines, c) flows which are diverted, accelerated or decelerated due to variations in surface contours, temperature, and roughness in the absence of separation or recirculation, and d) flows where backflows and recirculation may occur as a result of obstacle separation, valley drainage circulations, sea/lake circulations, etc.. Parallel with these flow categories one can identify six categories of numerical modeling:

i) Hill intercept models,
ii) Phenomenalogical models,
iii) Mass consistent or objective analysis models,
iv) Depth integrated models,
v) Linear perturbation models, and
vi) Full primitive equation models.

MODEL DESCRIPTION AND CRITIQUE

It will not be possible to review all complex terrain models here. A comprehensive list of models by name, type and author will be provided in tables. Prominent members of each category will be described to identify the advantages and disadvantages of each approach. Copies of almost all model source codes are available by request or purchase.

A. Dividing Streamline Models

Field measurements by Start et al. (1975) in Huntington Canyon, Utah, revealed that dispersion in complex terrain exceeded that in flat terrain by as much as an order of magnitude. Thus plume impaction assumptions led to overly conservative predictions. Hanna et al. (1984) proposed a Gaussian model where plume path took into effect atmospheric stratification through a hill Froude number effects. More recently RTDM (Rough Terrain Dispersion Model) which uses an ad hoc approach was tentatively approved by EPA for a "third level" screening model, and most recently the CTDM (Complex Terrain Diffusion Model) has been proposed which corrects for atmospheric stratification effects on plume paths around isolated hills and ridges (Hanna and Strimaitis, 1990). Unfortunately, these models are intended for plume impact on features closest to the source. They are not intended for application with many hills and valleys, nor do they contain any wake algorithms for simulating the mixing and recirculation found in cavity zones in the lee of a hill.

B. Phenomenological Models

Phenomenological models are those which use simple and specific insight about a limited phenomena to predict flow motions. For example Harvey and Hamawi (1986) modified the Gaussian dispersion equation to accommodate restricted lateral dispersion in deep river valleys. Multiple eddy reflections are assumed to occur between valley walls, the ground and the inversion over the valley; this leads to a simple imaging approach to estimating valley dispersion. Unfortunately the model presumes no temporal variation in valley conditions.

The boundary layer evolution of narrow mountain valleys during the early morning has been studied extensively, and a detailed description of this phenomena is provided by Whiteman (1990). Whiteman and Allwine (1985) and Bader and Whiteman (1989) proposed a phenomenological model titled VALMET for well-defined deep mountain valley diffusion based on the principles that:

> The nocturnal stable layer in a valley is destroyed by the growth of the convective boundary layer over the valley floor and sidewalls and the subsidence of the stable air mass in the valley center as the upslope motions transport mass out of the valley.
>
> Asymmetric heating of the valley sidewalls by the sun can skew the development of the boundary layer, with a tendency towards upslope motions on the heated sidewall and residual stability on the shaded sidewall.

The (1985) version of the model presumes that the valley air is "loaded" with pollution during the night, and then the early-morning motions fumigate this pollution downwards to the valley floor and sidewalls. The assumption is made that the night-time plume is "frozen" within the stable core. To work effectively twenty-seven input parameters are necessary to drive the model which includes topographic, temperature inversion, downvalley wind speeds, atmospheric stability and sensible heat flux characteristics. The model is driven by thermodynamic equations for the convective boundary layer (cbl) ascent and inversion descent coupled with continuity relations to maintain mass conservation and calculate up-slope wind speeds.

The model has not been validated quantitatively against field measurements. It would require substantial revision to incorporate the segments of airplane delivered elevated aerosol clouds delivered over a range of valley locations. Finally, the model is limited to well-defined narrow valleys; thus, emission above or below the stable core, cross valley flows, tributary flows, etc. are not be accounted for in the VALMET model.

TABLE 1: PHENOMENALOGICAL MODELS

GAUS PLUME MODEL FOR VALLEYS	Yankee Atmomic Electricity Massachussetts	Harvey and Hamawai (1986)
U. OF UTAH	Meteorology Department, U. of Utah	Lee and Kau (1984)
VALMET	Battelle PNWL	Whiteman and Allwine (1985)

C. Mass Consistent or Objective Analysis Models

This class of models combines some objective (regression or maximizing or minimizing some variable) analysis of available wind data to form a wind field. The wind field analysis typically forces the resulting flow to satisfy air mass continuity by constraining the flow between the ground surface and some elevated inversion height. Such models may either produce a fully three-dimensional wind field, or they may solve the depth integrated continuity equation in a horizontal plane, and then recreate a vertical field assuming certain similarity profiles.

Table 2 lists objective analysis models which attempt to adjust wind fields rather than just interpolate between field data. Recognition of the need to include terrain effects in mass-consistent calculations led to the development of three-dimensional, time-independent, finite-difference, regional wind field models like MATHEW (Mass-Adjusted Three dimensional Wind field model) or FEMASS its finite element counterpart. In both models the Sasaki variational analysis technique is used in adjusting a discrete field of time-averaged interpolated winds for mass consistency. Basically, the procedure entails minimizing the squares of the differences of the observed (interpolate) and analyzed velocity components subject to the imposed constraint of incompressibility. MATHEW uses a traditional approach in simulating terrain by representing the boundary surface as a system of regular blocks whose impenetrable sides lie along coordinate lines. FEMASS produces the shape of the boundary surface by the lowest row of nodes in the grid which, when interconnected, form a system of curvilinear patches. Thus FEMASS produces a more precise representation of an irregular surface. NOABL is a modification of MATHEW to use a terrain-following coordinate system.

The atmosphere's thermal structure is not explicitly considered in the model equations of MATHEW or FEMASS, but the phenomenological effect of stability can be simulated to a certain extent by making a judicious choice of the Gauss precision moduli weights. The IMPACT model uses a series of "transparencies" which overlay the grid points and use a $1/r^4$ weighing of stability at the data points. IMPACT also treats thermal drainage winds by adding a component to the vertical velocity near the surface, but the inclusion of thermally generated winds appears to be done without regard to local ground slope.

Mass consistent models have been modeled against mathematical tests, wind-tunnel terrain flows, and field data (Lewellen and Sykes, 1985; Lewellen, Sykes and Oliver, 1982). The block terrain feature in MATHEW induces 0(1) errors near the surface, and yet with the exception of the layer immediately adjacent to terrain changes, the mass adjustment imposes relatively minor adjustments to the interpolated wind fields. Lewellen et al. (1982) question whether such minor

TABLE 2: MASS CONSISTENT AND OBJECTIVE ANALYSIS MODELS

MODEL NAME	ORGANIZATION	REFERENCE
ATMOS1	Los Alamos Ntl. Lab.	Davis and Bunker (1980)
BLM/TM	NOAA/NWS	Long, Schaffer and Kemler (1978)
CHAPEAU	Dupont/SRL	Pepper and Baker (1979)
COMPLX	SRI International	Englich and Lee (1983)
FEMASS	LLNL	Gresho, et al., (1978)
IMPACT	Form and Substance Inc.	Fabrick, et al., (1977)
(Now called SMOG)		Wacker and Londergan (1984)
MASCON	LLNL	Dickerson (1978)
MATHEW/ADPIC	LLNL	Sherman, Lange (1978)
MESOGRID	ER&T	Morris, Berkley and Bass (1979)
NOABL	Science Applications Inc.	Phillips (1979)
PATRIC	LLNL	Lange (1978)
PHOENIX	Oak Ridge Ntl. Lab.	Murphy (1979)
PIC	Systems, Science & Software	Sklarew, et al, (1971)
RADM	Dames and Moore	Runchel, et al., (1979)
PDM	Systems Applications Inc.	Liu, et al, (1976)
TAPAS	USDA-Forest Service	Fox, et al., (1987)
(NUWNDS)		Ross, et al., (1988)
(NUATMOS)		"
U. of Hawaii BL Model	Meteorology Department U. of Hawaii	Erasmus (1984)

TABLE 3: PERTURBATION MODELS (LINEARIZED)

FLOWSTAR	Cambridge Environmental Services	Carruthers, et al., (1988)
MS3DJH/1,2,3,3R	Atmospheric Environment Service, Canada	Walmsley, et al., (1980 1982, 1986)
MS-MICRO	Atmospheric Environment Service, Canada	Walmsley, et al. (1987)
WAsP	Danish National Laboratory Denmark	Troen et al. (1987)

TABLE 4: DEPTH INTEGRATED MODELS

2D FLOW	--	Garrett and Smith (1984)
Integrated Drainage Model	NOAA/ATDL/ARL	Dobosy (1987)

changes justify the computer time spent on MATHEW. NOABL and FEMASS were found to produce substantial improvement in near surface wind predictions. NOABL seems unreliable when computing flows which go around obstacles, because the numerical scheme can diverge if the stability parameter is pushed too far in the direction of no vertical motion. IMPACT contains substantial numerical diffusion when flows move diagonally across the numerical grid. Many mass consistent models are not constructed to handle flow separation over ridges or valleys or temporal variations of wind data; however, modifications to include temporal effects should be possible. Finally objective models depend critically on the quality as well as quantity of the observed data and the empirically chosen constants involved in the models.

TAPAS (Topographic Air Pollution Analysis) is a computer modelling system being developed jointly by the Centre for Applied Mathematical Modeling at Chisholm Institute of Technology, Australia, and the Rocky Mountain Forest and Range Experiment Station, USDA-Forest Service. It contains simulation models of varying complexity, input data management routines, an on-line digital terrain data base, and graphical display procedures designed to assist non-computer oriented forrest service personnel. The TAPAS system currently uses wind-generation sub-modules called NUWNDS for low-cost two-dimensional screening and NUATMOS for a three-dimensional characterization of wind flow in complex terrain.

NUATMOS (version 6) is a highly improved version of the ATMOS1 code, which is now claimed to be completely stable, efficient and optimized to the extent that it will run on a PC-386 personal computer. NUATMOS employs terrain-following coordinates and variable vertical grid spacing. NUATMOS incorporates atmospheric stability effects via a characteristic Froude number to set the horizontal/vertical adjustment parameter α; hence, it is purported to account satisfactorily for terrain speed-up and even lee-wave behavior. The authors assert that it is the "most comprehensively tested and evaluated model of its type."

NUWND and NUATMOS have been compared against laboratory measurements of flow over isolated ridges and hills. They have also been compared against field data from the CTMD and ASCOT program. The model appears to correctly predict streamline splitting, plume impaction, and nocturnal drainage flows. The models have also been compared with data from four measurement sets from the Latrobe Valley, Australia. Surface winds were predicted with 50 to 70% reliability by the models.

Lee and Kau (1984) divided the flow over complex terrain into a drainage flow component, V_D, and a boundary layer component, V_B. The local drainage component was calculated from Prandtl's analytic solution which is a function of local slope, potential temperature surface to air differences, surface roughness, and height. The boundary layer component was derived from an analytic solution which includes geostrophic wind conditions, Monin-Obukhov stability length, surface roughness, and the Coriolis parameter. The resulting velocity field is then "adjusted" by an objective analysis until the flow is divergence free. Predictions of the model were compared observations from the 1979 ASCOT experiment over the California Geysers area. One might consider this approach a "phenomenological" objective analysis method.

Another mass-consistent model which incorporates phenomenological arguments to adjust for surface roughness variation, cross-valley separation, ridge amplification and wind direction shear was developed by Erasmus (1986). The model was solved for grid spacing of only 100 m x 75 m over Kahuku Point, Oahu. The model presumes flow is dominated by mechanical rather than thermal processes; hence, it may not be suitable for early-morning forest spray applications.

D. Depth-Integrated Models

Integrated models have been applied to the atmospheric boundary layer for a number of years. Equations in horizontal parameter result from direct integration of the full primitive equations through the vertical. The resulting two-dimensional expressions may be solved for depth-averaged winds, temperatures, humidities, concentrations, etc. once entrainment relations are specified at the boundaries. They have been particularly popular for calculating cold-air drainage and winds over complex terrain in a terrain-following layer. Such models employ a two-dimensional horizontal grid. They work well over reasonably smooth terrain having resolvable features, but they can not handle ridge separation or deep, narrow valleys. A 2D FLOW model was prepared by Garrett and Smith (1984) which includes a Lagrangian particle diffusion model. Dobosy (1987) constructed a depth-integrated model which predicts night-time drainage flow in a trapezoidal shape valley. Conceptually any number of features including a main valley, its tributaries, sidewalls, head region and pooling region may be combined to form a representation of an entire drainage. The Dobosy model has not been widely validated, does not predict local in-valley winds without presumptions about similarity, and is limited to night-time drainage situations.

E. Linear or Perturbation Models

The equations of motion can be written in terms of flow perturbations induced by roughness, stratification, and terrain shape and linearized by eliminating higher order terms. Solutions for the effect of each disturbance can then be individually calculated and superimposed to determine the total wind field. A linear three-dimensional theory has been developed by Hunt, Leibovich and Richards (1988) (HLR) which is the foundation for the FLOWSTAR complex terrain model. The method of calculation is to compute Fourier transforms of the velocity field following HLR; then the transform is inverted numerically to calculate the actual flow variables at a point. In contrast to numerical models which solve the equations of motion on a grid, there is no iteration involved. Also the solution is determined explicitly once the algorithms and their assumptions have been agreed.

This solution approach is very appropriate for use on small personal computers. FLOWSTAR is currently configured to operate on PC-AT or 386 systems. Post processing graphic programs can produce a wide variety of streamline, flow vector, or profile graphs. The wind field can then be input into a puff dispersion model. A major advantage of the approach is that turbulence information is also predicted. The major limitations of the linearized analytical models are that they exclude large positive or negative changes in the mean flow and they exclude more complex models of turbulent shear stresses. Linear theories cannot describe large non-linear perturbations to the flow or non-linear synergism where two or more effects combines such as roughness change and separation.

There are a number of conditions which must be satisfied in order for the model to give useful results:

i) the slopes of the terrain are small (typically less than 1/4),
ii) the changes in the natural logarithm of the roughness length, z_o, are small (less than 1.0),
iii) the profile of potential temperature can be approximated by a simple form,
iv) the upwind velocity profile increases from the ground upwards with no strong elevated shear layer,
v) the upwind conditions are varying slowly on a time scale compared to times required for a parcel to cross the calculation domain, and
vi) rapid hill-side heating or cooling does not occur.

The model will give results for flows where Fr > 1 and the terrain is gently rolling as opposed to deep narrow valleys.

The MS3DJH (Mason and Sykes 3-Dimensional version of the Jackson and Hunt's theory) series of models (MS3DJH/1, MS3DJH/2, MS3DJH/3, and MS3DJH/3R) are fully described in Walmsley et al. (1980, 1982, 1986). Again finite-area Fourier transform methods are used to obtain expressions for perturbation pressure, velocity and surface stress fields from the linearized equations of motion. These are evaluated numerically using discrete Fast Fourier Transforms. These models compare quite well when compared with more sophisticated models. Again the potential of the method is calculation of flow parameters over complex, three-dimensional terrain. Salmon et al. (1988) compare this method against field observations and laboratory simulations of flow over Kettle Hill, Alberta, Canada. Wind speeds and wind directions were closely predicted for neutral flow over this low hill. MS3DJH and FLOWSTAR can provide much higher resolution than other models currently available at a fraction of the computational cost.

F. Full Primitive Equation Models

Primitive equation models, meso-scale models, predictive models, meteorological models, or K-models compute all meteorological variables (wind, temperature, turbulence, mixed-layer height, etc.) given specification of initial conditions and domain boundary conditions. Boundary conditions of larger scale must always be specified, and small subgrid-scale processes must always be parameterized. Because of computational requirements, atmospheric models using fluid dynamics equations cannot span scales beyond a factor of 50. Listed in the table below are the grid size and min and max phenomena length scales proposed by Kreitzberg, 1975.[2]

---

[2] In Table 7 the scale L_{min} should incorporate four grid intervals rather than two; since a two delta feature cannot be realistically represented.

TABLE 5: Atmospheric scales: model scope, characteristic length, and time scales (Kreitzberg, 1975).

	-	Model		Length	Time
Atmospheric scale	Grid (km)	L_{min} (km)	L_{max} (km)	$L \approx \lambda/4$ (km)	$T \approx P/4$
Regional	20	40	2000	20	3 hr
Mesoscale	1	2	100	10	1 hr
Local	0.08	0.16	8	1	15 min
Turbulent	0.01	0.02	1	0.2	1 min

Although Table 6 lists a few of the major primitive equation models used there are many other named and unnamed meso-scale model calculations which have been used to predict atmospheric flows ranging from mountain airflows, heat island flows, sea breezes, sudden roughness changes, etc. as shown in Table 7 extracted from Dickerson (1980). These models are quite complicated and require substantial computational resources. They contain many differences associated with computational molecules, grid systems, stability criteria, thermodynamics, boundary conditions, initial conditions, and turbulence models (closure *assumptions). The closure assumptions lead to a hierarchy of turbulence models and often additional transport equations (K-models, Kϵ-models (2nd moment), sub-grid scale models (large eddy simulation or Deardorff models). Presently, atmospheric modelers utilize parameterizations of subgrid scale turbulence, cumulus cloud effects, radiative flux divergence, etc., based on an "average" parameterization. One might wonder how such an approach is compatible with the desire to produce "real time" local values.

Ross et al. (1988) state "Predictive models are, in general, time consuming and impractical for real-time applications." Most predictive modelers have a more optimistic belief that their models may eventually be useful for real time applications on small scales.[3] There are also questions concerning model verification. Many models have been found to include rather

[3] Pielke (1990) believes that current supercomputer workstation capabilities have sufficiently advanced and reduced in cost, that primitive equation models coupled via "nudging" with observations should be the modeling platform of choice for Forest Service spray drift predictions. He has documented over 50 studies which provide qualitative validation of primitive equation numerical model approach and more than 10 studies which provide quantitative agreement.

large numerical pseudo-viscosity (Havens and Schreurs, 1985). Concern about "inherent" flow variabilities has led to discussion like that of Praegle et al. (1990) which suggest that "chaos" does indeed limit many connectively dominated meso-scale flows. Alternatively recent results suggest that complex terrain flows may be dominated by linear forcing due to terrain boundary conditions, synoptic scale pressure fields, and local solar cycle. (This may explain why objective analysis models have worked quite well in complex terrain.)

Most experience with primitive equations exists for mesoscales where minimum grid size is 0.5 to 2 km or larger. These models have not been thoroughly compared with detailed meteorological data, but they can be said to produce results which are "not counter-intuitive." Many well known phenomena are reproduced such as sea and land breeze cycles, lee waves, downslope and upslope winds, channeling, and valley drainage flow behavior. Less experience exists for smaller scale regions.

Very few cases are available where a full primitive model calculation is compared to a well-documented terrain flow. In a draft paper prepared by Dawson, Stock and Lamb (1990) the TEMPEST code was used to solve for flow over Steptoe Butte, Washington. The code used a $k\epsilon$-turbulence model, grid cell dimensions as small as 116 m by 175 m by 16 m, but a rather crude approximation to hill shape. Inaccuracy due to false diffusion was found to be quite significant (1 to 3 times as great as turbulent mass diffusivities in the recirculation and wake regions of the hill).

TABLE 6: MAJOR PRIMITIVE EQUATION MODELS

MODEL NAME	ORGANIZATION	REFERENCE
Argonne Model	Argonne Ntl. Lab. Los Alamos Ntl. Lab.	Yamada (1978)
ARAP	ARAP Inc.	Lewellen (1981)
CSU RAMS	Meteorology Department Colorado State University	Cotton, Pielke et al. (1982-90)
FEM-3	LLNL	Chan (1988)
HOTMAC	Yamada Science & Art Co.	Yamada (1989)
Penn State Model	Penn State and NCAR	Anthes and Warner (1978)
SIGMET	Science Applications Inc.	Davis and Freeman (1981)
TEMPEST	Battelle PNWL	Trent, et al., (1983)
UK Met Office Mesoscale Model	UK Meteorological Office	Tapp and White (1976)

TABLE 7: DICKERSON (1980)

Models that may be used to simulate airflow over a complex terrain area. Models are grouped according to main subject to which they have been applied: mountain airflow, heat island, sea breeze, or sudden roughness change.

* Includes topography

K MODEL

Mountain Airflow

Anthes & Warner 1974*
Fosberg 1967, 1969*
Jacobs & Pandolfo 1974*
Klemp & Liffy 1978*
Mahrer & Pielke 1975*
Mason & Sykes 1978*
Nickerson & Magaziner 1976*
Taylor 1977*

Heat Island

Bornstein 1975
Delage & Taylor 1970
Estoque & Bhumralkar 1969
Estoque & Bhumralkar 1970
Gulman & Torrance 1975
Mahrer & Pielke 1976
Ochs 1975 (Ref. 87)
Pielke & Mahrer 1975
Yu & Wagner 1975

Sea breeze

Estoque 1961
Estoque 1962
Fisher 1961
Magata 1965
McPherson 1970
Moroz 1967
Neumann & Mahrer 1974
Pielke 1974
Tapp & White 1976

Sudden roughness change

Huang & Nickerson 1974
Taylor 1969

CLOSURE MODEL

Mountain Airflow

Benque & Dewagenaere 1977*
Rao et al. (1974)
Yamada 1978*

DEARDORFF'S MODEL

Deardorff 1974

V. CONCLUSIONS AND RECOMMENDATIONS

The randomness inherent in atmospheric turbulence imposes a natural limit on flow predictability, which provides an upper bound on model accuracy as a function of available data. Nonetheless, recent analysis suggests that some degree of stratification may be obtained in flows strongly influenced by local boundary shapes, strong wind fields, or the diurnal cycle.

Given the desire to use the "best available" science and numerical models in the forest spray program limited by the desire to use "off-the-shelf" codes, a selection among the models reviewed can be made. Computational models most suitable for adoption wind energy-meteorology are:

TAPAS (NUATMOS) - This model is attractive because it is a) oriented toward forest and land-management personnel, b) contains attractive input and output modules, and c) can operate quickly on mini or micro computers.

The model should predict flow over undulating or rolling terrain in situations where drainage movements are small, ridge separation does not occur, and winds are moderate or high.

FLOWSTAR -

MS3DJH/3R - These models are also attractive because they are a) fully documented, b) input and output modules could be modified to fit siting needs, and c) they can operate on mini or micro computers.

The type model can provide almost infinite resolution over undulating or rolling terrain in situations where drainage movements are absent, ridge separation does not occur, and winds are moderate or high.

SUMMARY OF ADVANTAGES AND DISADVANTAGES OF VARIOUS MODEL CLASSIFICATIONS:

Phenomenological Models:

Advantages

1. Models are designed to reproduce specifically the dominant features of the identified flow system,
2. Models like VALMET can inherently handle complicated temporal variations of valley flows, and
3. Recent versions of the model can operate on mini size computers.

Disadvantages

1. Models are limited to terrain geometries for which they were created (e.g. VALMET is limited to narrow valleys of simple planform),
2. Models usually can not handle flow systems beyond their design range (e.g. cross-valley flows, tributary flows, sudden change in terrain shape or direction), and
3. Models will require extensive development to make them flexible.

Mass Consistent Objective Analysis Models:

Advantages

1. Models can be terrain specific and provide for terrain steering of winds,
2. Models can handle wind shear,
3. Versions of these models can handle stratification, surface roughness and lee wave behavior, and.
4. Recent versions of the model can operate on mini or micro computers.

Disadvantages

1. Requires substantial input data to yield accurate results (results are possible with minimal input, but accuracy degrades),
2. Turbulent diffusion parameters such as sigmas must be determined separately,
3. Models can not handle flow separation or strong drainage flows, and
4. Does not provide any estimate of variance from predicted values.

Depth Integrated Models:

Advantages

1. Grid reduction by depth integration increases substantially the computer space available for horizontal domain size or horizontal resolution; hence, large domains can be examined on mini or micro size computers, and

2. Models have been extensively validated against oceanographic and atmospheric flows as well as heavy gas spills.

Disadvantages

1. Models can not handle flow separation, strong vertical shear, or recirculation situations, and
2. Models are effectively limited to situations where inversions or other boundaries cap the layer being examined.

Linear or Perturbation Models:

Advantages

1. Models can be terrain specific and provide for terrain steering of winds,
2. Models can provide almost infinite resolution over the domain chosen,
3. Models can adjust for atmospheric stratification, wind shear, and inhomogeneities in surface roughness, and
4. Models can operate on mini or micro computers.

Disadvantages

1. Requires substantial input data to yield accurate results (results are possible with minimal input, but accuracy degrades),
2. Turbulent diffusion parameters such as sigmas must be determined separately,
3. Models can not handle flow separation or strong drainage flows, and
4. Models do not provide any estimate of variance from predicted values.

Primitive Equation Models:

Advantages

1. Models can provide simulations of almost all meteorological variables,
2. Models contain all the necessary physics to predict wind shear, flow separation, secondary flows, etc., and
3. Models can be structured to take advantage of almost all of available data in providing a best-guess simulation.

Disadvantages

1. Models require very large computing resources,
2. Further development work will be required to reduce response time and make input and output modules user friendly,
3. Boundary condition data may often be difficult to obtain,
4. Some tests suggest many models contain large numerical pseudo-viscosity which distorts the predictions, and
5. Many of these models are still not very well validated.

REFERENCES

Albini, F.A. ,(1981), "A Phenomenological Model for Wind Speed and Shear Stress Profiles in Vegetation Cover Layers," J. Appl. Meteorol., Vol. 20, 1325-1335.

Arya, S.P.S., Shipman, M.S. and Courtney, L.Y., (1981), "An experimental investigation of flow and diffusion in the disturbed boundary layer over a ridge--II. Diffusion from a continuous point source," Atmospheric Environment, Vol. 15, 1185-1194.

Arya, S.P.S. and Gadiyaram, P.S., (1986), " An experimental study of flow and dispersion in the wakes of three-dimensional low hills," Atmospheric Environment, Vol. 20, 729-740.

Bader, D.C. and C.D. Whiteman, 1989: "Numerical simulation of cross-valley plume dispersion during the morning transition period," J. Appl. Meteorol., Vol. 28, pp. 652-664.

Baron, Y., (1981), "A method for power-law index estimation," M.S. Thesis, Civil Engineering Department, Colorado State University, Fort Collins, Co, 115 pp.

Bayton, H.W., Biggs,W.G., Hamilton Jr., H.L. et al., (1965) "Wind Structure in and above a Tropical Forest," J. Appl. Meteorol., Vol. 4, 670-675.

Belcher, S.E., Xu, D.P. and Hunt, J.C.R., (1990), "The response of a turbulent boundary layer to arbitrarily distributed two-dimensional roughness changes," Q. J. R. Meteor. Soc., Vol. 116, pp. 611-635.

Bilanin, A.J. Teske, M.E., Barry, J.W. and R.B. Ekblad, 1989: "AGDISP: The Aircraft Spray Disperion Model, Code Development and Experimental Validation," Transactions of the ASAE, Vol. 32 (1), pp. 327-334.

Blumen, W. ed., (1990), Current Directions in Atmospheric Processes Over Complex Terrain, W. Blumen, ed., American Meteorological Society Monograph Volume 23, Number 45, 323 pp..

Bouwmeester, R.J.B., Meroney, R.N. and Sandborn, V.A., (1978), Sites for Wind-power Installations: Wind characteristics over ridges, Dept. of Energy Report RLO/2438-78/1, FMWE Report CER77-78RJBB-RNM-VAS51), 206 pp.

Bowne, N.E., Londergan, R.J., Murray, D.R., and H.S. Borenstein, 1983: "Overview, Results, and Conclusions for the EPRI Plume Model Validation and Development Project: Plains Site," EPRI Report EA-3074.

Bradley, E.F. (1978), An experimental study of the profiles of wind speed, shearing stress and turbulence at the crest of a large hill, Division of Environmental Mechanics, CSIRO, Canberra, Australia.

Britter, R.E., Hunt, J.C.R. and Richards, K.J., (1981), Air flow over a two-dimensional hill: studies of velocity speed-up, roughness effects and turbulence," Q .J. R. Meteor. Soc., Vol. 107, pp. 91-110.

Carruthers, D.J. and Hunt, J.C.R., (1990), "Fluid Mechanics of Airflow Over Hills: Turbulence, Fluxes and Waves in the Boundary Layer," Chapter 5 of AMS Monograph on Current Directions in Atmospheric Processes over Complex Terrain, W. Blumen, ed., pp.

Chan, S.T., ROdean, H.C., and D.L. Ermak, 1984: "Numerical Simulations of Atmospheric REIease of Heavy Gases over Vairiable Terrain," Air Pollution Modeling and Its Application III, Plenum Press, pp. 295-341.

Cionco, R.M., (1965), "A Mathematical Model for Air Flow in a Vegetative Cover," J. Appl. Meteorol., Vol. 4, 517-522.

Cionco, R.M., (1982), "A Meteorological Approach to Chemical Defense Over Complex Terrain with Vegetation," Workshop on the Parameterization of Mixed Layer Diffusion, R.M. Cionco, ed., 20-23 October, Las Cruces, New Mexico, pp. 323-328.

Cook, N.J., (1985), The Designer's Guide to Wind Loading of Building Structures, Part 1, Butterworths, London.

Cooper, R.W. (1965), Wind movement in pine stands, Georgia Forest Research Council, Macon, Ga.

Counihan, J., (1975), "Adiabatic Atmospheric Boundary Layer: A Review and Analysis of Data from the Period 1880-1972, Atmospheric Environment, Vol. 9, 871-905.

Cowan, I.R., (1968), "Mass, Heat and Momentum Exchange Between Stands of Plants and Their Atmospheric Environment," Quart. J. Roy. Mėteorol. Soc., Vol. 94, 523-544.

Davenport, A.G., (1960), "Rationale for Determining Design Wind Velocities," J. of the Structural Division, Proceedings ASCE, Vol. 86, No. ST5, 39-68.

Davenport, A.G., (1965), "The relationship of wind structure to wind loading," Wind Effects on Buildings and Structures, Proc. Conf. held at National Physical Laboratory, Teddington, London, H.M. Stationary Office, London, 53-111.

Davis, C.G. and Bunker, S.S., 1980: "Mass Consisent Windfields - July 22 Geyeser's Area," Los Alamos Scientific Laboratory, LA-UR-80-1092, 14 pp.

Davis, C.G. and B.E. Freeman, 1981: "Modeling Drainage Flow with SIGMET," Los Alamos National Laboratory, LA-UR-81-1329, ASCOT-81-1, 14 pp.

Deaves, D.M., (1981), "Computations of wind flow over changes in surface roughness," J. Wind Eng. and Industrial Aerodyn., Vol. 7, 65-94.

Denmead, O.T., (1964), "Evaporation Sources and Apparent Diffusivities in a Forest Canopy," Applied Meteorology, Vol. 3, 383-389.

Derickson, R.G. and Meroney, R.N., (1977), "A simplified physic airflow for evaluating wind power sites in complex terrain," Proceedings Summer Computer Simulation Conference, July 1977, Chicago, Illinois, 14 pp.

Derickson, R.G. and Peterka, J.A., (1992), "A method for calculating mean velocity profiles with multiple changes in surface roughness," Task 6 Report, NSF CSU/TTU Cooperative Program in Wind Engineering, Colorado State University, Fort Collins, CO, 51 pp. , (DRAFT)

Dolman, A.J. (1986), "Estimates of Roughness Length and Zero Plane Displacement for a Foliated and Non-Foliated Oak Canopy," Agric. Forest Meteorol., Vol 36, 241-248.

Dickerson, M.H., 1978: "MASCON-A Mass Consistent Atmospheric Flux Model for Regions with Complex Terrain," Journal of Applied Meteorology, Vol. 17, No. 3, pp. 241-253.

Dickerson, M.H. (editor), 1980: "Atmospheric Studies in Complex Terrain (ASCOT) Information Study," Lawerence Livermore National Laboratory, University of California, Report UCID-18572, ASCOT-80-3.

Dobosy, R., 1987: "An Integrated Model for Atmospheric Drainage Flow in a Valley," Proceedings of Fourth Conference on Mountain Meteorology, 25-28 August, 1987, Seattle, Washington, pp. 134-138.

Dumbauld, R.K. (1981), "Aerial Spray Application and Long-term Drift," Workshop on the Parameterization of Mixed Layer Diffusion, (R.M. Cainca, editor), 20-23 October, Las Cruces, New Mexico, p 289 ff.

Egan, B.A. and F.A. Schiermeier, 1986: "Dispersion in Complex Terrain: A Summary of the AMS Workshop held in Keystone, Colorado, 17-20 May 1983," Bulletin AMS, Vol. 67, No. 10, pp. 1240-1247

Eimern, I., ed. (1964), Windbreaks and Shelterbelts, I. Eimern, ed., World Meteorological Organization Technical Note No. 59, 188 pp.

Ekblad, R., Windell, K., Thompson, B. and B. Thompson, 1990: "EMCOT Weather Station," U.S.D.A. Forest Service, Program Wind Report.

Elliott, D.L. and Barnard, J.C., (1990a), "Effects of Trees on Wind Flow Variability and Turbulence," Transactions of the ASME, Vol. 112, 320-325.

Elliott, D.L. and Barnard, J.C., (1990b), "Observations of wind turbine wakes and surface roughness effects on wind flow variability," Solar Energy, Vol. 45, 265-283.

Erasmus, D.A., 1986: "A Model for Objective Simulation of Boundary-Layer Winds in an Area of Complex Terrain," Journal of Climate and Applied Meteorology, Vol. 25, pp. 1832-1841.

Finnigan, J.J. and Mulhearn, P.J., (1978), "Modelling Waving Crops in a Wind Tunnel," Boundary-Layer Meteorol., Vol. 14, 253-277.

Fons, W.L., (1940), Influence of forest cover on wind velocity, J. of Forestry, Vol. 38, 481-486.

"Forests, weather and climate," (1989) P.G. Jarvis, ed., Philosophical Transactions of the Royal Society of London, Series B, Vol. 324, No. 1223., 173-436.

Fosberg, M.A., (1969), "Airflow Over a Heated Coastal Mountain," J. Appl. Meteor., Vol. 8, 436-442.

Fowler, W.B., Helvey, J.D., and Felix, E.N., (1987)," Hydrologic and climatic changes in three small watersheds after timber harvest," Res. Pap. PNW-PR-379. Portland, OR: U.S.D.A., Forest Service, Pacific NW Research Station, 13 p.

Fox, D.G., Dietrich, D.L., Mussard, D.E., Riebau, A.R. and W.E. Marlatt, 1986: "The Topographic Air Pollution Analysis System," Proceedings of the Int. Conf. on Development and Application of Computer Techniques to Environmental Studies, (P. Zannetti, editor), pp. 123-144.

Fox, D.G., Dietrich, D.L., Mussard, D.E., Riebau, A.R. and W.E. Marlatt, 1987: "An Update on TAPAS and Its Model Components," Ninth Conf. on Fire and Forest Meteorlogy, April 21-24, Sand Diego, AMS, pp. 1-7.

Frost, W. (1979), "Summary of guidelines for siting wind turbine generators relative to small-scale, two-dimensional terrain features," Dept of Energy Report RLO/2443-77/1, 62 pp.

Frost, W., Masu, J.R. and Fichtl, G.H., (1974), " A boundary layer analysis of atmospheric motion over a semi-elliptical surface obstruction," Boundary-Layer Meteor., Vol. 7, 165-184.

Frost, W. and Nowak, D.K. (1977), "Sample Chapter 4.0 on Handbook for WTG Siting Relative to Small-scale Terrain Features," Contract E(45-1)-2443, PNWL, Richland WA, 78 pp.

Frost, W. and Shieh, C.F. (1981), "Guidelines for siting WECS relative to small-scale terrain features," DOE Report DOE/ET/20242-78/1 (DE82009124), 195 pp.

Geiger, R., (1950), The climate near the ground, Harvard University Press, Cambridge.

Gong, W. and Ibbetson, A., (1989), "A wind tunnel study of turbulent flow over model hills," Boundary-Layer Meteorology, Vol. 49,113-148.

Gong, W., (1991), "A wind tunnel study of turbulent dispersion over two- and three-diemnsional gentle hills from upwind point sources in neutral flow," Boundary-Layer Meteorology, Vol. 54, 211-230.

Grant, R.H. (1984), "The Mutual Interference of Spruce Canopy Structural Elements," Agric. Forest Meteorol., Vol. 32, 145-156.

Grant, A.L.M. and Mason, P.J. (1990), "Observations of boundary-layer structure over complex terrain," Q.J. R. Meteor. Soc., Vol. 116, pp. 159-186.

Gross, G. (1987), "A numerical study of the air flow within and around a single tree," Boundary Layer Meteorology, Vol. 40, No. 4, pp. 311-327.

Gross, G. (1987), "Some effects of deforestation on nocturnal drainage flow and local climate--a numerical study," Boundary-Layer Meteorology, Vol. 38, pp 315-337.

Guo, X. and J.P. Palutikof, 1988: "A comparison of two simple mesoscale models to predict windspeeds in the lower boundary layer," Wind Energy Conversion - 1988, Proc. 10th British Wind Energy Ass. Conf, London, 22-24 March 1988, (D.J. Milborrow, editor), Mechanical Engineering Publications Limited, London, 105-112.

Hanna, S.R. and D.G. Strimaitis, 1990: "Rugged Terrain Effects on Diffusion," Chapter 6 of AMS Monograph on Current Directions in Atmospheric Processes over Complex Terrain (W. Blumen, editor) (draft), 90 pp.

Hanna, S.R., Egan, B.A., Vaudo, C.J. and A.J. Curreri, 1984: "A Complex Terrain Dispersion Model for REgulatory Applications at the Westvaco Luke Mill," Atmopsheric Environment, Vol. 18, pp. 685-699.

Harvey, R.B. Jr. and J.N. Hamawi, 1986: "A Modification of the Gaussian Dispersion Equation to Accommodate Restricted Lateral Dispersion in Deep River Valleys," APCA Journal, Vol. 36, No. 2, pp. 171-173.

Havens, J.A. and P.J. Schreurs, 1985: "Evaluation of 3-D Hydrodynamic Computer Models for Prediction of LNG Vapor Dispersion in the Atmosphere," Gas Research Institute Report, Contract NO. 5083-252-0788.

Hewson, E.W., Wade, J.E., and Baker, R.W. (1979), "A handbook on the use of trees as an indicator of wind power potential," DOE Report RLO-2227-79/3, 21 pp.

Hiester, T.R. and Pennell, W.T. (1981), "The Meteorological Aspects of Siting Large Wind Turbines," Pacific Northwest Laboratory Report PNL-2522, Richland WA

Hirata, T., (1953), "Fundamental studies on the formation of cutting series on the center pressure, the drag coefficient of a tree and one effect of shelter belts, Bull. Tokyo Univ. Forestry, No. 45, 61-87.

Hsi, G. and Nath, J., (1968), A laboratory study on the drag force distribution within model forest canopies in turbulent shear flow, U.S. Army Materiel Command, Grant No. DA-AMC-28-043-65-G20.

Hunt, J.C.R. (1978), "Wind over hills," Survey paper for NOAA-NSF Workshop, Boulder, Colorado, August 1978, 41 pp.

Hunt, J.C.R., (1981), " Turbulent stratified flow over low hills," Proceedings of Symposium on Designing with the Wind, Nantes, France, June 1981, pp. I-1-1 to I-1-23.

Hunt, J.C.R., (1984), "Analytical calculations and estimates of heat flux and temperature fluctuations in distorted flows and flows over hills," Report C to Flow Analysis Associates, Ithaca, N.Y. 30 pp.

Hunt, J.C.R., Holyyroyd, R.J., Carruthers, D.J., Robins, A.G., Aspley, D.D., Smith, F.B., and Thomson, D.J. (1990), "Developments in modelling air pollution for regulatory uses," Proceedings of the 18th NATO-CCMS Int. Conf. on Air Pollution Modelling and its Applications, Vancouver, Canada, p. 1-42.

Hunt, J.C.R., Leibovich, S., and K.J. Richards, 1988: "Turbulent shear flow over hills," Q.J. Roy. Met. Soc., Vol. 114, pp. 1435-1470.

Hunt, J.C.R. and Simpson, J.E. (1982), "Atmospheric Boundary Layers Over Non-Homogeneous Terrain," Chapter 7 from Engineering Meteorology, E.J. Plate, ed., Elsevier Scientific Pub. Co., pp. 269-318.

Huston, J.S., (1964), Observations of the micrometeorology and intensity of turbulence within a deciduous forest, CRDL Technical Memorandum 5-6, August 1964.

Hutchison, B.A. and Hicks, B.B., eds. (1985), The Forest-Atmosphere Interaction, D. Reidel Publishing.

Iizuka, H., (1952), "On the width of windbreak,"Bulletin of the Government Forest Experiment Station, No. 56, Tokyo, Japan, December 1952.

Iizuka, H., (1956), "On the width of windbreak," Proc. Intern. Union of Forest Res. Organ., 12th Congress, Oxford, Section 11, IUFRO, 1-4.

Inoue, E., (1963), "On the Turbulent Structure of Airflow within Crop Canopies," J. Meteorol. Soc. Japan, Vol. 41, 317-326.

Jackson, P.S. and Hunt, J.C.R., (1975), "Turbulent wind flow over a low hill," Q.J. Roy. Met. Soc., Vol. 101, 929ff.

Jackson, P.S. (1977), "Aspects of Surface Wind Behavior," J. of Wind Engineering, Vol. 1, No. 1, pp. 1-14.

Jackson, P.S. (1979), "The influence of local terrain features on the site selection for wind energy generating systems," Research Report BLWT-1-1979, U. of Western Ontario, London, Canada, 83 pp.

Jaeger, L., (1985), "Estimations of surface roughnesses and displacement heights above a growing pine forest from wind profile measurements over a period of ten years," The Forest-Atmosphere Interaction, B.A. Hutchison and B.B. Hicks, eds., D.Reidel Publishing Company, pp. 71-90.

Jensen, N.O., (1978), "Change of surface roughness and the planetary boundary layer," Quart. J. R. Met. Soc., Vol. 104, 351-356.

Jensen, N.O. and Peterson, E.W., (1978), "On the escarpment wind profile," Quart. J. R. Meteor. Soc., Vol. 104, 719-728.

Jensen, N.O., Petersen, E.L. and Troen, I. (1984), Extrapolation of mean flow statistics with special regard to wind energy applications, WMO Report WCP-86, WMO/TD-No. 15.

Kawatani, T.and Meroney, R.N., (1968), The Structure of Canopy Flow Fields, Report to U.S. Army Material Command, Contract No. DA-AMC-28-043-65-G20, 122 pp.

Kawatani, T. and Meroney, R.N., (1970), "Turbulence and Wind Speed Characteristics within a Model Canopy Flow Field," J. of Agricultural Meteorology, Vol. 7, 143-158.

Kawatani, T, (1971), An Investigation of Turbulent Boundary Layer on High Roughness, Ph.D. Dissertation, Civil Engineering, Colorado State University, Fort Collins, CO, 1971.

Lai, W., (1955), Aerodynamic drag of several broadleaf tree species, Internal Tech. Rept. AFSWP-863, U.S. Dept. of Agriculture, Forest Service, 1955.

Lalas, D.P., Tombraou, M., and Petrakis, M. (1988), "Comparison of the performance of some wind energy siting codes in rough terrain," Proceedings of European Community Wind Energy Conference, Herning Denmark, 6-10 June 1988, pp. 110-114.

Laniccci, J.M. (1985), "Sensitivity Tests of a Surface Layer Windflow Model to Effects of Stability and Vegetation," Air Force Geophysics Laboratory, Report AFGL-TR-85-0265, 56 pp.

Leahey and Hansen, M.C., (1987), "Short Communications: Observations of winds above and below a forest canopy located near a clearing," Atmospheric Environment, Vol. 21, No. 5, 1227-1229

Lee, H.N. and Kau, W.S., 1984: "Simulation of Three-Dimensional Wind Flow Over Complex Terrain in the Atmospheric Boundary Layer," Boundary-Layer Meteorlogy, Vol. 29, pp. 381-396.

Lee, R.L. and J.M. Leone, Jr., 1988a: "Appliations of a Three-Dimensional Finite Element Model to Mountain-Valley Flows," Int. Conf. on Computational Methods in Flow Analysis, Okayam, Japan, September 5-8, 1988, Lawrence Livermore National Laboratory, UCRL-97389, preprint, 8 pp.

Lee, R.L. and J.M. Leone, Jr., 1988b: "A Modified Finite Element Model for Mesoscale Flows Over Complex Terrain," Comput. Math. Applic., Vol. 16, No. 1/2, pp. 41-56.

Lewellen, W.S. and R.I. Sykes, 1985: "A Scientific Critique of Available Models for Real-Time Simulations of Dispersion," Nuclear Regulatory Commission Report NUREG/CR-4157, ARAP Report No. 472.

Lewellen, W.S., Sykes, R.I., and D. Oliver, 1982: "The Evaluation of MATHEW/ADPIC as a Real-Time Dispersion Model," Nucelar Regulatory Commission Report NUREG/CR-2199, ARAP Report No. 442.

Lewellen, W.S., Sykes, R.I., and S.F. Parker, 1985: "Comparison of the 1981 INEL Disperion Data With Results from a Number of Different Models," Nuclear Regulatory Commision Report NUREG/CR-4159, ARAP Report No. 505.

Lewellen, W.S., Teske, M., Contiliano, R., Hilst, G., and C. duP. Donaldson, 1974: "Invariant Modeling of Turbulence and Diffusion in the Planetary Boundary Layer," Aeronautical Research Associates of Princeton, Report No. 225, 319 pp.

Lin, J.T., Veenhuizen, S.D., and Qualmann, R.L. (1985), "Numerical Estimates of Three-Dimensional Wind Flow for the Cape Blanco Area of Oregon," United Industries Report No. 8514 for Bonneville Power Administration, Portland, Oregon, 113 pp.

Lin, J.T. (1989), "Study on Reduction of Fugitive Dust Using Wind Energy for Taichung Coal-fired Power Plant," Interim Report. United Industries Report No. 8907, for Environmental Protection Department, Taiwan Power Company, Taipei, Taiwan R.O.C

Lin, J.T. (1990), "A Numerical Model for Predicting Wind Turbine Array Performance in Complex Terrain-Phase II," Final Report, United Industries Report No. 8917 for SBIR Program, US Dept. of Energy, 112 pp.

Malina, F.V., (1941), "Recent developments in the dynamics of wind erosion," Trans. Amer. Geophys. Union, 279.

Mason, P.J. (1986), "Flow over the summit of an isolated hill," Boundary-Layer Meteorology, Vol. 37, pp. 385-405.

Massman, W., (1987), "A comparative study of some mathematical models of the mean wind structure and aerodynamic drag of plant canopies," Boundary-Layer Meteorology, Vol. 40, 179-197.

McNider, R.T. and R.A. Pielke, 1984: "Numerical simulation of slope and mountain flows," J. Climate Appl. Meteor., Vol. 10, pp. 1441-1453.

McNaughton, K.G. (1989), "Micrometeorology of shelter belts and forest edges," Phil. Trans. R. Soc. Lond., B, Vol. 324, 351-368.

Meroney, R.N., (1968), "Characteristics of Wind and Turbulence in and above Model Forests," Journal of Applied Meteorology, Vol. 7, No. 5, 780-788.

Meroney, R.N. (1977), "Wind in the perturbed environment: Its influence on WECS," Proceedings of AWEA Spring Conference, May 11-14, 1977, Boulder, CO, 27 pp.

Meroney, R.N. (1980), "Wind-tunnel simulation of the flow over hills and complex terrain," J. of Ind. Aerodynamics, Vol. 5, 297-321.

Meroney, R.N. (1990), "Review and Classification of Complex Terrain Models for Use with Integrated Pest Management Program Spray Models," Forest Service Technology and Development Program, USDA, Forest Service, Missoula, Montana, 22 pp. [CEM89-90-RNM-1].

Meroney, R.N., Bowen, A.J., Lindley, D.L., and Pearse, J.R. (1978), "Wind characteristics over complex terrain: Laboratory simulation and field measurements at Rakaia Gorge, New Zealand," Department of Energy Report RLO/2438-77/2, 219 pp.

Meroney, R.N., Kesic, D.and Yamada, T., (1968), Gaseous Plume Diffusion Characteristics Within Model Peg Canopies, Technical Report to U.S. Army Electronics Command, ECOM C-0423-1, 71 pp.

Meroney, R.N., Sandborn, V.A., Bouwmeester, R.J.B., and Rider, M.A., (1976), Sites for Wind Power Installations: Wind Tunnel Simulation of the Influence of Two-Dimensional Ridges on Wind Speed and Turbulence, U.S. National Science Foundation, Report NSF/RANN GAER 75-00702, July 1976.

Meroney, R.N. et al. (1978), Sites for Wind Power Installations: Physical Modeling of the Influence of Hills, Ridges and Complex Terrain on Wind Speed and Turbulence: Part II Executive Summary, Report RLO/2436-77/3, U.S. Dept. of Energy, 91 pp.

Meroney, R.N., Bowen, A.J., Lindley, D.L. and Pearse, J.R., (1978), Wind characteristics over complex terrain: Laboratory simulation and field measurements at Rakaia Gorge, New Zealand, Department of Energy Report RLO/2438-77/2, 219 pp.

Monteith, J.L., ed., (1975-76), Vegetation and the Atmosphere Vols 1 and 2, J.L. Monteith, ed., Academic Press, London, 278 pp, 439 pp.

Park, J. Schwind, D., (1977), Wind Power for Farms, Homes and Small Industry, Nielsen Engineering and Research, Inc., Mountain View, California.

Paegle, J., Pielke, R.A., Dalu, G.A., Miller, W., Garrat, J.R., Vukicevic, T., Berri, G. and M. Nicolini, 1990: " Predictability of Flows Over Complex Terrain," Chapter 10 of AMS Monograph on Current Directions in Atmospheric Processes over Complex Terrain (W. Blumen, editor) (draft), 48 pp.

Panofsky, H.A. and Dutton, J.A., (1984), Atmospheric Turbulence: Models and Methods for Engineering Application, John Wiley and Sons, New York, 397 pp.

Pendergrass, W. and Arya, S.P.S., (1984), "Dispersion in Neutral Boundary Layer Over a Step Change in Surface Roughness--I. Mean Flow and Turbulence Structure," Atmospheric Environment, Vol. 18, 1267-1279.

Pendergrass, W. and Arya, S.P.S., (1984), "Dispersion in Neutral Boundary Layer Over a Step Change in Surface Roughness--II. Concentration Profiles and Dispersion Parameters," Atmospheric Environment, Vol. 18, 1281-1296.

Plate, E.J. and Quarishi, A.A., (1965), "Modeling of Velocity Distributions Inside and Above Tall Crops," J. of Applied Meteorology, Vol. 4.

Poppendiek, H.F. (1949), Investigation of velocity and temperature profiles in air layers within and above trees and brush, U. of California, Dept. of Engineering, Los Angeles, March 1949.

Priestly, C.H.B., (1959), Turbulent Transfer in the Lower Atmosphere, Univ. of Chicago Press.

Raupach, M.R., Thom, A.S. and Edwards, L., (1980), "A Wind Tunnel Study of Turbulent Flow Close to Regularly Arrayed Rough Surfaces," Boundary-Layer Meteorol., Vol. 18, 373-397.

Raupach, M.R. and Thom, A.S., (1981), "Turbulence in and above Plant Canopies," Ann. Rev. Fluid Mech., Vol. 13, 97-129.

Rayner, W.G., (1962), Wind resistance of conifers, Aero. Rept. 1008, National Physical Laboratory, U.K., 1962.

Reifsnyder, W. (1955), "Wind Profiles in a Small Isolated Forest Stand," Forest/Science Washington D.C.,Vol. 1, 289-297.

Ross, D.G. and I. Smith, 1986: "Diagnostic Wind Field Modelling for Complex Terrain - Testing and Evaluation," Centre for Applied Mathematical Modelling, Chisholm Institute of Technology, CAMM Report No. 5/86, 93 pp.

Ross, D.G., Smith, I.N., Manins, P.C. and Fox, D.G. (1988), "Diagnostic Wind Field Modeling for Complex Terrain: Model Development and Testing," Journal of Applied Meteorology, Vol. 27, 785-796.

Ruck, B. and Adams, E., (1991), "Fluid Mechanical Aspects of the Pollutant Transport to Coniferous Trees," Boundary-Layer Meteor., Vol. 56, 163-195.

Sadeh, W.Z., Baron, Y., and Fox, D.G. (1982), "Estimating the Power-Law Index for Wind," Rocky Mountain Forest and Range Experiment Station, Forest Service, USDA Report, Fort Collins, CO, 38 pp.

Sadeh, W.Z. and Fox, D.G. (1981), "Canopy Effects on Turbulence and Diffusion," Workshop on the Parameterization of Mixed Layer Diffusion, (R.M. Cainca, editor), 20-23 October, Las Cruces, New Mexico, pp. 217-234.

Sadeh, W.Z., Law, F.W., Marlatt, W.E., et al., (1982), A survey of micrometeorological parameters within a forest canopy at Fort Polk, Louisiana, U.S. Army Elect. Res. and Devel. Command, Atmospheric Sciences Laboratory, White Sands Missile Range, NM, Report ASL-CR=82-0100-1, 175 pp.

Salmon, J.R., Teunissen, H.W., Mickle, R.E., and P.A. Taylor, 1988: "The Kettles Hill Project: Field Observations, Wind-Tunnel Simulations and Numerical Model Predictions for Flow Over a Low Hill," Boundary-Layer Meteorology, Vol. 43, pp. 309-343.

Sauer, F.M., Fons, W.L. and Arnold, K. (1951), Experimental investigation of aerodynamic drag in tree crowns exposed to steady wind - conifers, Div. Forest Fires Res., U.S. Dept. of Agriculture, Forest Service.

Sherman, C.A., 1978: "A Mass-Consistent Model for Wind Fields over Complex Terrain," Journal of Applied Meteorology, Vo. 17, pp. 312-319.

Simiu, E. and Scanlan, R.H., (1978), Wind Effects on Structures, John Wiley and Sons, New York, 458 pp.

Snyder, W.H., (1981), Guideline for fluid modeling of atmospheric diffusion, U.S. Environmental Protection Agency, Report 600/8-81-009, 185 pp

Snyder, W.H. and Britter, R.E., (1987), "A wind tunnel study of the flow structure and dispersion from sources upwind of three-dimensional hills," Atmospheric Environment, Vol. 21, 735-751.

Snyder, W.H. (1990), "Fluid modeling applied to atmospheric diffusion in complex terrain," Atmospheric Environment, Vol. 24A, No. 8, pp. 2071-2088.

Sutton, O.G., (1949), Atmospheric Turbulence, Metheun, London, 111 pp.

Taylor, P.A. and Gent, P.R., (1974), "A model of atmospheric boundary layer flow above an isolated two-dimensional hill; an example of flow above 'gentle topography'," Boundary-Layer Meteor., Vol. 7, 349-362.

Taylor, P.A. and Teunissen, H.W. (1987), "The Askervein Hill Project: Overview and background data," Boundary-Layer Meteor., Vol. 39, 107-132 (1987)

Taylor, P.A., Sykes, R.I, and Mason, P.J. (1989), "On the parameterization of drag over small-scale topography in neutrally-stratified boundary-layer flow," Boundary-Layer Meteorology, Vol. 48, pp. 409-422.

Teunissen, H.W., Shokr, M.E., Bowen, A.J. et al., (1987), "The Askervein Hill Project: wind-tunnel simulations at three length scales," Boundary-Layer Meteor., Vol. 40, 1-29.

Tiren, L., (1927), "Einige Intersuchungen ober die Schaftform," Meddel. Statens. Skogsforsoksanstalt, Hafte 24, No. 4, 81-152.

Tourin, M.H. and Shen, W.C., (1966), Deciduous Forest Diffusion Study, Final Report to U.S. Army, Dugway Proving grounds, Contract DA42-007-AMC-48(R).

Townsend, A.A., (1966), "The flow in a turublent boundary layer after a change in surface roughness," J. Fluid Mech., Vol. 22, 799 ff.

Townsend, A.A., (1976), Structure of turbulent shear flow, Cambridge Univ. Press, New York, 429 pp.

Trent, D.S., Eyler, L.L., and M.J. Budden, 1983: "TEMPEST a three-dimensional time-dependent computer program for hydrothermal analysis - Vol. I: Numerical methods and input instructions," Pacific Northwest Laboratory, PNL-4348 Vol. I.

Veenhuizen, S. and Lin, J.T., (1982), Numerically Estimated Areal Distribution of the Wind Field for the Cape Blanco area of Oregon, United Industries Report No. 8204, December.

Veenhuizen, S. and Lin, J.T., (1983), Numerical Estimates of Three-Dimensional Wind Flow for the Goodnoe Hills Area, U.S. Dept. of Energy, Bonneville Power Administration, United Industries Report No. 8305, February.

Veenhuizen, S.D. and Lin, J.T. (1985), "Numerical Estimates of Three-Dimensional Wind Flow for the Goodnoe Hills Area of Washington and Oregon," United Industries Report No. 8305 for Bonneville Power Administration, Portland, Oregon, 131 pp.

Walmsley, J.L., Salmon, J.R. and P.A. Taylor, 1982: "On the Application of a Model of Boundary-Layer Flow Over Low Hills to Real Terrain," Boundary-Layer Meterol., Vol. 23, pp. 17-46.

Walmsley, J.L. and Taylor, P.A. (1987), "A preliminary demonstration of the use of boundary-layer models of flow in complex terrain for high resolution surface wind forecasting," Proc. Symp. Mesoscale Analysis and Forecasting, Vancouver, Canada, 17-19 August 1987, ESA SP-282, pp. 539-543.

Walmsley, J.L., Taylor, P.A., and R. Mok, 1980: "MS3DJH-A Computer Model for the Study of Neutrally Stratified Boundary-Layer Flow Over Isolated Hills of Moderate Slope," Research REport AQRB-80-008-L, Atmospheric Enviornment Service, Toronto, Canada.

Walmsley, J.L., Taylor, P.A., and T. Keith, 1986: "A Simple Model of Neutrally Stratified Boundary-Layer Flow Over Complex Terrain with Surface Roughenss Modulations (MS3DJH/3R)," Boundary-Layer Meteorol., Vol. 36, pp. 157-186.

Walshe, D.E. and Fraser, A.I., (1963), Wind-tunnel tests on a model forest, Aero. Rept. 1078, National Physical Laboratory, U.K., 1963.

Wegley, H.L., Orgill, M.M., and Drake, R.L. (1978), "A Siting Handbook for Small Wind Energy Conversion Systems," Pacific Northwest Laboratory Report PNL-2521, Richland, WA.

Whiteman, C. and K.J. Allwine, 1985: "VALMET-A VAlley AIr Pollution Model," Battelle Pacific Northwest Laboratory Report PNL-4728 Rev 1, 176 pp.

Woodruff, N.P. and Zingg, A.W., (1952), Wind tunnel studies of fundamental problems related to windbreaks, U.S. Dept. of Agriculture, Soil Conservation Service, Report SCS-TP-112, August 1952.

Wu, G., (1993), Wind-Tunnel Simulation of Turbulence Structure and Dispersion Processes for Air Flow Over a Step Change of Surface Roughness, Ph.D. Dissertation, Civil Engineering, Colorado State University, Fort Collins, 259 pp.

Yamada, T. (1982), "A numerical model study of turbulent airflow in and above a forest canopy," Journal of the Meteorological Society of Japan, Vol. 60, No. 1, pp.439-454.

Yamada, T. and Bunker, S. (1988), "Development of a nested grid, second moment turbulence closure model and application to the 1982 ASCOT Brush Creek data simulation," Journal of Applied Meteorology, Vol. 27, pp. 562-578.

Yamada, T. and Bunker, S., (1989), "A numerical model study of nocturnal drainage flows with strong wind and temperature gradients," Journal of Applied Meteorology, Vol. 28, 545-554.

Yamada, T., Kao, C.Y.J., and S. Bunker, 1989: "Airflow and Air Quality Simulations Over the Western Mountainous Region with a Four-Dimensional Data Assimilation Technique," Atmospheric Enviornment, Vol. 23, No. 3, pp. 539-554. (HOTMAC and RaPTAD)

Zeman, O. and Jensen, N.O. (1987), "Modification of turbulence characteristics in flow over hills," Q.J.R. Meteor. Soc., Vol. 113, pp. 55-80.